การสังเคราะห์สารลดจุดเริ่มไหลจากกรดไดคาร์บอกซิลิกสำหรับไบโอดีเซลจากน้ำมันถั่วเหลืองและน้ำมันปาล์ม

นางสาวสุจิตรา วารสนาม

วิทยานิพนธ์นี้เป็นส่วนหนึ่งของการศึกษาตามหลักสูตรปริญญาวิทยาศาสตรมหาบัณฑิต
สาขาวิชาปิโตรเคมีและวิทยาศาสตร์พอลิเมอร์
คณะวิทยาศาสตร์ จุฬาลงกรณ์มหาวิทยาลัย
ปีการศึกษา 2555

SYNTHESIS OF POUR POINT DEPRESSANT FROM DICARBOXYLIC ACID FOR BIODIESEL FROM SOYBEAN OIL AND PALM OIL

Miss Sujitra Warasanam

A Thesis Submitted in Partial Fulfillment of the Requirements
for the Degree of Master of Science Program in Petrochemistry and Polymer Science
Faculty of Science
Chulalongkorn University
Academic Year 2012

Thesis Title	SYNTHESIS OF POUR POINT DEPRESSANT FROM DICARBOXYLIC ACID FOR BIODIESEL FROM SOYBEAN OIL AND PALM OIL
By	Miss Sujitra Warasanam
Field of Study	Petrochemistry and Polymer Science
Thesis Advisor	Associate Professor Somchai Pengprecha, Ph.D.

Accepted by the Faculty of Science, Chulalongkorn University in Partial Fulfillment of the Requirements for the Master's Degree

…………………………………………Dean of the Faculty of Science
(Professor Supot Hannongbua, Dr.rer.nat.)

THESIS COMMITTEE

…………………………………………Chairman
(Associate Professor Tharapong Vitidsant, Ph.D.)

…………………………………………Thesis Advisor
(Associate Professor Somchai Pengprecha, Ph.D.)

…………………………………………Examiner
(Associate Professor Wimonrat Trakarnpruk, Ph.D.)

…………………………………………External Examiner
(Suchada Butnark, Ph.D.)

สุจิตรา วารสนาม : การสังเคราะห์สารลดจุดเริ่มไหลจากกรดไดคาร์บอกซิลิกสำหรับไบโอดีเซลจากน้ำมันถั่วเหลืองและน้ำมันปาล์ม. (SYNTHESIS OF POUR POINT DEPRESSANT FROM DICARBOXYLIC ACID FOR BIODIESEL FROM SOYBEAN OIL AND PALM OIL) อ.ที่ปรึกษาวิทยานิพนธ์หลัก: รศ.ดร.สมใจ เพ็งปรีชา, 107 หน้า.

จุดมุ่งหมายของงานวิจัยนี้ คือการสังเคราะห์สารลดจุดเริ่มไหล (PPDs) จากกรดไดคาร์บอกซิลิกเพื่อปรับปรุงสมบัติการไหลที่อุณหภูมิต่ำของไบโอดีเซลจากน้ำมันถั่วเหลืองและไบโอดีเซลจากน้ำมันปาล์ม สารลดจุดเริ่มไหล 16 ชนิด คือ ไดเมทิลซัคซิเนต (DMS), ไดเมทิลอะดิเปต (DMAD), ไดเมทิลอซีเลท (DMAZ), ไดเมทิลพทาเลท (DMP), ไดไอโซโพรพิลซัคซิเนต (DIS), ไดไอโซโพรพิลอะดิเปต (DIAD), ไดไอโซโพรพิลอซีเลท (DIAZ), ไดไอโซโพรพิลพทาเลท (DIP), ได-2-บิวทิลซัคซิเนต (DBS), ได-2-บิวทิลอะดิเปต (DBAD), ได-2-บิวทิลอซีเลท(DBAZ), ได-2-บิวทิลพทาเลท (DBP), ได-2-เอทิลเฮกซิลซัคซิเนต (DBS), ได-2-เอทิลเฮกซิลอะดิเปต (DBAD), ได-2-เอทิลเฮกซิลอซีเลท (DBAZ), และได-2-เอทิลเฮกซิลพทาเลท (DBP) ถูกสังเคราะห์โดยปฏิกิริยาเอสเทอริฟิเคชัน โครงสร้างของสารเหล่านี้ถูกพิสูจน์เอกลักษณ์โดยเทคนิค FT-IR และ ^{1}H-NMR จุดหมอก (CP) และจุดเริ่มไหล (PP) ของน้ำมันไบโอดีเซลจากน้ำมันถั่วเหลืองและไบโอดีเซลจากน้ำมันปาล์มถูกปรับปรุงโดยการเติมสารลดจุดเริ่มไหลปริมาณ 10,000, 100,000 และ 300,000 ส่วนในล้านส่วน เมื่อเติมสารลดจุดเริ่มไหล 300,000 ส่วนในล้านส่วน จุดหมอกและจุดเริ่มไหลของไบโอดีเซลทั้งสองชนิดมีค่าลดลงอยู่ในช่วง 2.70±1.0 ถึง 6.00±1.0 องศาเซลเซียส และ 2.00±1.0 ถึง 6.00±1.0 องศาเซลเซียส สารกลุ่ม 2-บิวทิลเอสเทอร์ สามารถปรับปรุงสมบัติการไหลของไบโอดีเซลจากน้ำมันถั่วเหลืองและไบโอดีเซลจากน้ำมันปาล์มได้ดี ยิ่งไปกว่านั้นผลการทดลองแสดงให้เห็นว่า DBAZ มีประสิทธิภาพมากที่สุดเมื่อเปรียบเทียบกับสารลดจุดเริ่มไหลชนิดอื่น เนื่องจากหมู่แทนที่ซึ่งเป็นกิ่ง (2-บิวทิล) ในโครงสร้างของมัน เมื่อเติม DBAZ 300,000 ส่วนในล้านส่วน จุดหมอกและลดจุดเริ่มไหลของไบโอดีเซลจากน้ำมันถั่วเหลืองสามารถลดลงได้ 5.15±1.0 องศาเซลเซียส และ 5.40±1.0 องศาเซลเซียส ในขณะที่ทั้งจุดหมอกและจุดเริ่มไหลของไบโอดีเซลจากน้ำมันปาล์มลดลง 6.00±1.0 องศาเซลเซียส

สาขาวิชา ปิโตรเคมีและวิทยาศาสตร์พอลิเมอร์ ลายมือชื่อนิสิต..............................
ปีการศึกษา ....2555.......... ลายมือชื่อ อ.ที่ปรึกษาวิทยานิพนธ์หลัก..........

5372361023: MAJOR PETROCHEMISTRY AND POLYMER SCIENCE
KEYWORDS: BIODIESEL / DICARBOXYLIC ACID / POUR POINT DEPRESSANT

SUJITRA WARASANAM: SYNTHESIS OF POUR POINT DEPRESSANT FROM DICARBOXYLIC ACID FOR BIODIESEL FROM SOYBEAN OIL AND PALM OIL. ADVISOR: ASSOC. PROF. SOMCHAI PENGPRECHA, Ph.D., 107 pp.

The purpose of this research is to synthesize pour point depressants (PPDs) from dicarboxylic acids for improving cold flow properties of soybean methyl ester (SME) and palm methyl ester (PME). The 16 types of PPDs (dimethyl succinate (DMS), dimethyl adipate (DMAD), dimethyl azelate (DMAZ), dimethyl phthalate (DMP), diisopropyl succinate (DIS), diisopropyl adipate (DIAD), diisopropyl azelate (DIAZ), diisopropyl phthalate (DIP), di 2-butyl succinate (DBS), di 2-butyl adipate (DBAD), di 2-butyl azelate (DBAZ), di 2-butyl phthalate (DBP), di 2-ethyl hexyl succinate (DES), di 2-ethyl hexyl adipate (DEAD), di 2-ethyl hexyl azelate (DEAZ) and di 2-ethyl hexyl phthalate (DEP)) were synthesized by esterification reaction. Their structures were characterized by FT-IR and ^{1}H-NMR techniques. The cloud point (CP) and pour point (PP) of SME and PME were improved by addition of PPDs at 10,000, 100,000, and 300,000 ppm. At 300,000 ppm, could point and pour point of both biodiesels were reduced in the range of 2.70±1.0 °C to 6.00±1.0 °C and 2.00±1.0 °C to 6.00±1.0 °C. 2-Butyl esters gave good results on improving flow property of both SME and PME. Moreover, the results indicated that DBAZ was the most effective when compared with other PPDs, due to branch substituent (2-butyl) in its structure. At 300,000 ppm of DBAZ, the CP and PP of SME were reduced by 5.15±1.0 °C and 5.40±1.0 °C while the CP and PP of PME were reduced 6.00 ±1.0 °C in both CP and PP.

Field of Study : Petrochemistry and Polymer Science Student's Signature…………
Academic Year :………..2012……………….......... Advisor's Signature………..

ACKNOWLEDGEMENTS

I would like to express my deepest appreciation and gratitude to my advisor, Associate Professor Dr. Somchai Pengprecha, for his excellent suggestion, guidance, encouragement and supportiveness throughout the entire period of conducting this thesis. I would also like to thank Associate Professor Dr. Tharapong Vitidsant, Associate Professor Dr. Wimonrat Trakarnpruk and Dr. Suchada Butnark attending as the chairman and members of my thesis committee, respectively, for their kind guidance and valuable suggestions and comments.

Additionally, I would like to thank Mr. Sirawat Satapimolphan, Miss Urailuk Leeruang and Miss Nattaya Sinsakulroj in Research Centre for Bioorganic Chemistry for their suggestion, helping and teaching me the experimental techniques throughout this work.

Finally, I would like to express thanks to my family for their care and supports to make my study successful. Thanks are also due to everyone who has contributed suggestions and supports throughout my research.

CONTENTS

Page

Page

LIST OF TABLES

Table **Page**

Table **Page**

LIST OF FIGURES

Figure **Page**

LIST OF ABBREVIATIONS

µl	microliter
µm	micrometer
ASTM	American Standard Test Method
°C	Degree Celsius
cSt	Centistroke
°F	Degree
FFA	Free fatty acid
FT-IR	Fourier Transform Infrared Spectroscopy
g	gram
GC	Gas Chromatography
h	hour
NMR	Nuclear Magnetic Resonance Spectroscopy
kg/cm^3	Kilogram per cubic metre
L	Liter
MJ/kg	Millijule per kilogram
min	Minute
mg	Miligram
ml	Milliter
mm	Millimeter
nm	Nanometer
ppm	parts per million
rpm	Revolution per minute
v/v	Volume by volume
w/v	Weight by volume
%wt	percent weight
δ_H	Chemical shift of ^{1}H NMR
CP	Cloud point
PP	Pour point
PPDs	Pour Point Depressants

SME	Soybean methyl ester
PME	Palm methyl ester
DMS	Dimethyl succinate
DMAD	Dimethyl adipate
DMAZ	Dimethyl azelate
DMP	Dimethyl phthalate
DIS	Diisopropyl succinate
DIAD	Diisopropyl adipate
DIAZ	Diisopropyl azelate
DIP	Diisopropyl phthalate
DBS	Di 2-butyl succinate
DBAD	Di 2-butyl adipate
DBAZ	Di 2-butyl azelate
DBP	Di 2-butyl phthalate
DES	Di 2-ethylhexyl succinate
DEAD	Di 2-ethylhexyl adipate
DEAZ	Di 2-ethylhexyl azelate
DEP	Di 2-ethylhexyl phthalate

CHAPTER I

INTRODUCTION

Numerous researches on renewable energy sources have become crucial due to the decreasing of fuel and increased pollution from burning of fossil fuel. Among all renewable and alternative energies, biodiesel fuel is one of the most representative fuels. Biodiesel normally referred to fatty acid methyl ester (FAME). Common vegetable oils and animal fats as well as used frying oils and fats can be transesterified with anhydrous alcohol, especially methanol in the presence of an alkali catalyst to produce biodiesel [1, 2]. The advantages of using biodiesel include that it is biodegradable and it can be used without modifying existing engines helping to produce less harmful gas emissions such as sulfur oxide, resulting in toxicity reduction and environmental friendly. However, one major technical problem confronting the use of biodiesel fuel is its poor cold flow properties in comparison with fossil-based diesel fuel [3]. The crystallization temperature of biodiesel fuel is generally higher than that of fossil-based diesel fuel, so the formation of crystals at relatively high temperatures can plug fuel lines and filters, causing problems in fuel pumping and engine performance during cold temperature operation. The biodiesel is composed of both saturated fatty acid and unsaturated fatty acid. Some previous researches have reported that biodiesel with significant amount of saturated fatty acid compounds will display higher cloud point (CP) and pour point (PP) [4]. The CP is defined as the temperature at which a cloud of wax crystals first appear in a liquid. The PP is defined as the temperature at which the fuel can no longer be poured due to gel formation. For example, the reported CP and PP of palm oil methyl ester (PME) were 21 and 19 °C respectively because palm oil consists of mainly saturated fatty acid especially 63.1% of palmitic acid. While the values for soybean oil methyl ester (SME) reported CP and PP were 0 and -2°C respectively due to soybean oil consists of mainly unsaturated fatty acid particularly 52.8% of linoleic acid. Several approaches have been attempted to improve cold-flow properties of biodiesel such as winterization process, blending biodiesel with fossil diesel fuel, preparation of fatty esters with branched chain and using of additive. The uses of additives in biodiesel are an interesting solution with simple, economical and variable methods. The additive was called Pour Point Depressants (PPDs) [5]. PPDs should be soluble in oil with an ability to co-crystallize in the growing wax crystals from the oil below its cloud point [5].

Therefore, the purpose of this research is to synthesize PPDs from dicarboxylic acid. The dicarboxylic acid is selected because its structure consists of polar and nonpolar parts which similar to the main structure of biodiesel. Thus, dicarboxylic acid ester should be soluble in biodiesel. We expect that the molecular structure of dicarboxylic acid ester will interact with biodiesel yielding the biodiesel crystallinity reduction.

1.1 Objectives of the research:

1. To synthesize pour point dispersant (PPDs) from dicarboxylic acid.
2. To improve the cold flow property of soybean and palm biodiesel by dicarboxylic acid ester.

CHAPTER II

THEORY AND LITERATURE REVIEWS

2.1 Background

The world is gradually heading toward severe energy crisis due to limited availability of fossil fuels, such as petroleum oil, natural gas and coal. Fossil oils are fuels which come from pristine animals and microorganisms. The formation of fossil oils require millions of years. These fossil fuels are classified as nonrenewable energy resources that cannot be replaced in a relatively short time after being utilized. However, people are still heavily dependent on fossil fuels for transportation, electricity generation and development. The major reason that caused the fast diminishing of energy resources is due to rapid population and industrialization growth globally. Moreover, combustion of fossil fuels contributes most to emissions of greenhouse gases, which lead to atmospheric pollution and global warming. Therefore, the search of an alternative and renewable energy source has emerged as one of the key challenges in this century in order to protect the environment and creating a sustainable world for future generation [6].

There are a lot of renewable energy sources that have been explored such as solar, hydropower, wind, wave, geothermal and nuclear energy. However, most of these energy are not economically feasible because the requirement of high capital and operating cost that has limited its usage in many countries over the world. Recently, biodiesel become as hope in the field of renewable energy because it has close similarity with conventional fossil diesel in terms of chemical structure and energy content. Moreover, modification of a diesel engine is not necessary that biodiesel is compatible with existing engine and can be blended direct with diesel fuel. Biodiesel is a promising nontoxic and biodegradable renewable fuel consisted of mono-alkyl esters of long chain fatty acids, which is produced by transesterification reaction of vegetable oils with short-chain alcohols (e.g., methanol, ethanol).

Biodiesel can be produced from a great variety of feedstock. These feed-stocks include common vegetable oils (e.g., soybean, palm, rapeseed/canola, sunflower and coconut) and animal fats (usually tallow) as well as waste oils (e.g., used frying oils) [7].

Although biodiesel has many advantages, one of the major disadvantage of biodiesel is the cold-flow properties of biodiesel may hinder its performance during cold weather. At low temperature, long chain saturated fatty acid in biodiesel nucleate and form crystals in the fuel. The crystals grow and agglomerate in size; it can restrict or block flow through fuel lines and filters. This is a challenge problem that must be resolved [8].

2.2 **Sources of biodiesel** [9]

Globally, there are more than 350 oil-bearing crops identified as potential sources for biodiesel production, soybean, rapeseed, sunflower and palm oils are among the common vegetable oils that are used in biodiesel production. The variety of feedstock for biodiesel production represents one of the most significant factors of producing biodiesel. The feedstock should fulfill two main requirements: low production costs and large production scale. The availability of feedstock for producing biodiesel depends on the regional climate, geographical locations, local soil conditions and agricultural practices of each country (Figure 2.1). Selecting the cheapest feedstock is necessary to ensure low production cost of biodiesel. Another factor to consider any feedstock as a biodiesel source, the oil percentage and the yield per unit area are important parameters. The problem of using feedstock, more than 95% of the world biodiesel is produced from edible oils such as rapeseed, sunflower oil, palm oil and soybean oil. Therefore, biodiesel production has shifted to other alternative feedstock such as waste frying oil (WFO) and nonedible oil (e.g., jatropha curcas, karanja and microalgae). Nevertheless, the use of WFO and nonedible oil also has a problem due to high free fatty acid (FFA) content that complicates in biodiesel processing steps.

Figure 2.1 Source of biodiesel around the word.

2.3 Triglyceride

Nearly all the commercially important fats and oils of animal and plant origin consist almost exclusively of the simple lipid class - triglyceride. The structure of triglyceride was shown in Figure 2.1. These include all the vegetable oils and animal fats. Triglycerides are made up of long chain fatty acids attached to glycerol, which is a type of alcohol. Each triglyceride contains one glycerol and three long chain fatty acids that there are many kinds of free fatty acid (R', R'' and R'''). The common fatty acid was shown in Table 2.1.

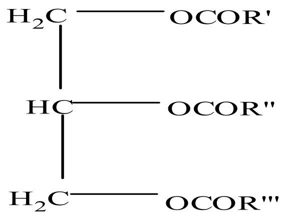

$$\begin{array}{ll} H_2C & \text{—— OCOR'} \\ | & \\ HC & \text{—— OCOR''} \\ | & \\ H_2C & \text{—— OCOR'''} \end{array}$$

Figure 2.2 Structure of a triglyceride.

In the Table 2.1, the chains of fatty acid differ in the number of carbon atoms and the number of double bonds in the chain. These double bonds show an important part in the stability of biodiesel. Biodiesel is not hydrocarbons because oxygen atoms are present in its structure while petro-diesel is true hydrocarbons, made up only of molecules of hydrogen and carbon.

Table 2.1 The common fatty acids in triglyceride. [10]

Fatty acid	**Systermatic name**	**Structure**	**Formular**
Lauric	Dodecanoic	12:0	$C_{12}H_{24}O_2$
Myristic	Tetradecanoic	14:0	$C_{14}H_{28}O_2$
Palmitic	Hexadecanoic	16:0	$C_{16}H_{32}O_2$
Stearic	Octadecanoic	18:0	$C_{18}H_{36}O_2$
Arachidic	Eicosanoic	20:0	$C_{20}H_{40}O_2$
Behenic	Docosanoic	22:0	$C_{22}H_{44}O_2$
Lignoceric	Tetracosanoic	24:0	$C_{24}H_{48}O_2$
Oleic	cis-9-Octadecenoic	18:1	$C_{18}H_{34}O_2$
Linoleic	cis-9,cis-12Octadecadienoic	18:2	$C_{18}H_{32}O_2$
Linolenic	cis-9,cis-12,cis-15-Octadecatrienoic	18:3	$C_{18}H_{30}O_2$
Erucic	cis-13-Docosenoic	22:1	$C_{22}H_{42}O_2$

The physical and chemical fuel properties of biodiesel commonly depend on the fatty acids distribution of the triglyceride used in the production. The fatty acid distributions of some feedstock for biodiesel production were shown in Table 2.2.

Table 2.2 Chemical composition of vegetable oils. [9]

Feedstock	**Fatty acid composition (%wt)**						
	12:0	**14:0**	**16:0**	**18:0**	**18:1**	**18:2**	**18:3**
Sunflower	-	-	6.08	3.26	16.93	73.73	-
Rapeseed	-	-	3.49	0.85	64.40	22.30	8.23
Soybean	-	-	10.58	4.76	22.52	52.34	8.19
Palm	-	1	42.8	4.5	40.5	10.1	0.2

Feedstock	**Fatty acid composition (%wt)**						
	12:0	**14:0**	**16:0**	**18:0**	**18:1**	**18:2**	**18:3**
Coconut	46.5	19.2	9.8	3	6.9	2.2	-
Soybean soapstock	-	-	17.2	4.4	15.7	55.6	7.2
Used frying oil	-	-	12	-	53	33	1
Tallow	-	3-6	24-32	20-25	37-43	2-3	-
Lard	-	1-2	28-30	12-18	4-50	7-13	-

Some properties of vegetable oil were shown in Table 2.3. The kinematics viscosity of vegetable oils varies in the range of 31–40 cSt. These oils have high viscosity due to large molecular weight and complex chemical structure of vegetable oil.

Table 2.3 Some properties of vegetable oil. [11]

Vegetable Oil	**Kinematic viscosity**	**Cetane number**	**Heating value (MJ/kg)**	**Cloud point (°C)**	**Pour point (°C)**	**Flash point (°C)**	**Density (Kg/l)**	**Carbon residue (wt%)**
Corn	34.9	37.6	39.5	−1.1	−40.0	277	0.9095	0.24
Cotton seed	33.5	41.8	39.5	1.7	−15.0	234	0.9148	0.24
Crumble	53.6	44.6	40.5	10.0	−12.2	274	0.9044	0.23
Linseed	22.2	34.6	39.3	1.7	−15.0	241	0.9236	0.22
Peanut	39.6	41.8	49.8	12.8	−6.7	271	0.9026	0.24
Rapeseed	37.0	37.6	39.7	−3.9	−31.7	246	0.9115	0.30
Safflower	31.3	41.3	39.5	18.3	−6.7	260	0.9114	0.25
Sesame	35.5	40.2	39.3	−3.9	−9.4	260	0.9133	0.25
Soybean	32.6	37.9	39.6	−3.9	−12.2	254	0.9138	0.27
Sunflower	33.9	37.1	39.6	7.2	−15.0	274	0.9161	0.23
Palm	39.6	42.0	—	31.0	—	267	0.9180	—
Tallow	—	—	40.0	—	—	201	—	6.21

The problems associated with using straight vegetable oil in diesel engines were classified into short term and long term. The problems, probable causes and the potential solutions of using vegetable oil were shown in Table 2.4. The major problems of using direct vegetable were high viscosity, low volatility, acid composition, gum formation due to oxidation and polymerization during storage and combustion, poor cold engine start-up, ignition delay, incomplete combustion, ring sticking, injector choking in engine and lubricating oil thickening. Therefore the chemical modification of vegetable oil was essential for using in diesel engine.

Table 2.4 Problems, probable cause and potential solutions for using straight vegetable oil in diesel engines. [12]

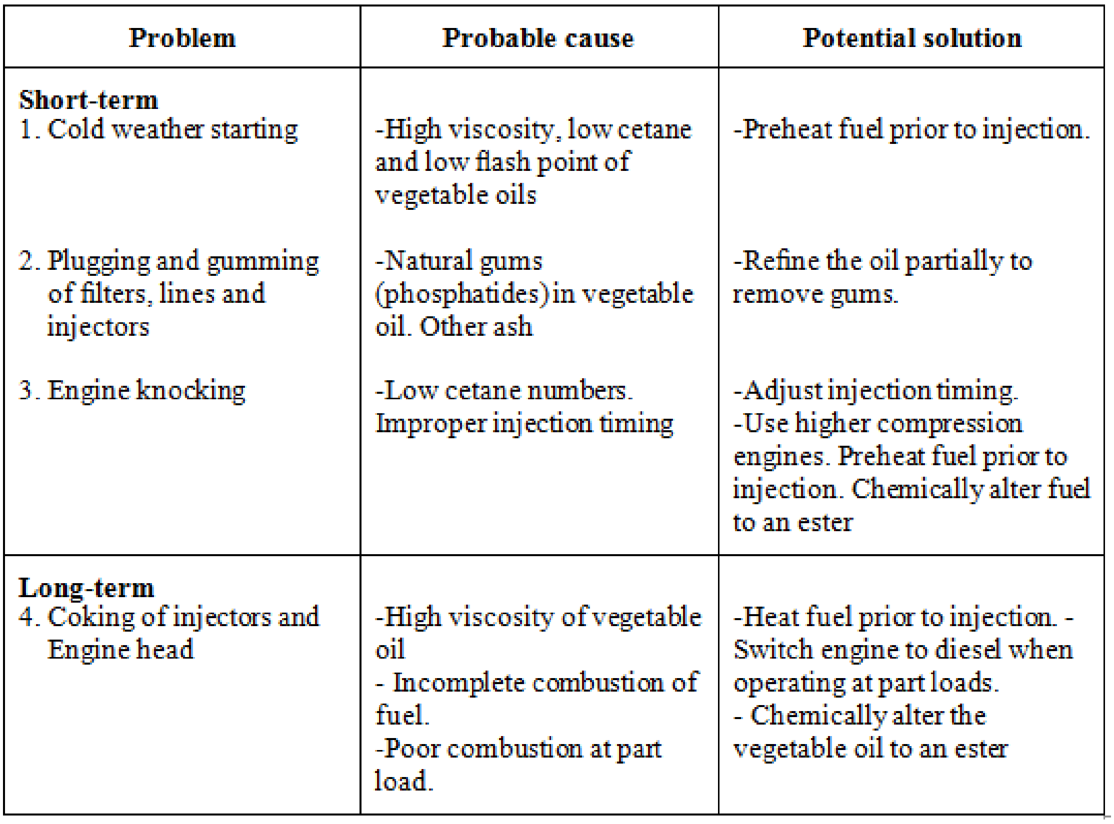

Problem	Probable cause	Potential solution
Short-term 1. Cold weather starting	-High viscosity, low cetane and low flash point of vegetable oils	-Preheat fuel prior to injection.
2. Plugging and gumming of filters, lines and injectors	-Natural gums (phosphatides) in vegetable oil. Other ash	-Refine the oil partially to remove gums.
3. Engine knocking	-Low cetane numbers. Improper injection timing	-Adjust injection timing. -Use higher compression engines. Preheat fuel prior to injection. Chemically alter fuel to an ester
Long-term 4. Coking of injectors and Engine head	-High viscosity of vegetable oil - Incomplete combustion of fuel. -Poor combustion at part load.	-Heat fuel prior to injection. -Switch engine to diesel when operating at part loads. - Chemically alter the vegetable oil to an ester

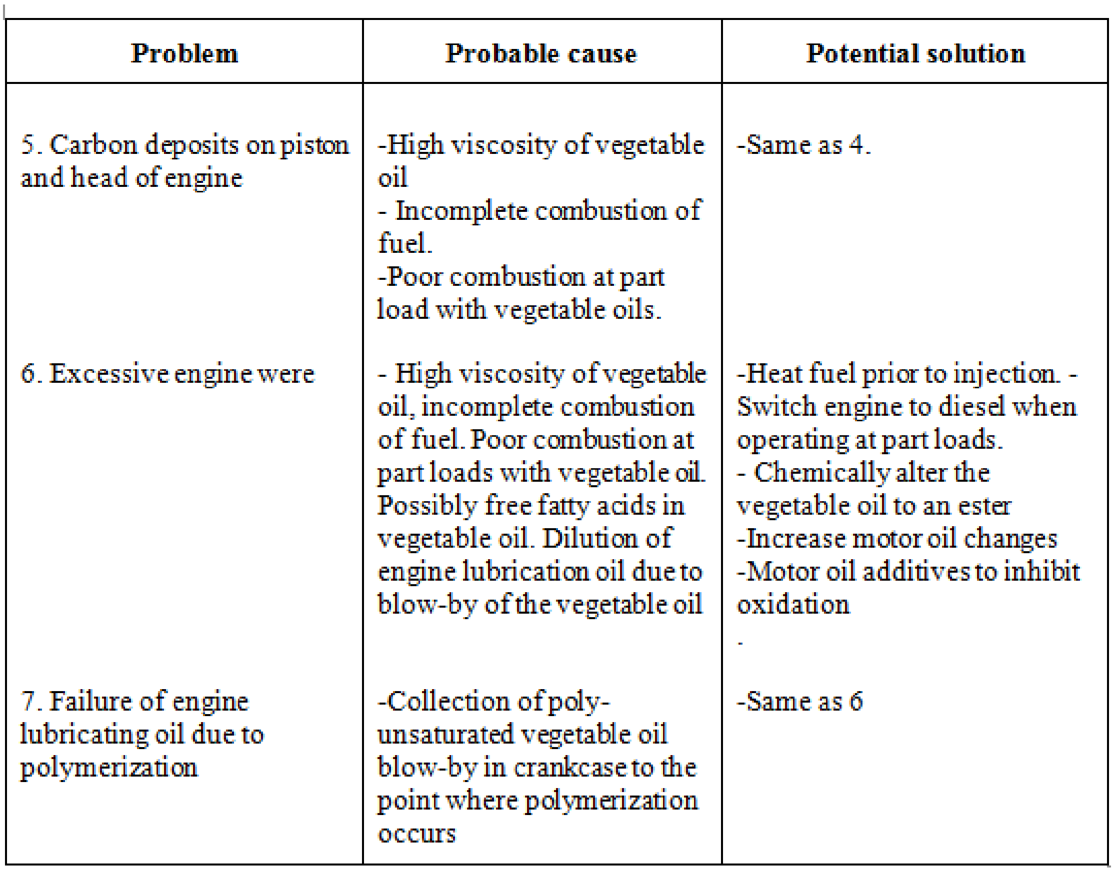

Problem	Probable cause	Potential solution
5. Carbon deposits on piston and head of engine	-High viscosity of vegetable oil - Incomplete combustion of fuel. -Poor combustion at part load with vegetable oils.	-Same as 4.
6. Excessive engine were	- High viscosity of vegetable oil, incomplete combustion of fuel. Poor combustion at part loads with vegetable oil. Possibly free fatty acids in vegetable oil. Dilution of engine lubrication oil due to blow-by of the vegetable oil	-Heat fuel prior to injection. - Switch engine to diesel when operating at part loads. - Chemically alter the vegetable oil to an ester -Increase motor oil changes -Motor oil additives to inhibit oxidation -
7. Failure of engine lubricating oil due to polymerization	-Collection of poly-unsaturated vegetable oil blow-by in crankcase to the point where polymerization occurs	-Same as 6

2.4 Biodiesel production [13, 14]

Vegetable oils are unsuitable as fuel for diesel engine. Considerable efforts have been made to develop vegetable oil for it had properties and performance like diesel fuels. The problem with using triglycerides for diesel fuel is mostly associated with high viscosity, low volatility and polyunsaturated characters. So the chemical structures of vegetable oil must be modified. Production of biodiesel can be performed at least four ways:

- Direct use and blending (dilution)
- Micro-emulsion
- Pyrolysis (Thermal cracking)
- Transesterification

2.4.1 Direct use and blending [15]

The vegetable oil is diluted with fossil fuel to run the engine. In 1980, Caterpillar Brazil used the mixture of 10% vegetable oil to maintain total power without any alteration or adjustment to the engine. At that point it was not practical to substitute 100% vegetable oil for diesel fuel. This experiment used up to a 50% of vegetable oil with diesel fuel. When blending of 20% vegetable oil and 80% diesel fuel was successful. The lower viscosity is good for performance of engine that viscosity can reduced when the percentage of diesel increased. Direct use of vegetable oils or the use of blends of the oils has normally been considered to be not satisfactory and impractical for both direct and indirect diesel engines. The problems of this method are still high viscosity, low volatility, reactivity of unsaturated hydrocarbon chains and low cetane number.

2.4.2 Micro-emulsions [13, 16]

A micro emulsion is define as a colloidal equilibrium dispersion of optically isotropic fluid microstructure with dimensions generally in the range of 1–150, formed spontaneously from two normally immiscible liquids. Micro-emulsion is method to solve the problem of the high viscosity of vegetable oils by blending oils with solvents such as simple alcohols e.g., methanol, ethanol and 1-butanol. In 2001, Ali studies on the use of hybrid fuels, formed by ethanol with soybean oil. These emulsions were evaluated by burning in a diesel engine. The fuels performed nearly as well as diesel, but lower cetane numbers and less energy content. However, the hybrid fuels are too expensive to compete with diesel fuel. The advantage of this method gives spray patterns during combustion better than diesel.

2.4.3 Pyrolysis [13,15]

Pyrolysis is a process of conversion of substance into another by heating in the absence of air or oxygen and cleavage of chemical bonds to yield small molecule with the help of the catalyst. Many researchers have studied the pyrolysis of triglycerides to obtain products suitable for diesel engines. Thermal decomposition or pyrolysis of triglycerides produces the compounds such as alkanes, alkenes, alkynes and carboxylic acids. The products from this method are chemically similar to petroleum-derived gasoline and diesel fuel, but pyrolysis process is high cost.

2.4.4 Transesterification [17, 18, 19, 20]

Transesterification (also called alcoholysis) is the most general process to produce biodiesel. Transesterification is the reaction of triglyceride in animal fat or vegetable oil with an alcohol to form fatty acid mono alkyl esters and glycerol as by product. A catalyst is usually used to improve the reaction rate and percentage yield. Alcohol that can be used in the transesterification process are methanol, ethanol, propanol, and butanol. Methanol and ethanol are used most frequently, especially methanol because it low cost and its physical and chemical advantages (polar and shortest chain alcohol) result in it can quickly react with triglycerides. Commonly, the relation between alcohol and oil is 3:1 but excess alcohol is used to push the equilibrium toward the product because of reversible nature of reaction. Transesterification is the most viable process for reduce viscosity of oils. The simplified form of transesterification reaction is represented in Figure 2.3.

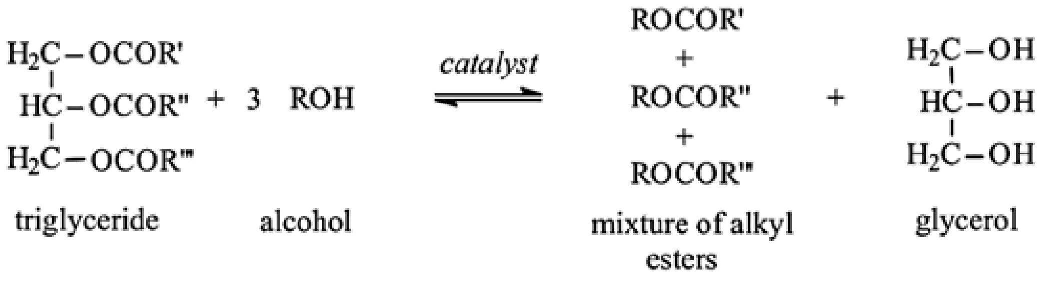

Figure 2.3 Transesterification of vegetable oils.

2.4.4.1 Transesterifcation kinetics and mechanism

The mechanism of transesterification is described in Figure 2.4. The first step is the conversion of triglycerides to diglycerides followed by the conversion of diglycerides to monoglycerides and the conversion of monoglycerides to glycerol yielding one alkyl ester molecule in each step. The step wise reactions are reversible and excess of alcohol is used to shift the equilibrium towards the formation of methyl esters. In presence of excess alcohol, the foreword reaction is pseudo-first order while the reverse reaction is found to be second order. The catalyst of transesterification reaction can be both homogeneous such as acids, alkalis, enzymes, non-ionic base and heterogeneous catalysts. In addition, noncatalytic process has been interested and it was developed to transesterification without using catalyst.

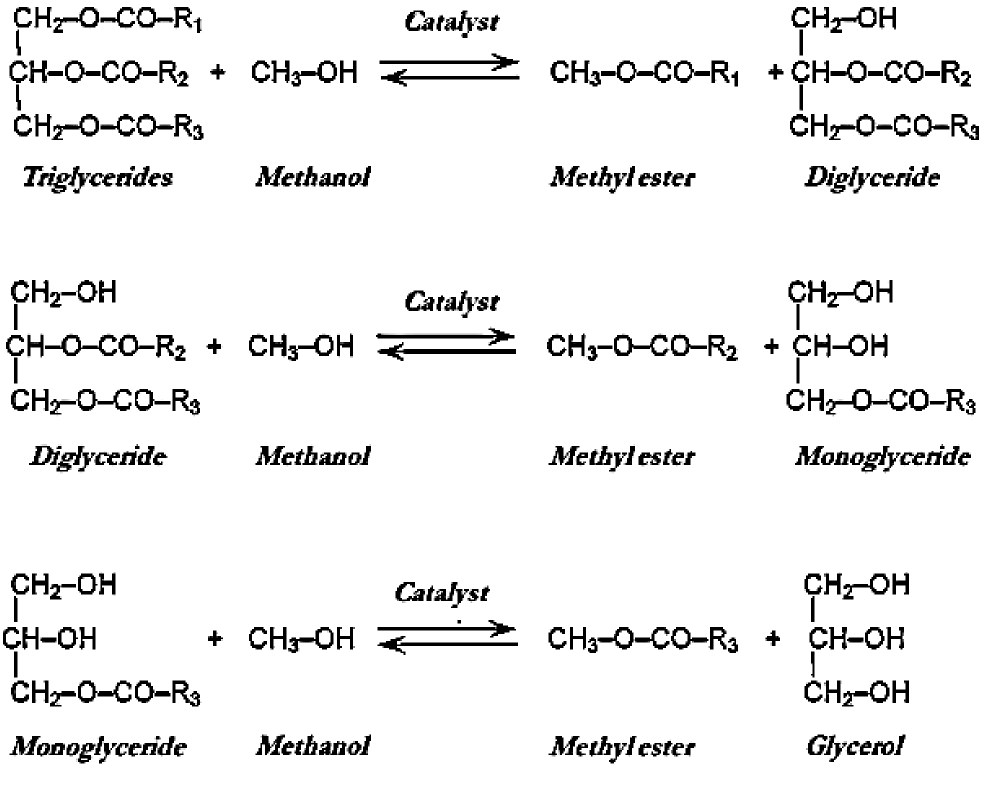

Figure 2.4 Transsesterification reaction step.

2.5 Type of catalysts in transesterification

2.5.1 Acid-catalyzed processes [21]

Acids are used for transesterification reaction in biodiesel production. Sulfuric acid, sulfonic acids, and hydrochloric acids are the usual acid catalysts but the most commonly used sulfuric acid. The advantages of using acid-catalyzed are insensitive to the presence of free fatty acid in vegetable oil or animal fat and it can catalyze esterification and transesterification simultaneously. However, acid-catalyzed system is not a popular for commercial applications because slower reaction rate, requirement of high reaction temperature, high molar ratio of alcohol to oil, separation of the catalyst, and corrosion related problem.

The steps involved during acid-catalyzed transesterification are shown in Figure 2.5. The carbonyl group of the ester is protonated by proton of acid lead to the carbocation, which after a nucleophilic attack of the alcohol produces a tetrahedral intermediate. This intermediate eliminates glycerol to form a new ester and to regenerate the catalyst. Acid-catalyzed transesterification should be carried out in the absence of water, in order to avoid the competitive formation of carboxylic acids which reduce the yields of alkyl esters.

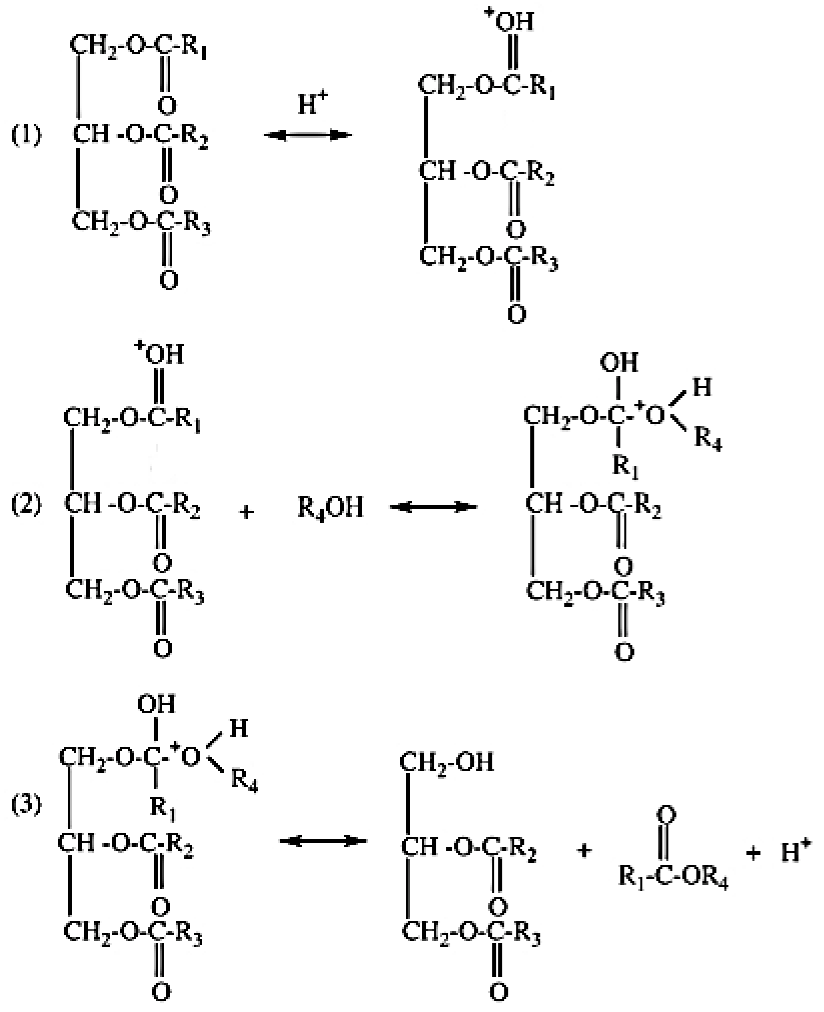

R_1,R_2,R_3: Carbon chain of fatty acid
R_4: Alkyl group of the alcohol

Figure 2.5 Mechanism of acid-catalyzed transesterification.

2.5.2 Alkaline-catalyzed processes [21]

Most of the commercial biodiesel is produced from oils using very effective alkali catalysts such as sodium or potassium hydroxides, carbonates or alkoxides. Application of alkali-catalyzed transesterification reaction provides faster rate, nearly 4000 times faster than that is catalyzed by the same amount of an acid catalyst and good corrosion resistance properties than acid catalyst. However, the alkali catalyzing process is very sensitive to the presence of water and free fatty acids in feedstock. When feedstocks have a high percentage of free fatty acids, the alkali catalyst will react with the free fatty acids to form soaps. The water in feedstock can hydrolyze the triglycerides into diglycerides and form more free fatty acids. Both of the reactions are reduce the yield of the biodiesel product. Moreover, the alkali catalysts need to neutralized, giving rise to wastewater and glycerol is obtained as an aqueous solution of relatively low purity.

The mechanism of alkali-catalyzed transesterification is described in Figure 2.6. The alkoxide ion is created initially and directly acts as a strong nucleophile, after that alkoxide ion attack on the carbonyl carbon of triglyceride to form a tetrahedral intermediate and then the rearrangement of the tetrahedral intermediate gives fatty acid ester and diglyceride.

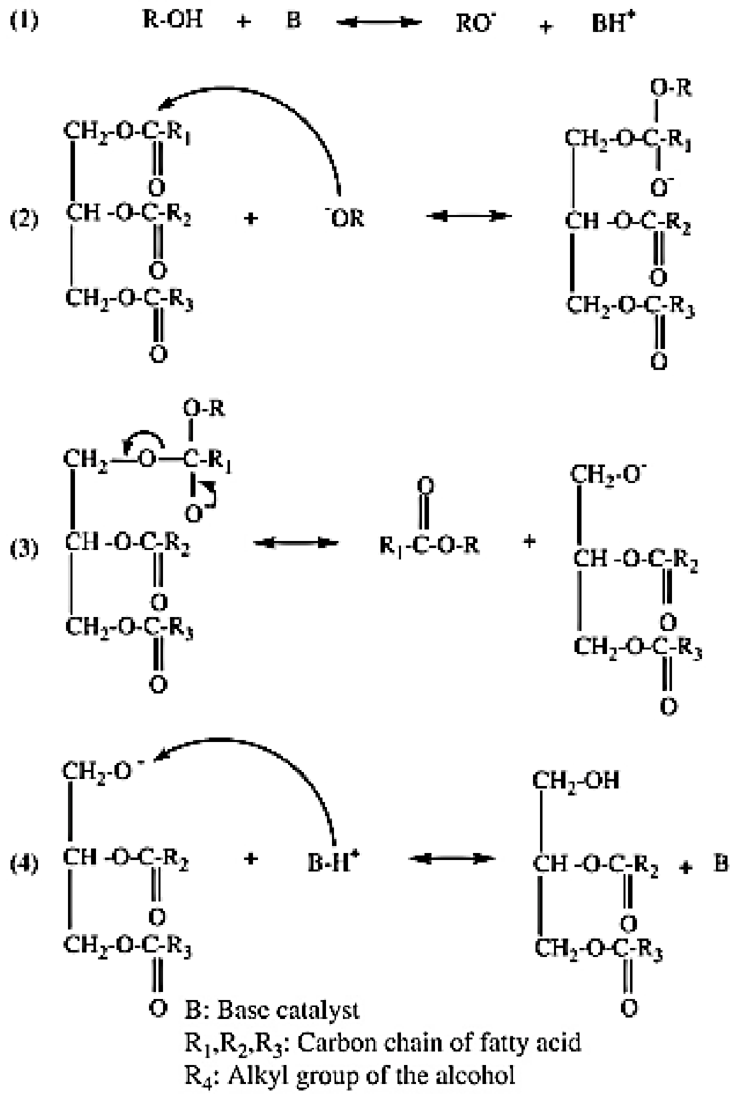

B: Base catalyst

R_1,R_2,R_3: Carbon chain of fatty acid

R_4: Alkyl group of the alcohol

Figure 2.6 Mechanism of alkaline-catalyzed transesterification.

2.5.3 Enzyme-catalyzed processes [22]

Enzymatic transesterification is interesting process due to the problem from using chemical transesterification. A lot of wastewater generation and difficulty in glycerol recovery are problems that eventually increase the overall biodiesel production cost and being not environmentally friendly. In contrast, enzyme catalysis process without the generation of by-products, easy recovery of product, mild reaction condition, insensitive to high free fatty acid of oil and catalyst can be reuse.

Lipase has been discovered that it can be used as catalyst for tranesterification and esterification due to its biocompatibility, biodegradability and environmental acceptability of the biotechnical procedure. However, enzyme-catalyzed still has disadvantage such as high cost of enzyme, slow reaction rate and enzyme deactivation.

2.5.4 Heterogeneously catalyzed processes [21]

The advantages of using heterogeneous catalyst are fast and easy separation from the reaction mixture without requiring the use of neutralization agent and do not formation soaps. Moreover heterogeneous catalyst can be regenerated and reused, and it has a less corrosive character, leading to safer, cheaper and more environment-friendly operation. Therefore, there is an increasing interest in the possibility of replacing the homogeneous catalyst by heterogeneous solid catalysts. The examples for heterogeneous catalysts are alkali earth or transition metal oxides such as CaO, MgO, BaO and ZnO/Al_2O_3, alkaline metal oxides supported on zeolites and MCM-41, ion exchange resins such as clay minerals with acidic reaction sites and sulfated metal oxides such as ferric sulfate ($Fe_2(SO_4)_3$).

Nevertheless it also has several drawbacks because it requires high temperatures and high pressures in the reaction, using solid support tend to show less activity than the active species in solution and leaching of catalyst active sites may result to product contamination.

2.5.5 Noncatalytic transesterification processes [23, 24, 25]

Transesterification in supercritical reaction conditions is used for catalyst-free biodiesel synthesis. In this condition, the solution between methanol and oil becomes a single homogeneous phase. Seeing that its nature, hydrophobic with a lower dielectric constant of supercritical alcohol resulting in non-polar triglycerides can be well solvated with supercritical methanol to form single phase oil to methanol mixture. It accelerates the reaction because there is no interphase mass transfer to limit the reaction rate. The non-catalytic supercritical process has environmental advantages due to there is no waste generated as a result of catalyst treatment and separation from the final product. Furthermore, this method requires no pretreatment of the feedstock because impurities do not strongly affect the reaction. When water and free fatty acid are present, transesterification, triglyceride hydrolysis and alkyl esterification of fatty acids occur simultaneously. Alkyl esterification is faster than transesterification and ensures that all free fatty acid feedstock are completely transformed into fatty acid alkyl esters. The separation of the biodiesel product and glycerol by product is simple because the products are not miscible in biodiesel. In addition, in this non-catalyzed process, there is no soap formation. However, high temperature, high pressure and high alcohol to oil ratio are required in this process.

2.6 Biodiesel quality

Biodiesel is a technologically possible alternative to fossil diesel. Table 2.5 shows the fuel ASTM standards of biodiesel and petroleum diesel fuels. The characteristics of biodiesel are close to petroleum diesel.

The standard of biodiesel in Thailand is described the minimum requirements for biodiesel. Table 2.6 shows characteristics and quality of biodiesel in Thailand.

Table 2.5 Comparison of fuel properties between diesel and biodiesel. [26, 27, 28, 29]

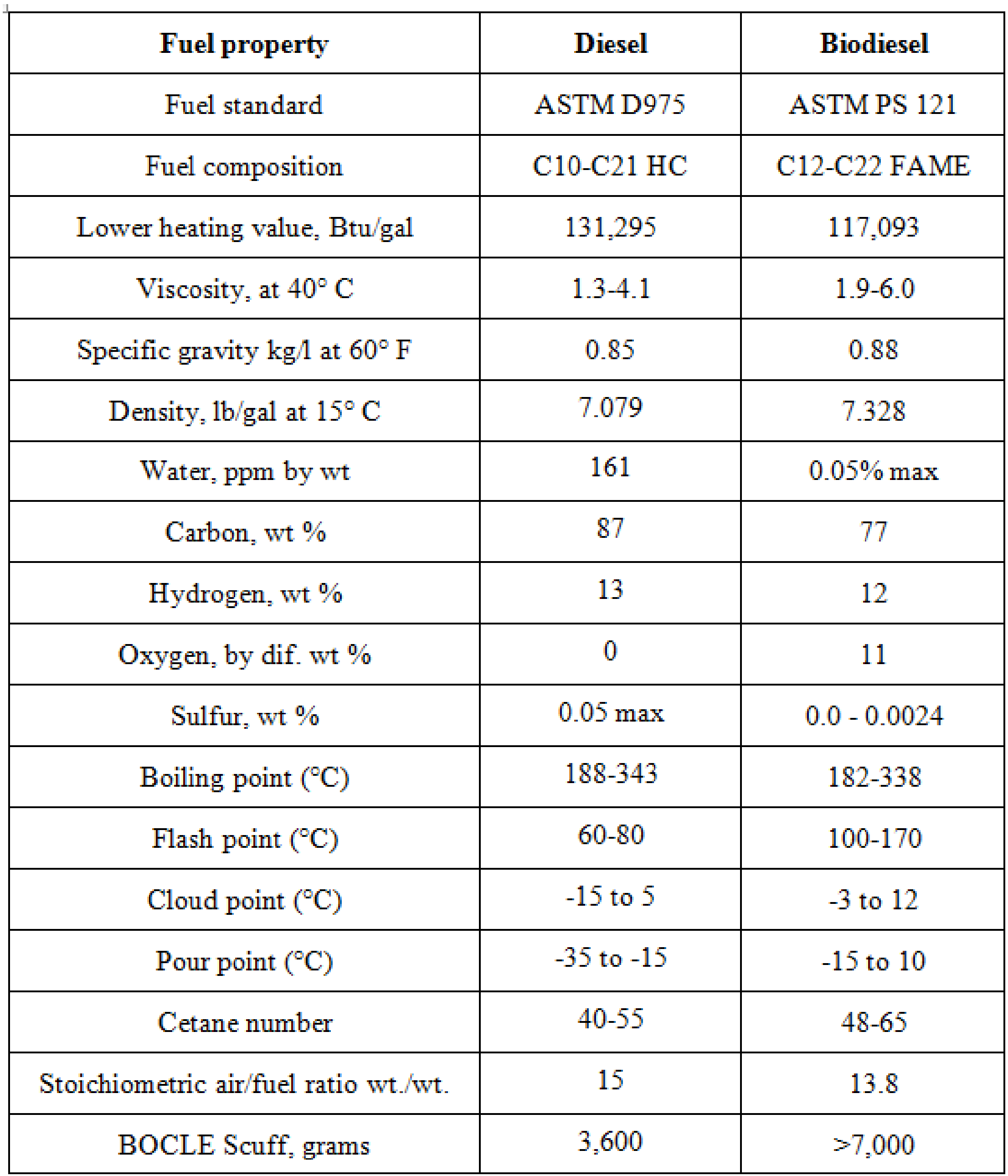

Fuel property	Diesel	Biodiesel
Fuel standard	ASTM D975	ASTM PS 121
Fuel composition	C10-C21 HC	C12-C22 FAME
Lower heating value, Btu/gal	131,295	117,093
Viscosity, at 40° C	1.3-4.1	1.9-6.0
Specific gravity kg/l at 60° F	0.85	0.88
Density, lb/gal at 15° C	7.079	7.328
Water, ppm by wt	161	0.05% max
Carbon, wt %	87	77
Hydrogen, wt %	13	12
Oxygen, by dif. wt %	0	11
Sulfur, wt %	0.05 max	0.0 - 0.0024
Boiling point (°C)	188-343	182-338
Flash point (°C)	60-80	100-170
Cloud point (°C)	-15 to 5	-3 to 12
Pour point (°C)	-35 to -15	-15 to 10
Cetane number	40-55	48-65
Stoichiometric air/fuel ratio wt./wt.	15	13.8
BOCLE Scuff, grams	3,600	>7,000

*The SL-BOCLE was developed by modifying the existing instrument (BOCLE) at SWI that had been used to measure the lubricity of jet fuel.

Table 2.6 Characteristic and quality of biodiesel in Thailand. [30]

Characteristic	**Value**	**Method of standard**
Methyl ester, %wt.	>96.5	EN 14103
Density at 15°C, kg/m^3	860-900	ASTM D 1298
Viscosity at 40°C, cSt	3.5-5.0	ASTM D445
Flash point, °C	>120	ASTM D 93
Carbon residue, on 10% distillation residue, %wt	<0.30	ASTM D 4530
Cetane number	>51	ASTM D 613
Sulfur, %wt.	<0.0010	ASTM D 2622
Sulfated ash, %wt.	<0.02	ASTM D 874
Water, %wt.	<0.050	ASTM D 2709
Total contaminate, %wt.	<0.0024	ASTM D 5452
Copper strip corrosion	<96.5	ASTM D 130
Oxidation stability at 110°C, h	>6	EN 14112
Acid value, mg KOH/g	<0.50	ASTM D 664
Iodine value, g Iodine/100 g	<120	EN 14111
Linolenic acid methyl ester, %wt.	<12.0	EN 14103
Methanol, %wt.	<0.20	EN 14110
Monoglyceride, %wt.	<0.80	EN 14105
Diglyceride, %wt.	<0.20	EN 14105
Triglyceride, %wt.	<0.20	EN 14105
Free glycerin, %wt.	<0.02	EN 14105
Total glycerin, %wt.	<0.25	EN 14105
Group I metals (Na+K)	<5.0	EN 14108 and EN 14109
Group II metals (Ca+Mg)	<5.0	EN 14538
Phosphorus, %wt.	<0.0010	ASTM D 4951

2.7 Cold flow property [10, 31, 32, 33]

Although most of the properties of biodiesel fuels are compared with diesel fuel but the flow properties of a biodiesel are very poor. Cold flow properties of fuel are usually characterized by the following four temperature measures.

1. Cloud point (CP)

The cloud point, which commonly occurs at a higher temperature than the pour point. Could point is the temperature at which liquid oil becomes cloudy or the first wax crystal is appeared in oil. The standard method to test cloud point of petroleum products is ASTM D2500.

2. Pour point (PP)

Pour point is the temperature at which the amount of wax out of solution is sufficient to fuel oil become gel, so it is the lowest temperature at which the fuel can flow. The standard method to test pour point of petroleum products is ASTM D97.

3. Cold filter plugging point (CFPP)

Cold filter plugging point (CFPP) refers to the temperature that the test filter starts to plug due to fuel components have started to gel or crystallize. The standard method to test cold filter plugging point of petroleum products is ASTM 6371.

4. Low temperature flow test (LTFT)

The low temperature flow test (LTFT) is a minimum temperature, at which 40 mL of oil safely passes through the filter within 60 s. The standard method to test low temperature flow of petroleum products is ASTM D4539-03.

The cold flow properties of biodiesel must be evaluated before they will be viable as alternative diesel fuel. The cold-flow properties of biodiesel may hinder its performance during cold weather. So there are many approaches for improving the cold-flow properties of biodiesel such as blending of biodiesel with conventional diesel fuel, winterization, preparation of biodiesel with branched/bulky in the chain and using of chemical additives.

2.7.1 The improvement of cold flow property [2, 11, 34]

1. Blending of biodiesel with conventional diesel fuel

Blending the biodiesel with petroleum diesel will reduce the fraction of saturated long-chain methyl esters in the mixture, which is reflected in improved low temperature characteristics of the fuel. This method is the simplest way.

2. Winterization

Winterization is used to reduce cold flow properties of biodiesel by removing saturated compound. Winterization is a method for separating of saturated fraction in oils with a solidification temperature. However, the problem of this process is low yield due to large blockage of crystals with the liquid.

3. Preparation of fatty esters with branched /bulky in the chain

The other possibility of improving cold flow properties of biodiesel is the synthesis, which branch chain such as *i*-propyl, *i*-butyl and 2-butyl instead of the methyl and synthesis of biodiesel with bulky substituent into the chain. A hypothesis exists that the branched chain and bulky substituent disrupts the regularity during the solid phase formation and the orientation in one direction.

4. Use of chemical additives

Treatment with chemical additives is the most convenient and economical way of improving the low temperature properties of fuel. When adding chemical additives, cloud point and pour point of fuels should be reduced. This technology is also very interesting in the biodiesel industry when compare with other methods.

2.8 Pour Point Depressants (PPDs) [5, 34]

The chemical additives for improving cold flow properties of biodiesel are called pour point depressants. The molecules of additives should be soluble in oil and contain with function groups, which prevent the crystal growth and agglomeration. The advantages of adding pour point depressant are simplicity and economy.

Figure 2.7 shows the major structure of pour point depressant; PPDs consist of two parts which are polar part and paraffin like part (non-polar part). Commonly, at or below the cloud point, the paraffin like part of pendant chains of the PPDs creates nucleation site and co-crystallizes with wax crystals, while the polar part of PPDs creates a barrier to the formation of interlocking wax network. Therefore PPDS can be prevented the crystal growth and agglomeration of wax crystal in oil result in a reduced cloud point and pour point.

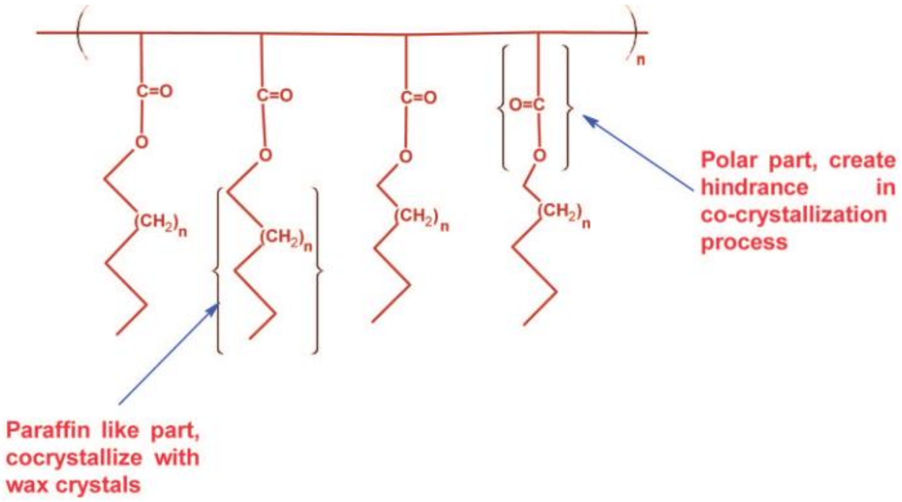

Figure 2.7 Characteristic structure of the general PPDs polymer additive.

2.9 Literature reviews

In 2006, Meher *et al.* [35] studied the transesterification for producing biodiesel from Karanja seeds by using potassium hydroxide as catalysts. The result showed that concentration of catalyst, molar ratio of the oil to alcohol, reaction time and reaction temperature had an effect to the transesterification reaction. The maximum yield of methyl ester was 97-98%, with 1:6 molar ratio of methanol: oil, 1 %wt of potassium hydroxide, 2 h and 65°C.

In 2007, Sern *et al.* [36] studied the effect of polymers and surfactants for improving the cold flow properties of palm oil methyl ester that the 12 type of compounds are various polarities, molecular size and structure. The results showed that seven out of the twelve polymeric compounds tested were miscible in palm oil methyl esters due to similar polarities of the compounds and biodiesel. From all compounds, poly (maleic anhydride-*alt*-1-octadecene) gave the best result. The pour point of palm oil methyl ester was reduced from 12 °C to 6 °C when 2 %wt of compound was added. The cloud point was reduced from 12.9 °C to 8.1 °C, and the cold filter plugging point was reduced from 12°C -7 °C.

In 2007, Soldi *et al.* [37] studied the synthesis of methacrylate copolymer for reducing the pour point of diesel oil. First step alkyl methacrylate monomer was synthesized by transesterification of methyl methacrylate with C_{14}, C_{16} and C_{18} fatty alcohol. Next, the copolymerization of these monomers with methyl methacrylate was performed, with molar ratios of 30:70, 50:50 and 70:30 for alkyl methacrylate: methyl methacrylate. 70% of octadecyl methacrylate with 30% of methyl methacrylate was shown the best performance. The pour point of diesel oil could be reduced 22 °C.

In 2009, Al-Sabagh *et al.* [38] studied synthesis of pour point depressants from styrene-maleic anhydride copolymer by reacted with alcohol which contain carbon 8, 12, 16 and 18 atoms to improve pour point of waxy crude oil. The result showed that, at 10000 ppm of long-branched chain (C18) gave maximum reduction (27°C to -3°C) while short-branched chain (C8) showed minimum reduction (27°C to 6°C). The efficiency of pour point depressant depends on branched chain length of alcohol.

In 2010, Panlek *et al.* [39] studied improving cold flow properties of biodiesel from Irvingia malayana Oliv. ex A. Benn by using four synthesized pour point depressants which were methyl laurate, methyl stearate, isopropyl laurate and isopropyl stearate. The results showed that isopropyl laurate gave the best efficiency. At 500,000 ppm of isopropyl laurate, the cloud point of biodiesel was reduced 8.70 °C and the pour point was reduced 9.0 °C. The branched chain of pour point depressant could prevent crystallisation. Furthermore, this research used commercial additives which were CD017, Zenith, Flozol 2251D, Flozol 112 and kerosene for improving cold flow properties of biodiesel. The results showed that kerosene gave the best result on reducing CP and PP of biodiesel.

In 2011, Joshi *et al.* [40] studied the effect of ethyl levulinate on cold flow properties of biodiesel from cottonseed oil and poultry fats. Both of biodiesesl were extremely poor low flow properties due to their high saturated fatty acid content. The could point and pour point of both biodiesel were decreased when the concentration of ethyl levulinate was increased, reductions of 4-5 °C in could point and 3-4 °C in pour point were observed at 20 vol % of ethyl levulinate. This may attribute to the low freezing point of ethyl levulinate (-79 °C), which was much lower than the CP values observed from cottonseed oil methyl ester (5 °C) and poultry fat methyl ester (8 °C).

CHAPTER III

EXPERIMENTAL

3.1 Materials and equipments

3.1.1 Raw materials

1. Cooking soybean oil
2. Palm biodiesel was obtained from Verasuwan CO., Ltd.

3.1.2 Chemicals

1. Adipic acid: analytical grade; Sigma-Aldrich
2. Azelaic acid: analytical grade; Sigma-Aldrich
3. 2-Butanaol: analytical grade; Merck
4. Chloroform-D: NMR spectroscopy grade; Merck
5. Cyclohexane: analytical grade; Merck
6. Dodecanoic acid: analytical grade; Sigma-Aldrich
7. Ethanol: analytical grade; Merck
8. Ethyl acetate: analytical grade; Lab-Scan
9. 2-Ethyl-1-hexanol: analytical grade; Merck
10. Heptane: analytical grade; Merck
11. Hexane: analytical grade; Lab-Scan
12. Methanol: analytical grade; Merck
13. Methyl heptadecanoate: analytical grade; Fluka
14. Phthalic acid: analytical grade; Sigma-Aldrich
15. phenolphthalein indicator: analytical grade; Merck
16. potassium permanganate: analytical grade; Lab-Scan
17. Potassium hydroxide: analytical grade; Lab-Scan

18. 2-Propanol: analytical grade; Merck
19. Sodium hydrogen carbonate: analytical grade; Merck
20. Sodium hydroxide: analytical grade; Sigma-Aldrich
21. Sodium sulfate: analytical grade; Sigma-Aldrich
22. Sodium thiosulfate: analytical grade; Lab-Scan
23. Succinic acid: analytical grade; Sigma-Aldrich
24. Sulfuric acid: analytical grade; Carlo Erba
25. Toluene: analytical grade; Merck
26. Wijs solution: analytical grade; Merck

3.1.3 Equipments

1. NMR Spectrometer: Mercury (400MHz); Varian
2. Cannon Automatic Viscometer: Model CAV-3; Cannon
3. Gas-liquid Chromatography; Model 3800; Varian
4. Fourier-Transform Infrared Spectroscopy: Nicolet
5. Rotary evaporator: Model; Buchi
6. Cloud point and pour point apparatus (ASTM D-2500 and ASTM D-97

3.2 Procedures

3.2.1 Synthesis of Pour Point Depressants (PPDs)

3.2.1.1 Synthesis of dimethyl succinate (DMS), dimethyl adipate (DMAD), dimethyl azelate (DMAZ) and dimethyl phthalate (DMP) as PPDs

The dimethyl ester was synthesized via esterification by using 20:1 molar ratio of methanol to dicarboxilic acid (succinic acid, adipic acid, azelaic acid and phthalic acid) and 2 %wt of sulfuric acid was added. Then, the mixture was heated at 65°C and stirring for 10 h. The reaction mixture was subjected to concentrate under reduced pressure. The dimethyl ester was taken into hexane. The organic layer extract was washed excessively with saturated sodium bicarbonate solution ($NaHCO_3$) and deionize water. Until products had pH value similar to deionized water. The organic extract was dried over anhydrous sodium sulfate (Na_2SO_4) and concentrated under vacuum at 60 °C to give the dimethyl succinate (DMS), dimethyl adipate (DMAD), dimethyl azelate (DMAZ) and dimethyl phthalate (DMP). The products were determined acid value according to ASTM D 974. The percentage conversion and functional group of DMS, DMAD, DMAZ and DMP were analyzed by ^{1}H-NMR and FTIR. Then the product yield of DMS, DMAD, DMAZ and DMP were calculated by:

$$\text{Product yield (wt\%)} \quad = \quad \frac{\text{Weight of PPDs}}{\text{Weight of dicarboxil ic acid}} \times 100$$

3.2.1.2 Synthesis of diisopropyl succinate (DIS), diisopropyl adipate (DIAD), diisopropyl azelate (DIAZ) and diisopropyl phthalate (DIP) as PPDs.

The synthesis of diisopropyl ester was carried out as similar to section 3.2.1.1, using isopropyl alcohol instead of methanol at 83°C. The diisopropyl succinate (DIS), diisopropyl adipate (DIAD), diisopropyl azelate (DIAZ) and diisopropyl phthalate (DIP) were obtained.

3.2.1.3 Synthesis of di 2-butyl succinate (DBS), di 2-butyl adipate (DBAD), di 2-butyl azelate (DBAZ) and di 2-butyl phthalate (DBP) as PPDs.

The synthesis of di 2-butyl ester was carried out as similar to section 3.2.1.1, using 2-butanol instead of methanol at 100°C. The di 2-butyl succinate (DBS), di 2-butyl adipate (DBAD), di 2-butyl azelate (DBAZ) and di 2-butyl phthalate (DBP) were obtained.

3.2.1.4 Synthesis of di 2-ethyl hexyl succinate (DES), di 2-ethyl hexyl adipate (DEAD), di 2-ethyl hexyl azelate (DEAZ) and di 2-ethyl hexyl phthalate (DEP) as PPDs.

The synthesis of di 2- ethyl hexyl ester was carried out as similar to section 3.2.1.1, using 2-ethylhexanol instead of methanol at 60°C. The products were purified by column chromatography. The 2-ethylhexyl succinate (DES), di 2-ethyl hexyl adipate (DEAD), di 2-ethylhexyl azelate (DEAZ) and di 2-ethylhexyl phthalate (DEP) were obtained.

3.2.2 Determination of properties from soybean oil

The properties of soybean oil such as % free fatty acid (FFA), saponification number (SN) and iodine value (IV) were determined according to ASTM D 5555, ASTM D 5558 and ASTM D 5554 Standard test method, respectively.

3.2.3 Synthesis of methyl ester from soybean oil (SME)

five hundred grams of soybean oil was added into 1,000 ml of round bottom flask equipped with condenser, The catalyst as 1% of sodium hydroxide (5 g) was dissolved in methanol (290 ml, 12:1 molar ratio of methanol to oil) by stirring in a small flask. After that the alcohol/catalyst mixture was added into the oil. The reaction mixture was heated at 65°C for 1.5 h. The reaction was checked by thin layer chromatography (TLC) developed by hexane: ethyl acetate: acetic acid (90:10:1 v/v) and visualized by vanillin solution. After the completion of transesterification reaction, the reaction mixture was transferred to a separatory funnel and cooled down to room temperature, the SME layer (upper layer) was separated, washed with warm deionized water and dried under reduced pressure. The conversion percentage of methyl ester and fatty acid profiles of biodiesel was analyzed by ^{1}H-NMR techniques. The product yield was calculated by:

$$\text{Product yield (\% wt)} = \frac{\text{Weight of Biodiesel}}{\text{Weight of Oil}} \times 100$$

3.2.4 Characterization and determination of SME and PME

3.2.4.1 The conversion percentage of SME and PME

The conversion percentage of SME and PME were determined by^{1}H NMR, integrated peak area of methoxy proton at δ_H 3.7 ppm and α-carbonyl methylene proton at δ_H 2.3 ppm calculated by following equation:

$$\boxed{\%\ \text{Conversion} = [(2I_{OMe}) / (3I_{CH2})] \times 100}$$

The ester content of SME and PME was determined by GC. The internal standard was methyl heptadecanoate. The ester content of SME and PME was calculated by the following equation:

$$C = \left(\frac{\sum A - Ai}{Ai} \right) \times \left(\frac{Ci \times Vi}{m} \right) \times 100$$

C = Methyl ester content

∑A = Total area of fatty acid methyl esters

Ai = Area of methyl heptadecanoate

Ci = Concentration of methyl heptadecanoate solution

Vi = Volume of methyl heptadecanoate solution

m = Mass of the sample

3.2.4.2 Determination of fatty acid compositions of SME and PME

The standard 37 fatty acid methyl esters were used to determined fatty acid compositions of SME and PME.

3.2.4.3 Determination of the properties of SME and PME

The main properties of SME and PME were determined according to the test methods shown in Table 3.1

Table 3.1 Test standard method of methyl ester.

Property	Method
Acid number (mg KOH/g)	ASTM D 974
Viscosity at 40°C (cSt)	ASTM D 445

3.2.5 Determination of cloud point (CP) and pour point (PP)

Soybean methyl ester (SME) and palm methyl ester (PME) were thoroughly with each of PPDs (DMS, DMAD, DMAZ, DMP, DIS, DIAD, DIAZ, DIP, DBS, DBAD, DBAZ, DBP, DES, DEAD, DEAZ and DEP) at various concentrations (0, 10,000, 100,000 and 300,000 ppm). Then the mixtures were subjected to measure CP and PP according to the ASTM D2500 for cloud point and ASTM D97 for pour point.

CHAPTER IV

RESULTS AND DISCUSSION

4.1 Synthesis of Pour Point Depressants (PPDs)

The appearance, conversion percentage, product yield percentage, acid value and viscosity at 40 °C of PPDs were summarized in Table 4.1.

Table 4.1 The appearance, conversion percentage, product yield percentage, acid value and viscosity at 40 °C of PPDs.

PPDs	Appearance	% Conversion	% product yield	Acid value (mg KOH/g oil)	Viscosity at 40 °C (cSt)
DMS	Colorless	99.50	84.48	0	1.51
DMAD	Colorless	96.62	88.80	0	1.89
DMAZ	Colorless	98.04	84.73	0	2.87
DMP	Colorless	98.04	86.13	0	5.57
DIS	Colorless	98.52	85.85	0	2.11
DIAD	Colorless	96.15	84.98	0	2.89
DIAZ	Colorless	98.04	87.78	0	4.56
DIP	Colorless	97.09	85.98	0	9.02
DBS	Colorless	98.04	87.53	0	2.65
DBAD	Colorless	97.09	87.38	0	3.47
DBAZ	Colorless	97.56	87.15	0	4.98
DBP	Colorless	96.15	84.90	0	13.21
DES	Colorless	99.01	84.95	0	3.79
DEAD	Colorless	97.09	84.13	0	5.03
DEAZ	Colorless	98.04	85.10	0	5.16
DEP	Colorless	96.15	86.60	0	25.10

According to Table 4.1, the appearances of 16 PPDs were colorless. The conversion percentage and product yield percentage were calculated, the values obtained were in the range of 96.15-99.50% and 84.13-88.80%, respectively. The acid value of PPDs were 0 mg KOH/g oil, that mentioned to no starting material (succinic acid, adipic acid, azelic acid and phthalic acid) remaining in PPDs. The viscosity at 40°C of PPDs was in the range of 1.51- 25.10 cSt. When the molecular weight of PPDs increased, the viscosity increased.

4.2 Characterization of PPDs

4.2.1 Fourier-Transform Infrared Spectroscopy (FT-IR)

The functional groups of 16 PPDs were characterized by FT-IR spectroscopy. The IR spectra of PPDs were presented in Figure A23-A38, All PPDs were ester group, the spectrum showed strong intensity peak at 1730-1740 cm $^{-1}$ corresponding to C=O stretching of carbonyl group and absorptions at1100-1350 cm $^{-1}$ attributable to C-O stretching peak of ester. In addition, the structures of DMP, DIP, DB and DEP were aromatic ring, the spectrum showed C-C stretching in aromatic ring at 1550-1600 cm $^{-1}$. From all spectra, the broad band of O-H stretching (2500-3300cm^{-1}) was not presented because all starting materials (dicarboxylic acid) were removed from PPDs.

4.2.2 Nuclear Magnetic Resonance (^{1}H^{-}NMR)

The structures of PPDs were characterized by ^{1}H-NMR (Figures A4-A19). The characteristic peaks of dimethyl esters, diisopropyl ester, di 2-butyl ester and di 2-ethyl hexyl ester were shown at δ 3.7, 5.0, 4.8 and 4 ppm, respectively.

4.3 Determination of properties from soybean oil

The initial properties of soybean oil as % free fatty acid (FFA), saponification number (SN) and iodine value (IV) were examined. From the results, the FFA of soybean oil was only 0.65%wt hence soybean oil was converted into methyl ester by means of transesterification process. The saponification number and iodine value of soybean oil were 180.67 mg KOH/g and 124.99 mg I_2/g, respectively.

4.4 Synthesis of methyl ester from soybean oil (SME)

Biodiesel from soybean oil was produced by transesterification reaction and the reaction was monitored by TLC. The triglyceride in soybean oil was completely converted to methyl ester. In Figure 4.1, the left side of TLC was the composition of soybean oil that it consists of mono-glyceride, di-glyceride and triglyceride. The right side of TLC showed the position of biodiesel, mono-glyceride and di-glyceride. The spot of biodiesel was higher than triglyceride, diglyceride and monoglyceride because biodiesel was minimum polar when using silica gel as stationary phase. There were traces of mono-glyceride and di-glyceride because the reaction of triglyceride occurs in three successive steps forming di-glycerides, mono-glycerides and glycerol. Each step was given one molecule of methyl ester as product. The color of SME was yellow and the product yield of SME was 89.82%.

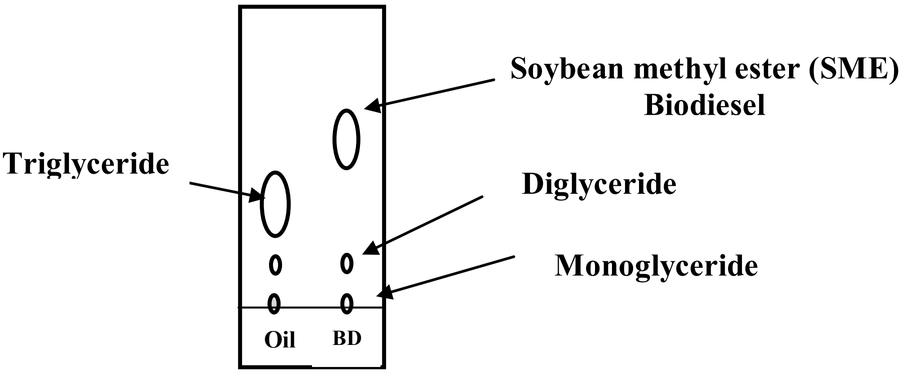

Figure 4.1 TLC of methyl ester from soybean oil when using hexane: ethyl acetate: acetic acid (90:10:1 v/v) solution as mobile phase.

4.5 Characterization and determination of SME and PME

4.5.1 Ester content of SME and PME

The percentage conversion or ester content of SME and PME were calculated from NMR technique. The data from NMR technique showed ester content of SME and PME were 96.62 % and 98.04 %. The percentage conversion of biodiesel should be higher than 96.5% according to EN 14103 standard.

4.5.2 Determination of fatty acid compositions of SME and PME.

From Table 4.2, the data from GC chromatogram of SME showed the major unsaturated fatty acids were linoleic acid (52.82%) and oleic acid (24.85%). For PME, the major fatty acids were palmitic acid (63.1%) and oleic acid (24.56%). The result indicated that SME had more amount of unsaturated fatty acid than PME. As a result, the CP and PP of SME lower than PME (showed in Table 4.5).

Table 4.2 Comparison of fatty acid composition from SME and PME.

Fatty acid compositions	**SME (wt%)**	**PME (wt%)**
C12:0 (Lauric acid)	-	0.24
C14:0 (Myristic acid)	-	1.38
C16:0 (Palmitic acid)	11.18	63.10
C18:0 (Stearic acid)	4.32	4.71
C18:1n9c (Oleic acid)	24.85	24.56
C18:1n9t (Elaidic acid)	1.31	0.32
C18:2n6c (Linoleic acid)	52.82	4.71
C18:2n6t (Linolelaidic acid)	0.63	-
C18:3n6 (γ-Linoleic acid)	4.36	-
C18:3n3 (α-Linoleic acid)	0.74	-

Fatty acid compositions	SME (wt%)	PME (wt%)
C20:0 (Arachidic acid)	-	0.33
C22:1n9 (Erucic acid)	-	0.43
C22:41n9 (Nervonic acid)	-	0.23

4.5.3 Determination of the properties from SME and PME

The properties of SME and PME such as acid value and viscosity were determined according to ASTM D 974 and ASTM D445.

Table 4.3 showed the SME and PME had acid value and viscosity at 40°C in the range of standard values. Furthermore, the viscosity of SME and PME after blending with PPDs was shown in Table 4.4. The viscosity was determined according to ASTM D445.

Table 4.3 Acid value and viscosity of SME and PME.

Properties	Standard value	SME	PME	Standard method
Acid value (mg KOH/g)	<0.5	0.26	0.39	ASTM D 974
Viscosity at 40°C (cSt)	3-5	4.13	4.19	ASTM D445

Table 4.4 showed viscosity at 40°C of SME and PME after blending with maximum concentrations of PPDs. The blending of PPDs in SME had viscosity values within the range of standard values except viscosity of blending SME with 300,000 ppm of di 2-ethyl hexyl phthalate (DEP). Similarly, when 300,000 ppm of DEP was added into PME result in viscosity was not standard (3-5 cSt).

Table 4.4 Viscosity of SME and PME when blending with 300,000 ppm of PPDs.

Additives	Viscosity at 40°C (cSt) of SME	Viscosity at 40°C (cSt) of PME
DMS	3.00	3.00
DMAD	3.27	3.20
DMAZ	3.70	3.71
DMP	4.31	4.22
DIS	3.33	3.34
DIAD	3.76	3.61
DIAZ	4.07	4.28
DIP	4.55	4.44
DBS	3.64	3.63
DBAD	3.81	3.76
DBAZ	4.42	4.35
DBP	4.37	4.78
DES	4.17	4.13
DEAD	4.47	4.47
DEAZ	4.57	4.49
DEP	5.87	5.79

Could point and pour point of SME, PME and PPDs were determined. The results were shown in Table 4.5.

Table 4.5 showed the CP and PP of SME, PME and PPDs. The CP and PP of SME were lower than PME because the SME contains unsaturated fatty acid while the composition of PME was saturated fatty acid (as showed in Table 4.2). The previous research stated that compositions of biodiesel with significant amount of saturated fatty acid compounds will display higher cloud (CP) and pour (PP) point.

Table 4.5 Could point (CP) and Pour point (PP) of SME, PME and PPDs.

Sample	*CPave*	*PPave*
SME	2.00±1.0	0.00±1.0
PME	21.00±1.0	19.00±1.0
DMS	9.00±1.0	13.50±1.0
DMAD	7.00±1.0	7.50±1.0
DMAZ	-3.50±1.0	-9.50±1.0
DMP	-1.20±1.0	-7.55±1.0
DIS	-10.25±1.0	-19.45±1.0
DIAD	-16.20±1.0	-25.00±1.0
DIAZ	-27.00±1.0	>-30.00±1.0
DIP	-21.00±1.0	-23.50±1.0
DBS	-15.30±1.0	-22.35±1.0
DBAD	-17.90±1.0	-25.75±1.0
DBAZ	-29.00±1.0	>-30.00±1.0
DBP	-21.00±1.0	-23.75±1.0
DES	3.00±1.0	-17.50±1.0
DEAD	-5.00±1.0	-23.00±1.0
DEAZ	-22.35±1.0	>-30.00±1.0
DEP	5.15±1.0	-27.00±1.0

4.6 Improvement of the cold flow properties of biodiesel

4.6.1 Using of DMS, DMAD and DMAZ as PPDs

Figures 4.2, 4.3, 4.4 and 4.5 showed the reduction of CP and PP in SME when blended with DMS, DMAD and DMAZ. At 300,000 ppm of DMS, the CP and PP of PME were reduced from 2.00 °C to -1.80 °C (ΔCP = 3.80 °C) and 0.00 °C to -2.00 °C (ΔPP = 2.00 °C).The CP and PP were decreased from 2.00 °C to -1.80 °C (ΔCP = 3.80 °C) and 0.00 °C to -3.40 °C (ΔPP = 3.40 °C) by using 300,000 ppm of DMAD. At the same concentration, the CP and PP of SME were reduced from 2.00 °C to -2.00 °C (ΔCP = 4.00 °C) and 0.00 °C to -4.50 °C (ΔPP = 4.50 °C) when blended with DMAZ.

The reduction of CP and PP was decreased after blending DMS, DMAD and DMAZ with PME (Figures 6 and 7). The values of CP and PP were decreased from 21.00 °C to 16.50 °C (ΔCP = 4.50 °C) and 19.00 °C to 14.30 °C (ΔPP = 4.70 °C) by using DMS at 300,000 ppm. Similarly, the values of CP and PP were reduced from 21.00 °C to 16.60 °C (ΔCP = 4.40 °C) and 19.00 °C to 14.20 °C (ΔPP = 4.80 °C) after blending with DMAD. In addition of 300,000 ppm of DMAZ, the CP and PP of SME were reduced from 21.00 °C to 16.30 °C (ΔCP = 4.70 °C) and 19.00 °C to 14.00 °C (ΔPP = 5.00 °C).

From the results, the cold flow properties of SME and PME were improved by using DMS, DMAD and DMAZ as PPDs. When using the small amount of DMS, DMAD and DMAZ (10,000 ppm), the reduction of CP and PP were changed slightly. In contrast, adding the large amount of DMS, DMAD and DMAZ (100,000-300,000 ppm) caused a significant change to CP and PP. These PPDs are preventing the crystal growth and agglomeration which will hinder the crystallization of biodiesel.

The comparison of PPDs' effectiveness in cold flow properties of SME and PME improvement indicated that DMAZ is more effective than DMAD and DMS, because the structure of three PPDs had different alkyl chain length (The hydrocarbon chain between carboxylic groups). The trends of CP and PP were decreased when the alkyl chain length increased. Therefore, the ratio of polar and nonpolar had affected to CP and PP values. When the PPDs were added in biodiesel, some molecules of PPDs could be interacted with themselves. The structure of DMS had a short chain between carboxylic group so carboxylic groups were close to each other. The molecule may be easily packed resulting in the crystallization occurrence which is easier than DMAD and DMAZ.

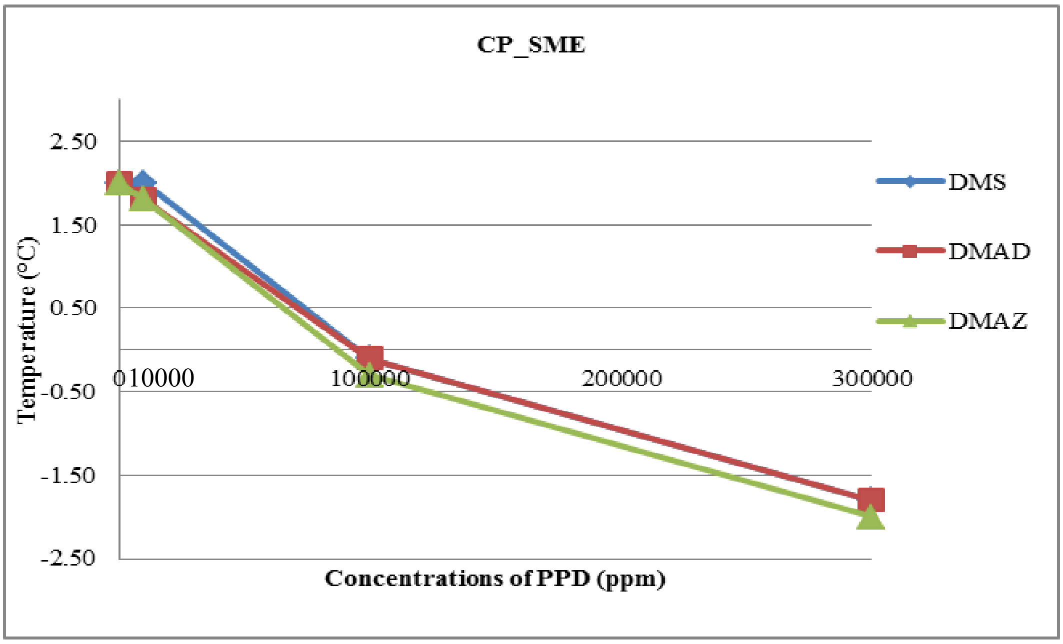

Figure 4.2 CP of SME with various concentrations of DMS, DMAD and DMAZ.

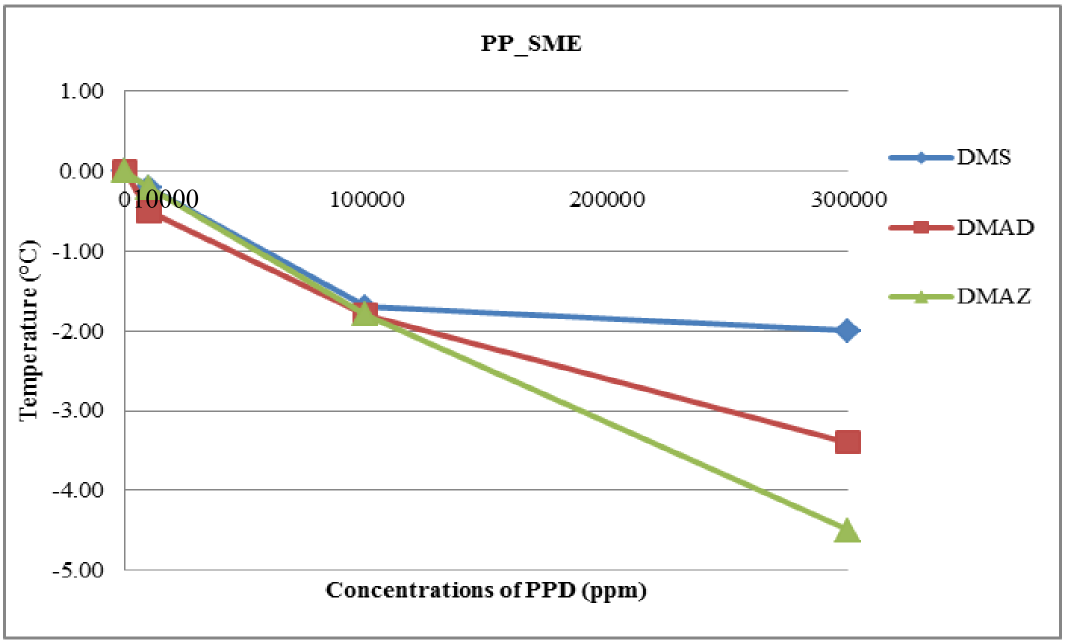

Figure 4.3 PP of SME with various concentrations of DMS, DMAD and DMAZ.

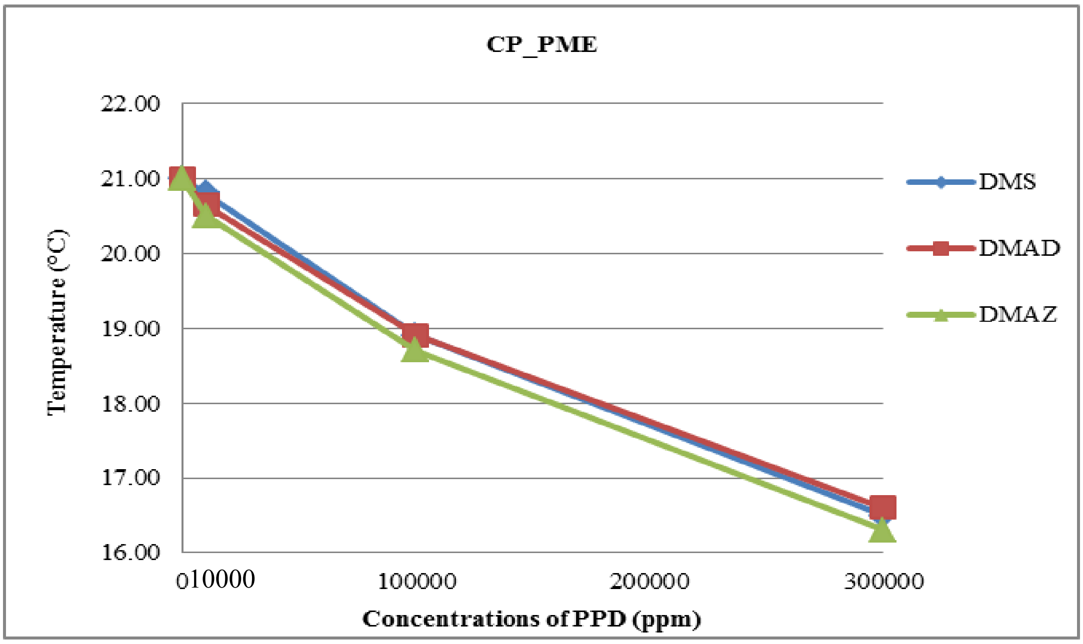

Figure 4.4 CP of PME with various concentrations of DMS, DMAD and DMAZ.

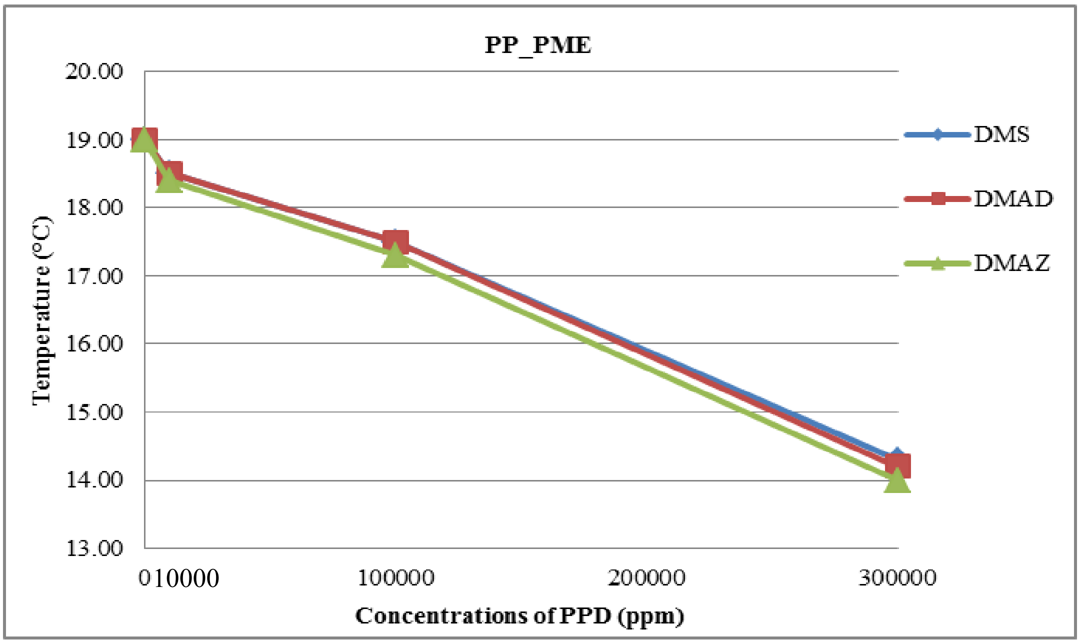

Figure 4.5 PP of PME with various concentrations of DMS, DMAD and DMAZ.

4.6.2 Using of DMAZ and DMP as PPDs

Three concentrations of DMAZ and DMP blends, i.e. (10,000, 100,000 and 300,000 ppm) were tested with SME and PME for cold flow properties (Figures 4.6 and 4.7) to enhance the cold weather functionality of biodiesel fuel. The reduction in CP and PP of SME was from 2.00 °C to -2.00 °C (ΔCP = 4.00 °C) and 0.00 °C to -4.50 °C (ΔPP = 4.50 °C) when blended with 300,000 ppm of DMAZ. Similarly to blending of DMP in PME, the CP and PP were reduced from 2.00 °C to -0.70°C (ΔCP = 2.70 °C) and 0.00 °C to -2.70 °C (ΔPP = 2.70 °C).

Figures 4.6 and 4.7 showed the CP and PP of PME when using DMAZ and DMP as PPDs. At 300,000 ppm of DMAZ, the CP and PP were decreased from 21.00 °C to 16.30 °C (ΔCP =4.70 °C) and 19.00 °C to 14.00 °C (ΔPP = 5.00 °C). The values of CP and PP were attested obviously when the concentration of DMP was 300,000 ppm, indicating decreased values from 21.00 °C to 16.60°C (ΔCP = 4.40 °C) and 19.00 °C to 14.90 °C (ΔPP = 4.10 °C), respectively.

The results could be concluded that The CP and PP of SME and PME were improved by using DMAZ and DMP. These PPDs inhibit the crystals size formation which was enough to clog fill-line and filters, and provide a barrier to crystal agglomeration.

Moreover, blending of DMAZ displayed CP and PP which was lower than DMP. DMAZ and DMP had different major structure; DMAZ was aliphatic hydrocarbon while DMP was aromatic hydrocarbon. The hypothesis suggested that there was interaction between DMP molecules; the crystalline aromatic ring involves perpendicular interaction between rings, thus the relatively positive periphery of one molecule associates with the relatively negative faces of the aromatic molecule aligned above and below it. The interaction between the aromatic rings would be better resulting in higher CP and PP.

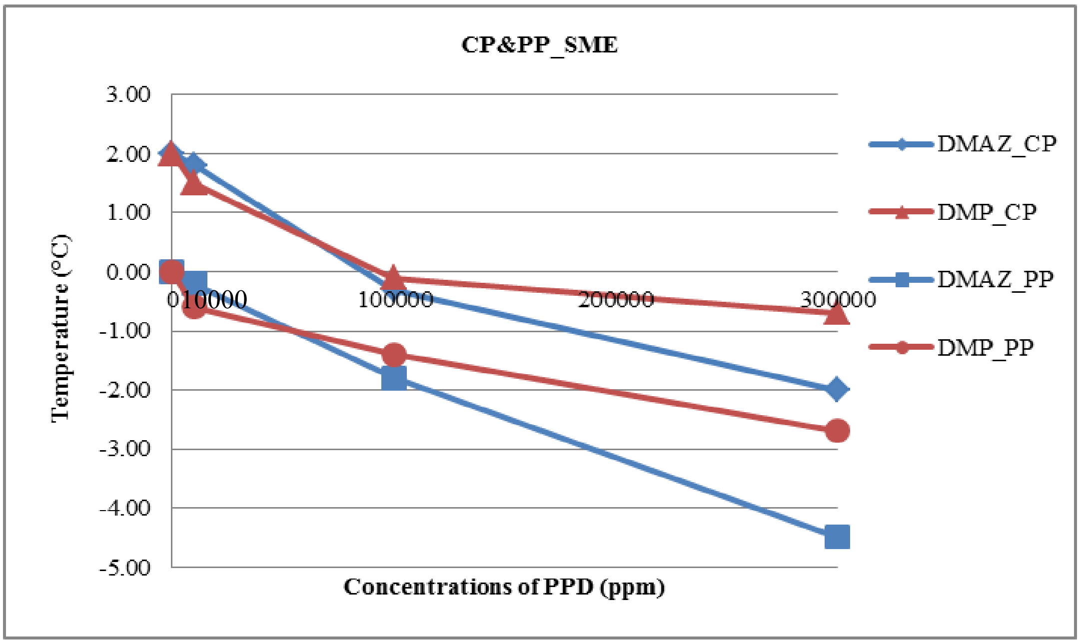

Figure 4.6 CP and PP of SME with various concentrations of DMAZ and DMP.

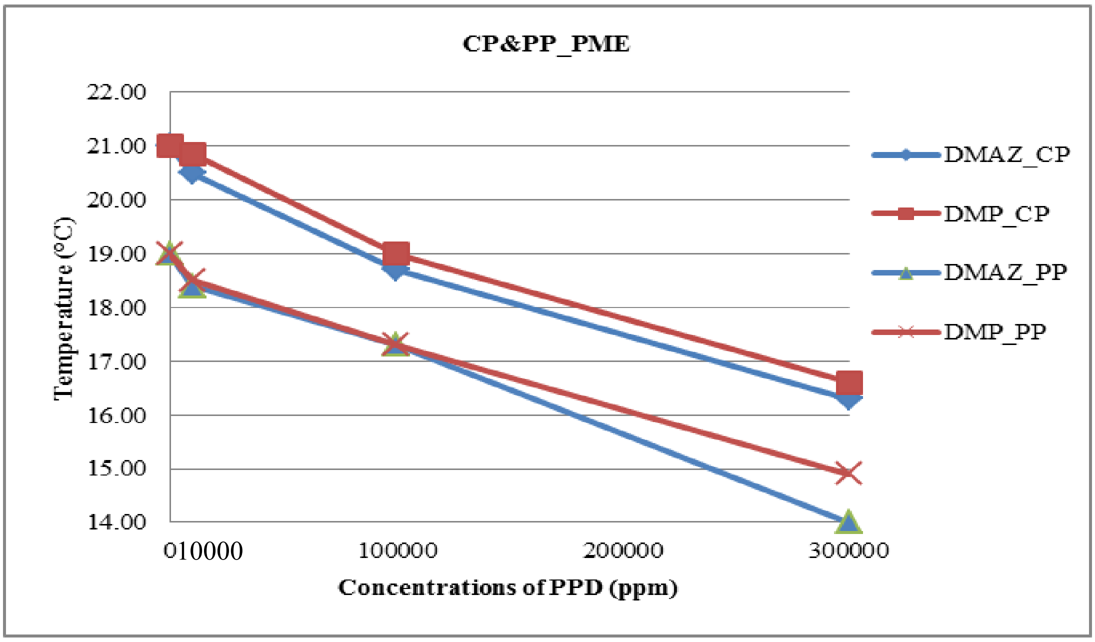

Figure 4.7 CP and PP of PME with various concentrations of DMAZ and DMP.

4.6.3 Using DMAZ, DIAZ, DBAZ, and DEAZ as PPDs

Addition of DMAZ, DIAZ, DBAZ and DEAZ to SME was resulted in lower CP and PP, as showed in Figures 4.8 and 4.9. The SME was displayed the reduction of CP and PP from 2.00 °C to -2.00 °C (ΔCP = 4.00 °C) and 0.00 °C to -4.50 °C (ΔPP = 4.50 °C) with addition of 300,000 ppm of DMAZ. Similarly, DIAZ reduced CP and PP from 2.00 °C to -2.90 °C (ΔCP = 4.90 °C) and 0.00 °C to -5.20 °C (ΔPP = 5.20 °C). When adding 300,000 ppm of DBAZ, the CP and PP were decrease from 2°C to -3.15°C (ΔCP = 5.15 °C) and 0.00 °C to -5.40 °C (ΔPP = 5.40 °C). Moreover, blending DEAZ at 300,000 ppm reduced CP and PP values from 2.00 °C to -2.70 °C (ΔCP = 4.70 °C) and 0.00 °C to -4.90 °C (ΔPP = 4.90 °C), respectively.

The results showed the reduction of CP and PP in PME when using DMAZ, DIAZ, DBAZ and DEAZ as PPDs. At highest concentration of DMAZ (300,000 ppm), the CP and PP of PME decreased from 21.00 °C to 16.30 °C (ΔCP =4.7 °C) and 19.00 °C to 14.00 °C (ΔPP = 5.00 °C). At the same condition, the CP and PP could be reduced from 21.00 °C to 15.35 °C (ΔCP = 5.65 °C) and 19.00 °C to

13.20 °C (ΔPP = 5.80 °C) after blending with DIAZ. The addition of 300,000 ppm in DBAZ decreased the CP and PP from 21.00°C to 15.00°C (ΔCP = 6.00 °C) and 19.00 °C to 13.00 °C (ΔPP = 6.00 °C). Finally, the reduction in CP and PP were from 21.00 °C to 15.90 °C (ΔCP = 5.10 °C) and 19 °C to 13.70 °C (ΔPP = 5.30 °C) when blended with DEAZ.

From the result, both SME and PME had pronounced decreases in CP and PP when the concentration of DMAZ, DIAZ, DBAZ and DEAZ were increased. This can be concluded that DMAZ, DIAZ, DBAZ and DEAZ could improve cold flow properties of SME and PME. The PPDs could be able to hinder the packing of wax crystals and solid formation. From the study, DBAZ had the highest efficiency, following with DIAZ, DEAZ and DMAZ. Four PPDs had different branched alkyl chain. DBAZ is the most active reducer in CP and PP because the structure of DBAZ consists of branch substituent which hindered the solid phase formation. The DIAZ is less effective than DBAZ because the molecule of DIAZ had less steric effect than DBAZ. Although DEAZ had a branch chain but DEAZ could reduce CP and PP less than DBAZ and DIAZ resulting from the branch substituent of DEAZ had a part of long chain hydrocarbon which may cause packing of hydrocarbon and crystallization. In addition, DMAZ had minimum efficiency due to the structure of DMAZ was not branch substituent. Thus, the packing of molecules occurred easily which caused crystallization.

In addition, the PPDs had 2-butanol as branch chain (DBS, DBAD and DBP) which gave the good results from the comparison of branch chain, followed by using isopropanol (DIS, DIAD and DIP) and 2-ethylhexanol (DES, DEAD and DEP) as branch substituent. The PPDS had methyl group which minimally improved flow properties of biodiesel. The results were shown in tables B1-B32 and the discussions were the same reasons as described above. All research showed that DBAZ gave the best result to improve cold flow properties of SME and PME. At 300,000 ppm of DBAZ, the CP and PP of SME were reduced 5.15 °C and 5.40 °C. Both CP and PP of PME were reduced 6.00 °C by using DBAZ as PPDs.

In this research, DBAZ was compared with poly (maleic anhydride-*alt*-1-octadecene) [36]. At 2 %wt of poly (maleic anhydride-*alt*-1-octadecene, the CP and PP of palm biodiesel were reduced 4.80 °C and 6.00 °C. Therefore, poly (maleic anhydride-*alt*-1-octadecene) is more effective than DBAZ because of more steric hindrance of poly (maleic anhydride-*alt*-1-octadecene). Furthermore, poly (maleic anhydride-*alt*-1-octadecene) is large molecule, so the molecules are more difficult to pack than DBAZ.

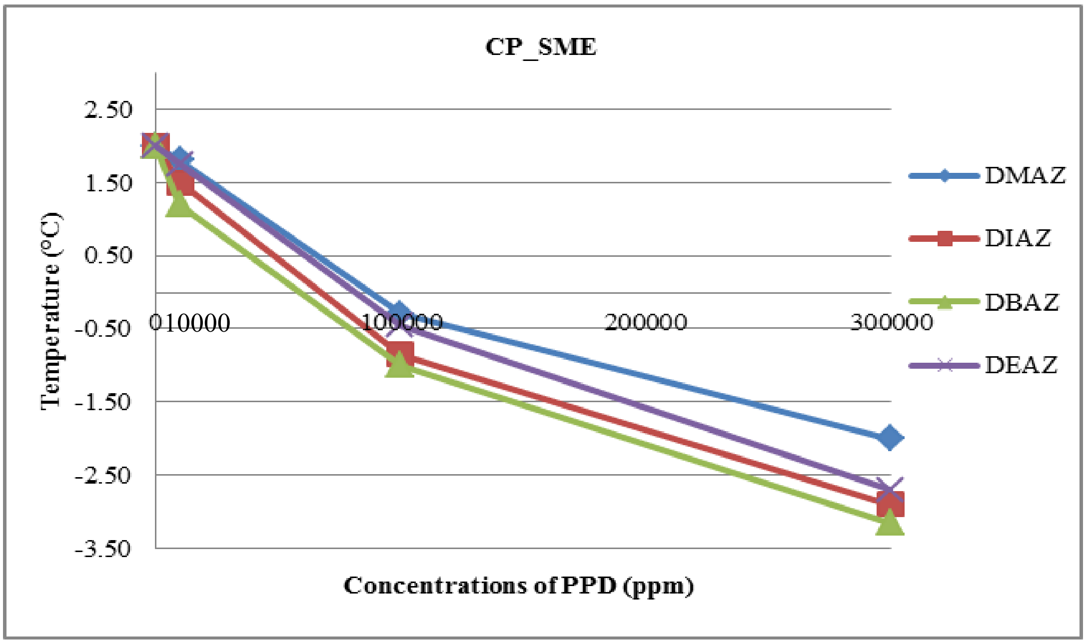

Figure 4.8 CP of SME with various concentrations of DMAZ, DIAZ, DBAZ and DEAZ.

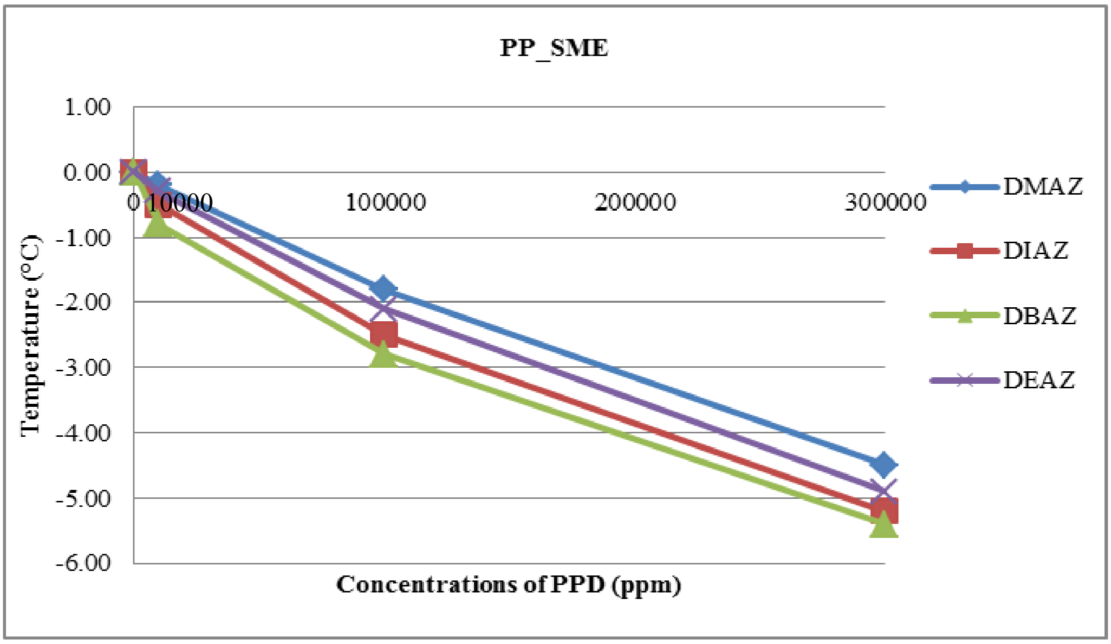

Figure 4.9 PP of SME with various concentrations of DMAZ, DIAZ, DBAZ, and DEAZ.

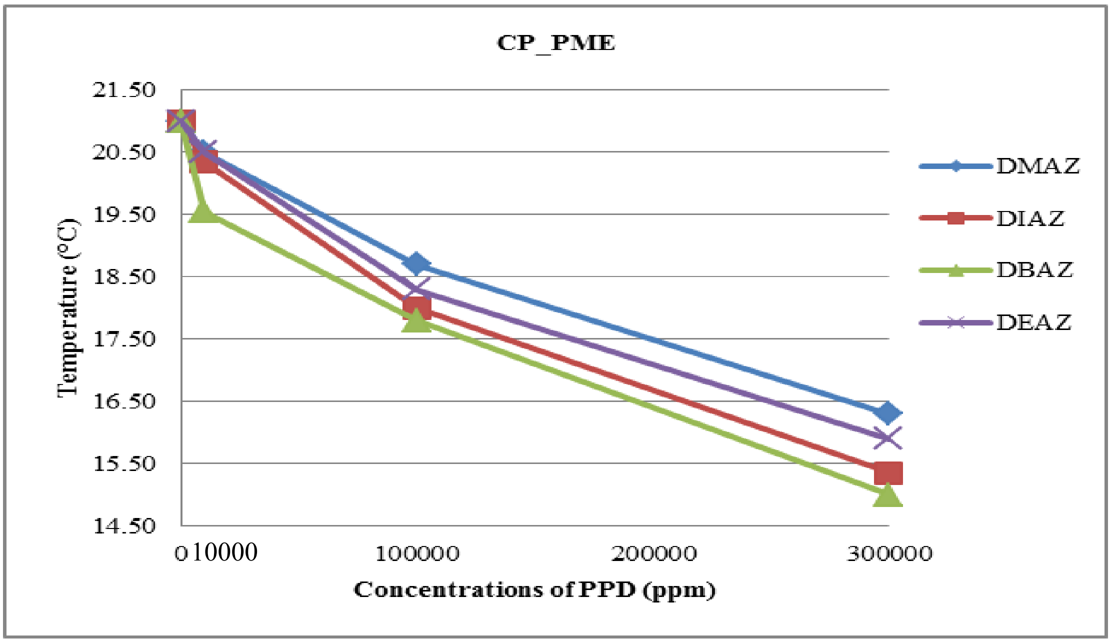

Figure 4.10 CP of PME with various concentrations of DMAZ, DIAZ, DBAZ and DEAZ.

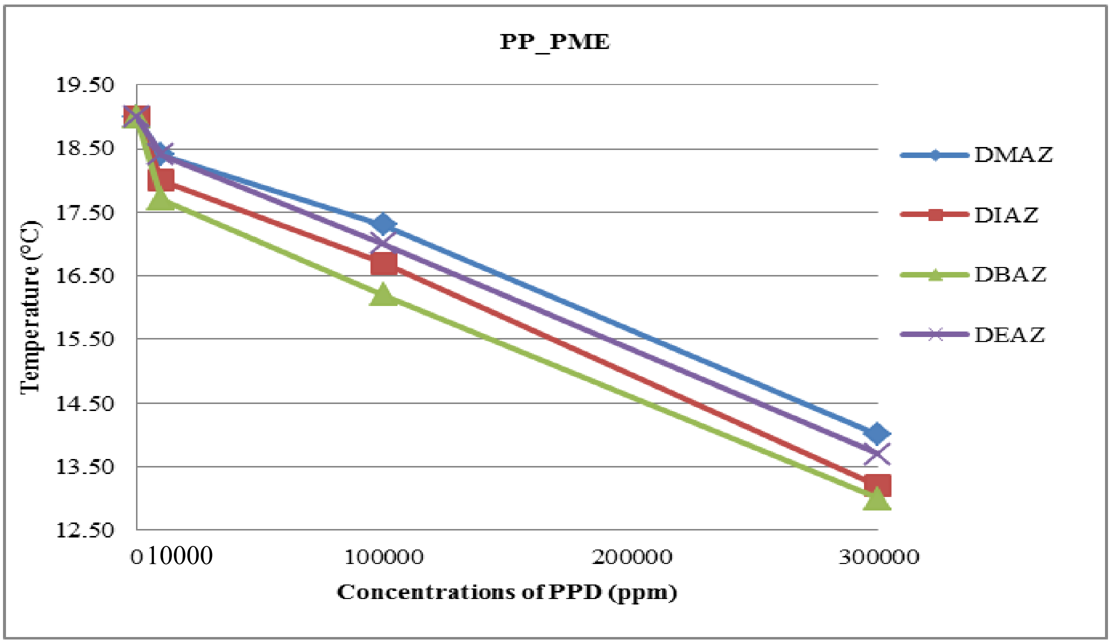

Figure 4.11 PP of PME with various concentrations of DMAZ, DIAZ, DBAZ and DEAZ.

CHAPTER V

CONCLUSION AND SUGGESTION

5.1 Conclusion

The objective of this research was to synthesize pour point depressants (PPDs) from dicarboxylic acid to improve flow properties of soybean methyl ester (SME) and palm methyl ester (PME) at low temperature. The diester could be synthesized from the esterification reaction by using sulfuric acid as catalyst. The CP and PP of SME and PME were reduced when diester was added. Moreover, the result also demonstrated that the branched chain of PPDs (DIS, DIAD, DIAZ, DIP, DBS, DBAD, DBAZ, DBP, DES, DEAD, DEAZ and DEP) is more effective than straight-chain (methyl) of PPDs (DMS, DMAD, DMAZ and DMP) because branched chain are more difficult to pack when compared with straight-chain. Aromatic PPDs (DMP, DIP, DBP and DEP) exhibited higher CP and PP compared with aliphatic PPDs. The aromatic ring had perpendicular interaction between rings caused aromatic molecule can be formed crystal. After that, comparison of alkyl chain length in structure of PPDs, the CP and PP of SME and PME were decreased when the alkyl chain length of PPDs increased. It indicated that increasing of alkyl chain length from C4 to C9 causes an increase of solubility resulting in an increase of the interaction between diester and wax in biodiesel therefore inhibition of the wax crystal formation should be obtained. Consequently, the good PPDs should have structure as follows: branched-chain, long alkyl chain length and aliphatic molecule. In addition, PPDs with large molecule were added in SME and PME results in viscosity of SME and PME was increased. Finally, di 2-butyl azelate (DBAZ) demonstrated the most advantageous cold flow properties by yielding the lowest CP and PP values. The maximum reduction of CP and PP in SME was obtained at 300,000 ppm which deceased 5.15 ± 1.0 °C and 5.40 ± 1.0 °C and both CP and PP could reduce 6.00 ± 1.0 °C in PME.

5.2 Suggestion

- PPDs should be synthesized from dicarboxylic acid which has longer alkyl chain length than azelaic acid (C_9) such as undecanedioic acid (C_{11}) and dodecanedioic acid (C_{12}) to improve the cold flow property of biodiesel.

REFERENCES

[1] Fernandes, D. M., Serqueira, D. S., Portela, F. M., Assunção, R. M. N., Munoz, R. A. A., Terrones, M. G. H. Preparation and characterization of methylic and ethylic biodiesel from cottonseed oil and effect of tert-butylhydroquinone on its oxidative stability. Fuel 97 (2012): 658-661.

[2] Kleinová, A., Paligová, J., Vrbová, M., Mikulec, J., Cvengroš, J. Cold flow properties of fatty esters. Process Safety and Environmental Protection 85 (2007): 390-395.

[3] Wang, Y., Ma, S., Zhao, M., Kuang, L., Nie, J., Riley, W. W. Improving the cold flow properties of biodiesel from waste cooking oil by surfactants and detergent fractionation. Fuel 90 (2011): 1036-1040.

[4] Bhale, P. V., Deshpande, N. V., Thombre, S. B. Improving the low temperature properties of biodiesel fuel. Renewable Energy 34 (2009): 794-800.

[5] Soni, H. P., Kiranbala., Bharambe. D. P. Performance-Based Designing of Wax Crystal Growth Inhibitors. Energy & Fuels 22 (2008): 3930-3938.

[6] Jin, F., Zeng, X., Cao, J., Kawasaki, K., Kishita, A., Tohji, K., Enomoto, H. Partial hydrothermal oxidation of unsaturated high molecular weight carboxylic acids for enhancing the cold flow properties of biodiesel fuel. Fuel 89 (2010): 2448-2454.

[7] Pérez, Á., Casas, A., Fernández, C. M., Ramos, M. J., Rodríguez, L. Winterization of peanut biodiesel to improve the cold flow properties. Bioresource Technology 2010, 101 (19), 7375-7381.

[8] Ramalho, E. F. S. M., Carvalho Filho, J. R., Albuquerque, A. R., de Oliveira, S. F., Cavalcanti, E. H. S., Stragevitch, L., Santos, I. M. G., Souza, A. G. Low temperature behavior of poultry fat biodiesel:diesel blends. Fuel 93 (2012): 601-605.

[9] Lin, L., Cunshan, Z., Vittayapadung, S., Xiangqian, S., Mingdong, D. Opportunities and challenges for biodiesel fuel. Applied Energy 88 (2011): 1020-1031.

[10] Atabani, A. E., Silitonga, A. S., Badruddin, I. A., Mahlia, T. M. I., Masjuki, H. H., Mekhilef, S. A comprehensive review on biodiesel as an alternative energy resource and its characteristics. Renewable and Sustainable Energy Reviews 16 (2012): 2070-2093.

[11] Srivastava, A., Prasad, R. Triglycerides-based diesel fuels. Renewable and Sustainable Energy Reviews 4 (2000): 111-133.

[12] Ma, F., Hanna, M. A. Biodiesel production: a review. Bioresource Technology 70 (1999): 1-15.

[13] Singh, S. P., Singh, D. Biodiesel production through the use of different sources and characterization of oils and their esters as the substitute of diesel: A review. Renewable and Sustainable Energy Reviews 14 (2010): 200-216.

[14] Leung, D. Y. C., Wu, X., Leung, M. K. H. A review on biodiesel production using catalyzed transesterification. Applied Energy 87 (2010): 1083-1095.

[15] Pramanik, K. Properties and use of jatropha curcas oil and diesel fuel blends in compression ignition engine. Renewable Energy 28 (2003), 239-248.

[16] Sahoo, P. K., Das, L. M. Process optimization for biodiesel production from Jatropha, Karanja and Polanga oils. Fuel 88 (2009): 1588-1594.

[17] Schuchardt, U., Sercheli, R., Vargas, R. M. Transesterification of vegetable oils: a review. Journal of the Brazilian Chemical Society 9 (1998): 199-210.

[18] Borges, M. E., Díaz, L. Recent developments on heterogeneous catalysts for biodiesel production by oil esterification and transesterification reactions: A review. Renewable and Sustainable Energy Reviews 16 (2012): 2839-2849.

[19] Sharma, Y. C., Singh, B., Upadhyay, S. N. Advancements in development and characterization of biodiesel: A review. Fuel 87 (2008): 2355-2373.

[20] Çaynak, S., Gürü, M., Biçer, A., Keskin, A., İçingür, Y. Biodiesel production from pomace oil and improvement of its properties with synthetic manganese additive. Fuel 88 (2009): 534-538.

[21] Lam, M. K., Lee, K. T., Mohamed, A. R. Homogeneous, heterogeneous and enzymatic catalysis for transesterification of high free fatty acid oil (waste cooking oil) to biodiesel: A review. Biotechnology Advances 28 (2010): 500-518.

[22] Fukuda, H., Kondo, A., Noda, H. Biodiesel fuel production by transesterification of oils. Journal of Bioscience and Bioengineering 92 (2001): 405-416.

[23] Quesada-Medina, J., Olivares-Carrillo, P. Evidence of thermal decomposition of fatty acid methyl esters during the synthesis of biodiesel with supercritical methanol. The Journal of Supercritical Fluids 56 (2011): 56-63.

[24] Anitescu, G., Bruno, T. J. Fluid properties needed in supercritical transesterification of triglyceride feedstocks to biodiesel fuels for efficient and clean combustion – A review. The Journal of Supercritical Fluids 63 (2012): 133-149.

[25] Tan, K. T., Gui, M. M., Lee, K. T., Mohamed, A. R. An optimized study of methanol and ethanol in supercritical alcohol technology for biodiesel production. The Journal of Supercritical Fluids 53 (2010): 82-87.

[26] Tyson, K.S. Biodiesel Handling and Use Guidelines National Renewable Energy Laboratory, Department of Energy, CO.USA, 2001.

[27] Atadashi, I. M., Aroua, M. K., Aziz, A. A. High quality biodiesel and its diesel engine application: A review. Renewable and Sustainable Energy Reviews 14 (2011): 1999-2008.

[28] Atadashi, I. M., Aroua, M. K., Aziz, A. R. A., Sulaiman, N. M. N. Refining technologies for the purification of crude biodiesel. Applied Energy 88 (2011): 4239-4251.

[29] Demirbas, A., Progress and recent trends in biodiesel fuels. Energy Conversion and Management 50 (2009): 14-34.

[30] ประกาศกรมธุรกิจพลังงาน เรื่อง กำหนดลักษณะและคุณภาพของไบโอดีเซลประเภทเมทิลเอสเทอร์ของกรดไขมัน. ราชกิจจานุเบกษา (2548), 122 (ตอนพิเศษ 70 ง).

[31] Dunn, R. Low-temperature flow properties of vegetable oil/cosolvent blend diesel fuels. Journal of the American Oil Chemists' Society 79 (2002): 709-715.

[32] Boshui, C., Yuqiu, S., Jianhua, F., Jiu, W., Jiang, W. Cold flow properties and crystal morphologies of biodiesel blends. Chemistry and Technology of Fuels and Oils 46 (2010): 52-57.

[33] Knothe, G. Dependence of biodiesel fuel properties on the structure of fatty acid alkyl esters. Fuel Processing Technology 86 (2005): 1059-1070.

[34] Soriano Jr, N. U., Migo, V. P., Matsumura, M. Ozonized vegetable oil as pour point depressant for neat biodiesel. Fuel 85 (2006): 25-31.

[35] Meher, L. C., Dharmagadda, V. S. S., Naik, S. N. Optimization of alkali-catalyzed transesterification of Pongamia pinnata oil for production of biodiesel. Bioresource Technology 97 (2006): 1392-1397.

[36] Sern, C. H., May, C. Y., Zakaria, Z., Daik, R., Foon, C. S. The effect of polymers and surfactants on the pour point of palm oil methyl esters. European Journal of Lipid Science and Technology 109 (2007): 440-444.

[37] Soldi, R. A., Oliveira, A. R. S., Barbosa, R. V., César-Oliveira, M. A. F. Polymethacrylates: pour point depressants in diesel oil. European Polymer Journal 43 (2007): 3671-3678.

[38] Al-Sabagh, A. M., Noor El-Din, M. R., Morsi, R. E., Elsabee, M. Z. Styrene-Maleic Anhydride copolymer esters as flow improvers of waxy crude oil. Journal of Dispersion Science and Technology 30 (2009): 420-426.

[39] Panlek, D. Improving cold flow properties of biodiesel from Irvingia malayana Oliv. ex A. Benn. Seeds. Master Thesis, Program of Petrochemistry and Polymer Science, Faculty of Science, Chulalongkorn University, 2010.

[40] Joshi, H., Moser, B. R.; Toler, J., Smith, W. F., Walker, T. Ethyl levulinate: A potential bio-based diluent for biodiesel which improves cold flow properties. Biomass and Bioenergy 35 (2011): 3262-3266.

APPENDICES

APPENDIX A

^{1}H-NMR SPECTRA, GC CHROMATOGRAMS AND IR SPECTRA

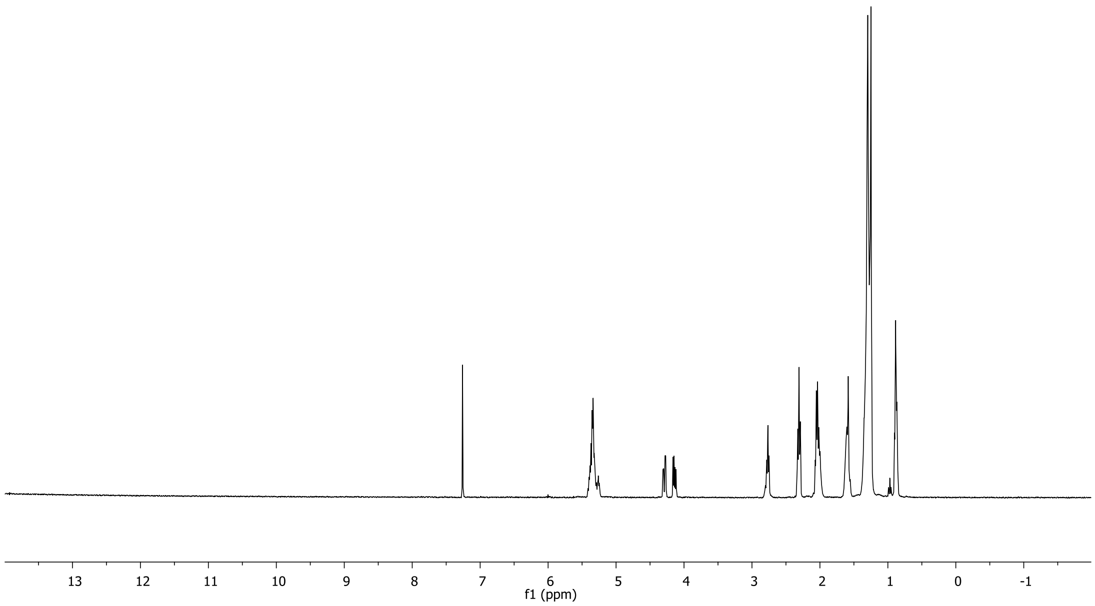

Figure A1 ^{1}H-NMR spectrum of Soybean oil.

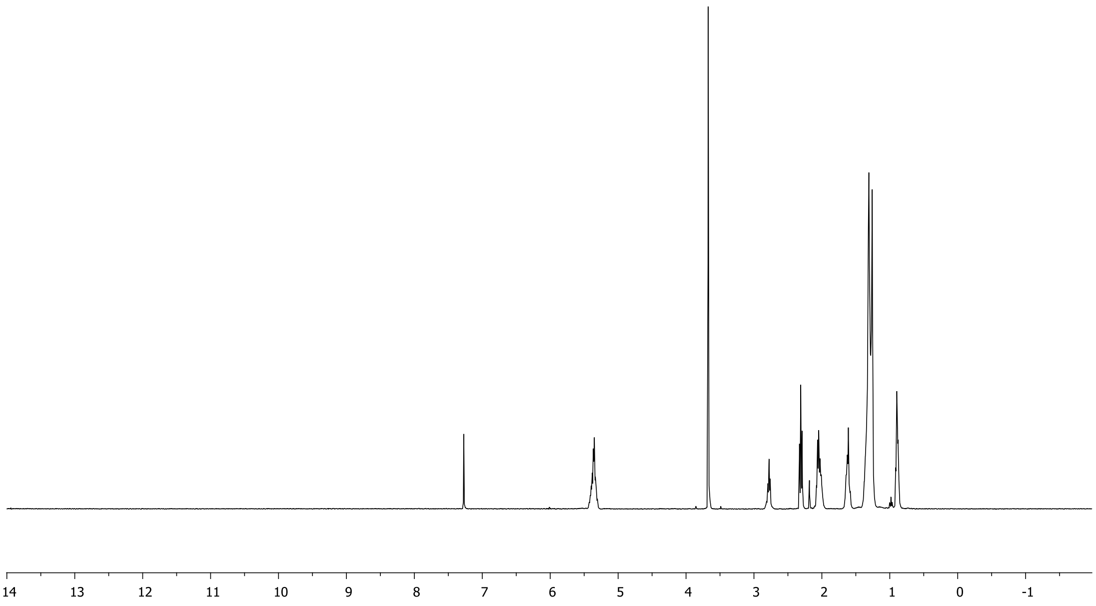

Figure A2 ^{1}H-NMR spectrum of SME.

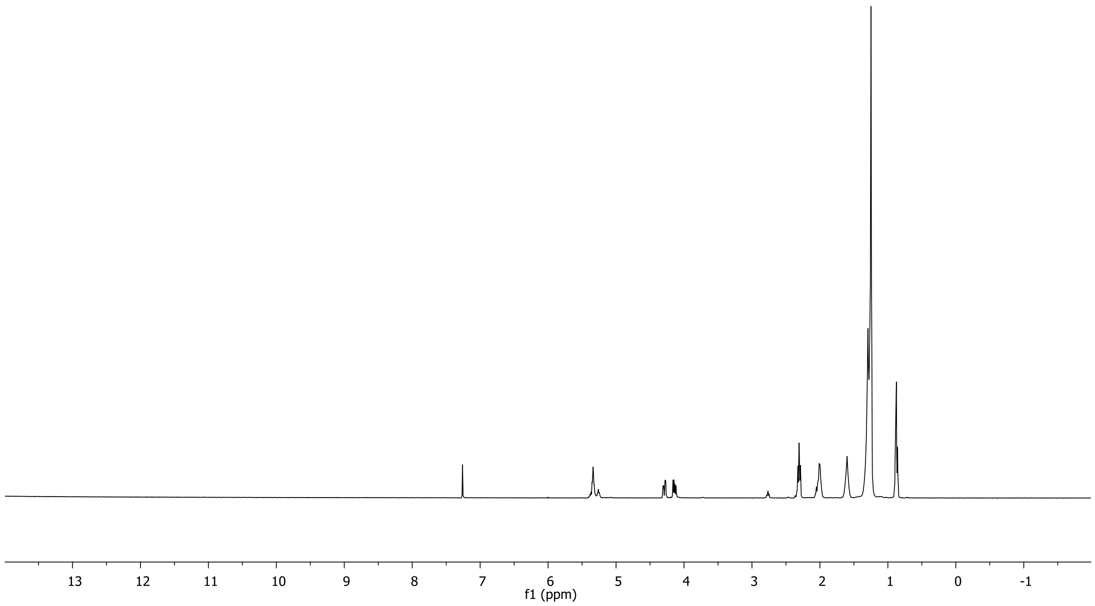

Figure A3 ^{1}H-NMR spectrum of PME.

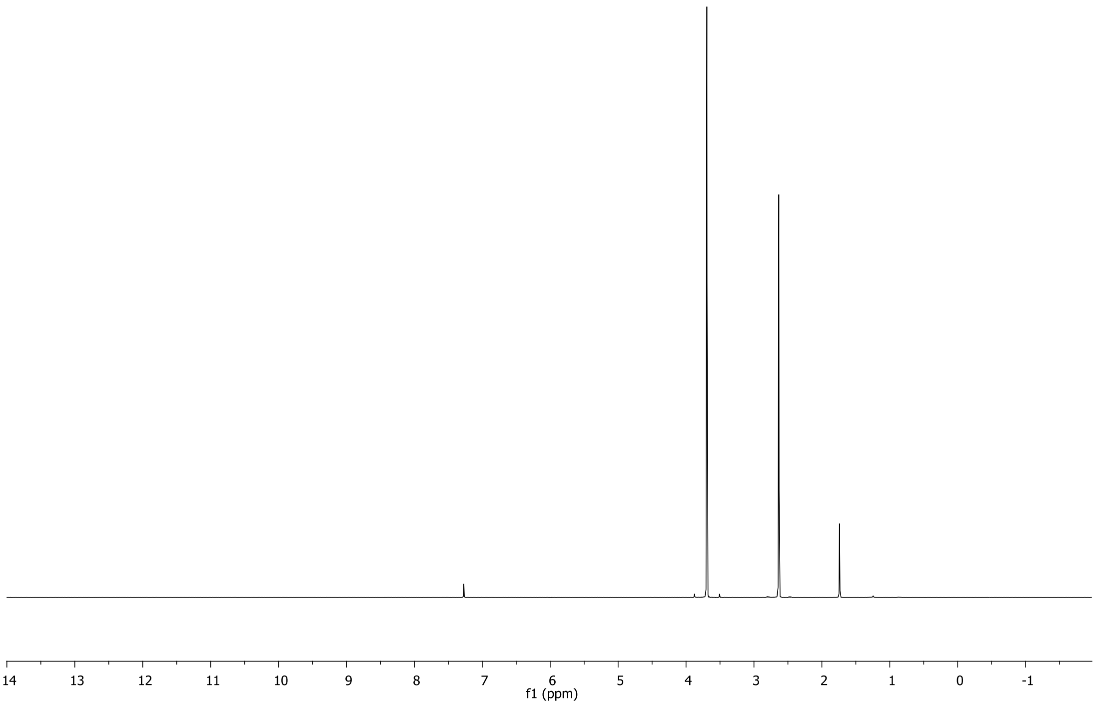

Figure A4 ^{1}H-NMR spectrum of DMS.

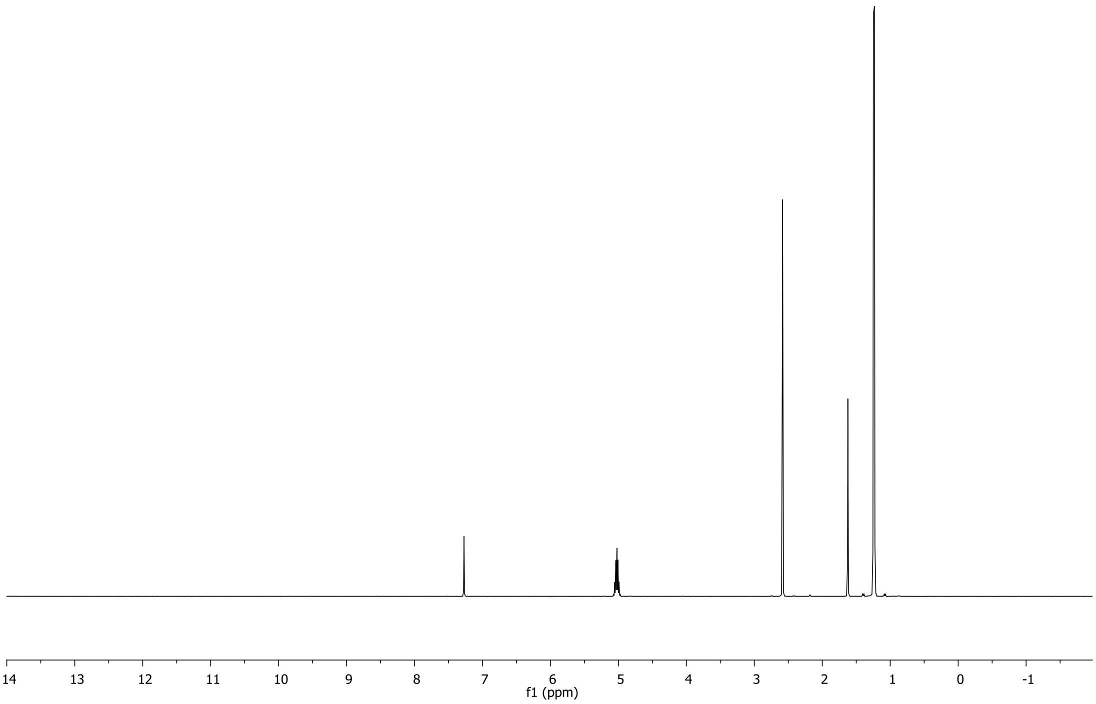

Figure A5 ^{1}H-NMR spectrum of DIS.

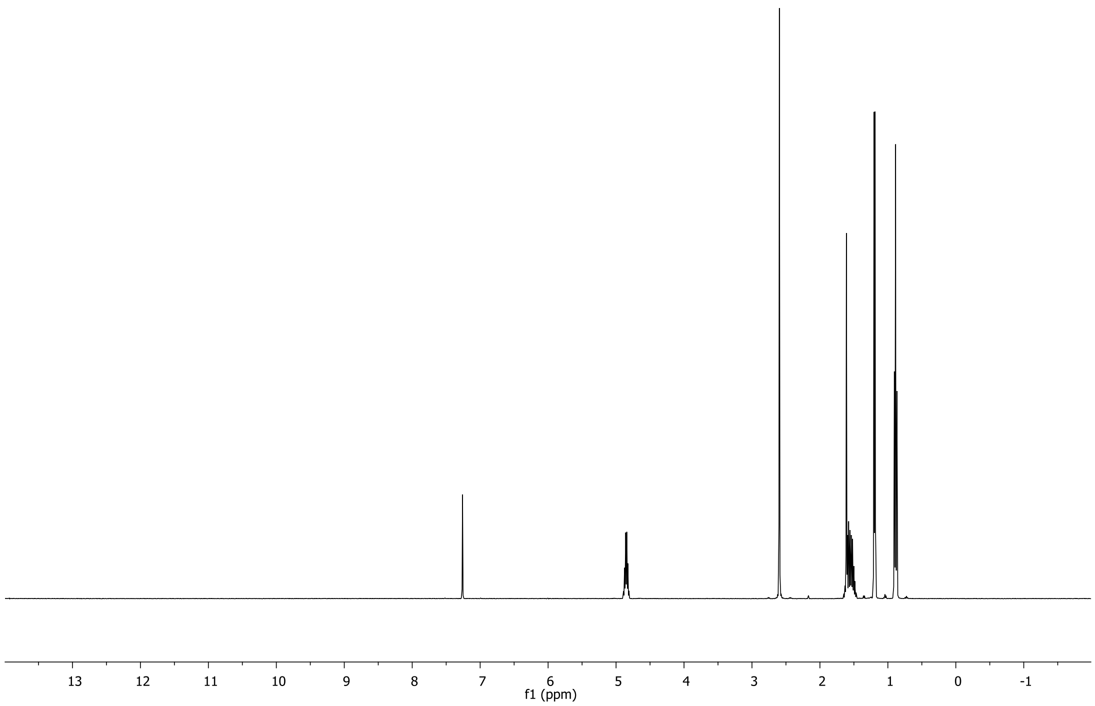

Figure A6 ^{1}H-NMR spectrum of DBS.

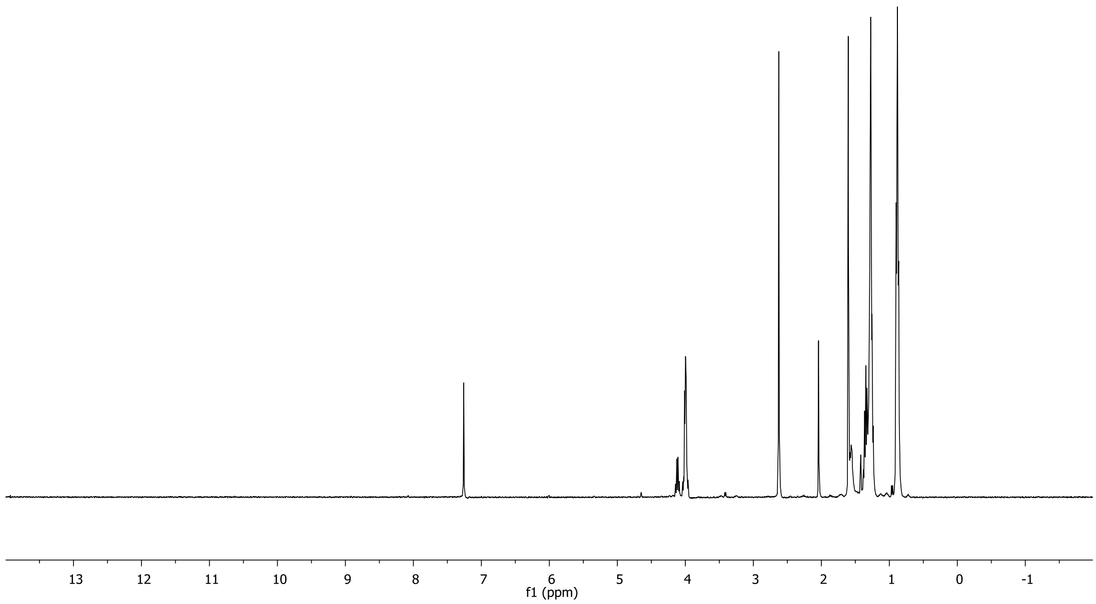

Figure A7 ^{1}H-NMR spectrum of DES.

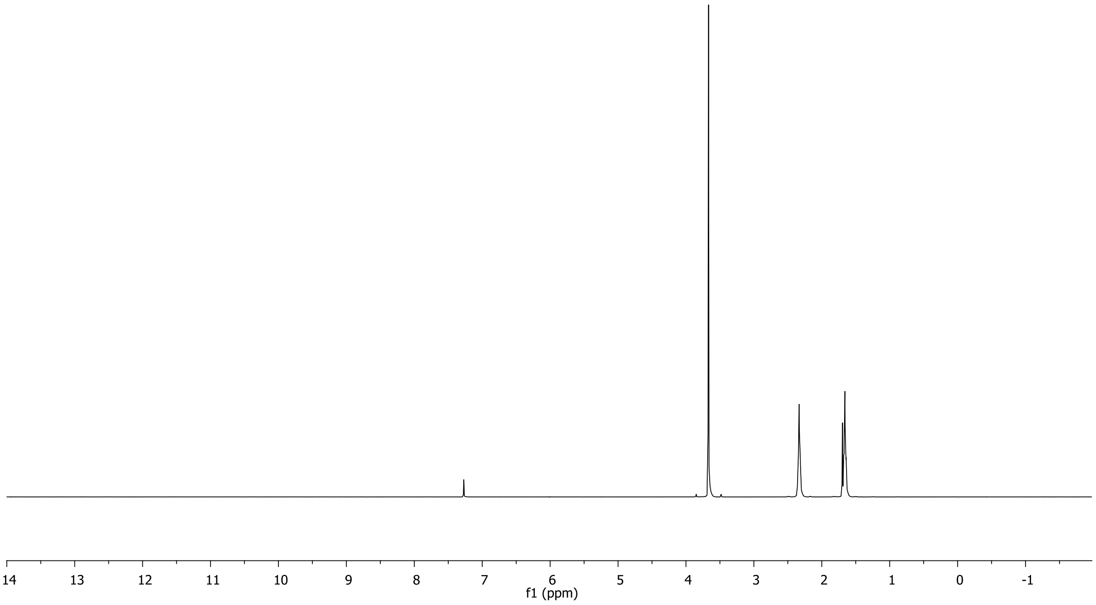

Figure A8 ^{1}H-NMR spectrum of DMAD.

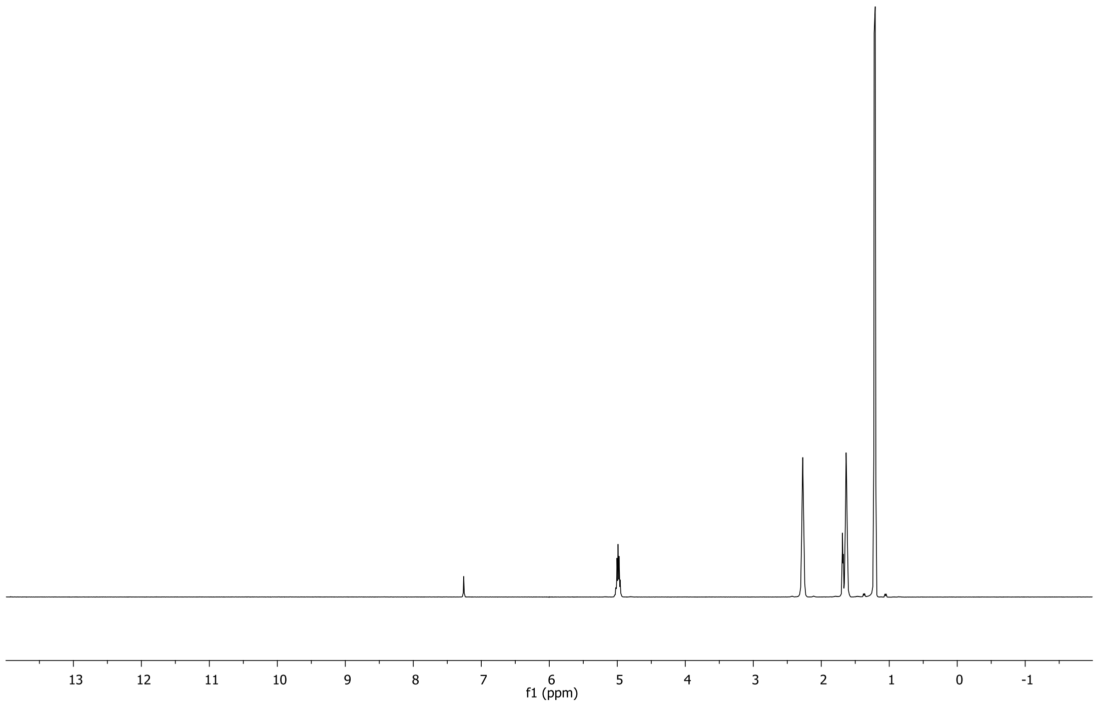

Figure A9 ^{1}H-NMR spectrum of DIAD.

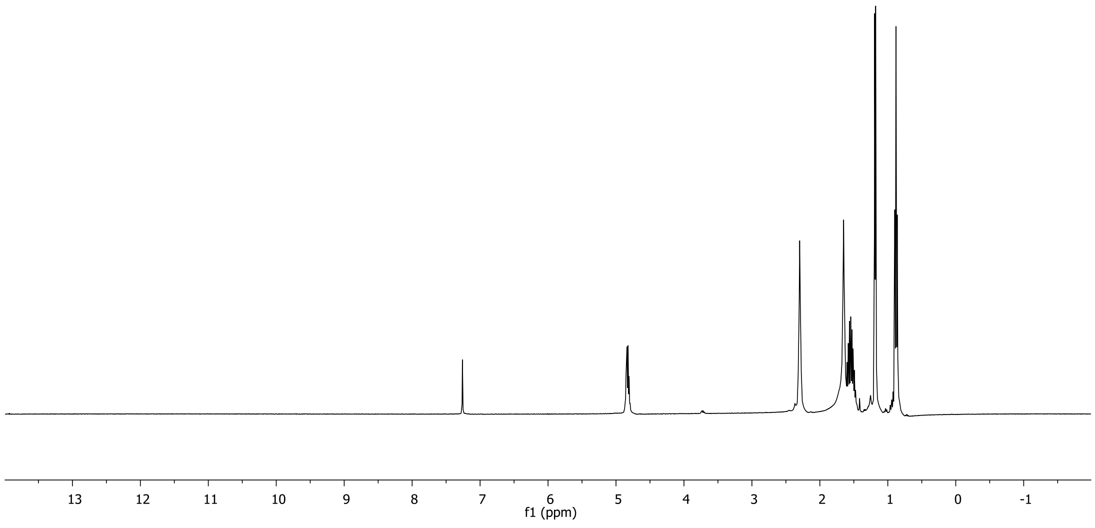

Figure A10 ^{1}H-NMR spectrum of DBAD.

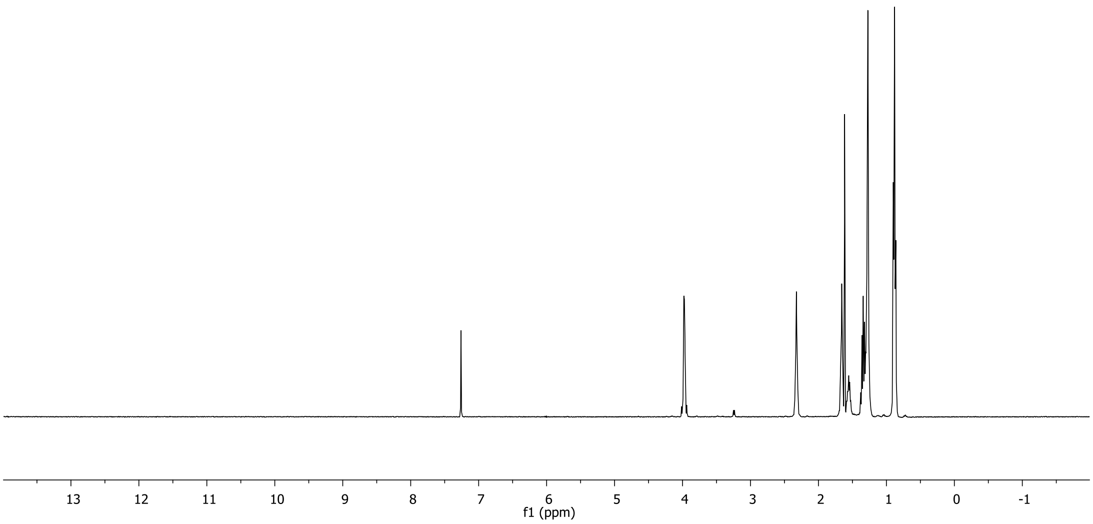

Figure A11 ^{1}H-NMR spectrum of DEAD.

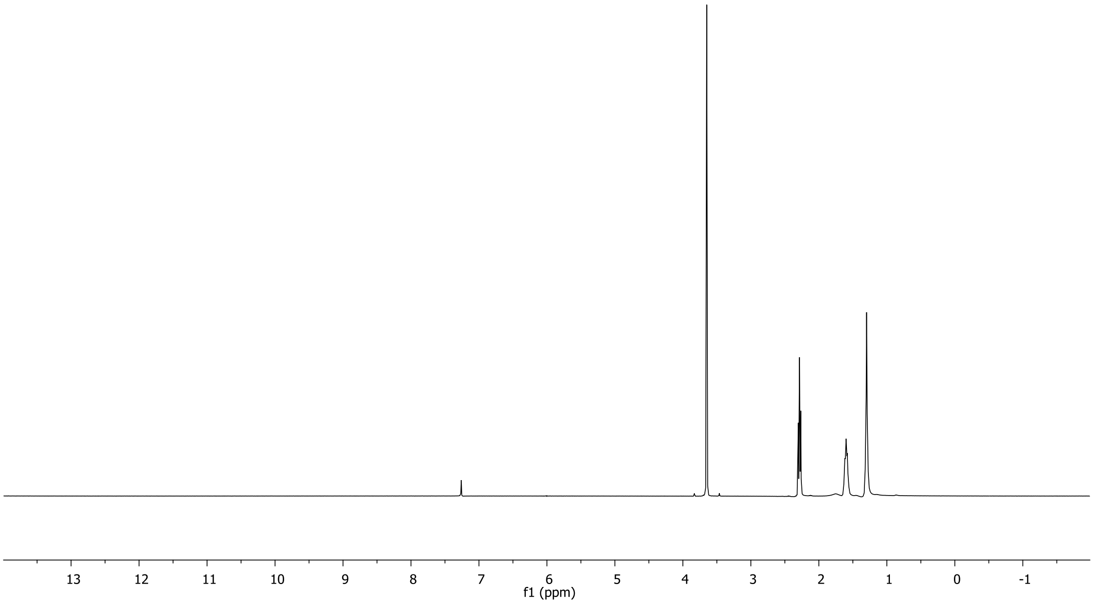

Figure A12 ^{1}H-NMR spectrum of DMAZ.

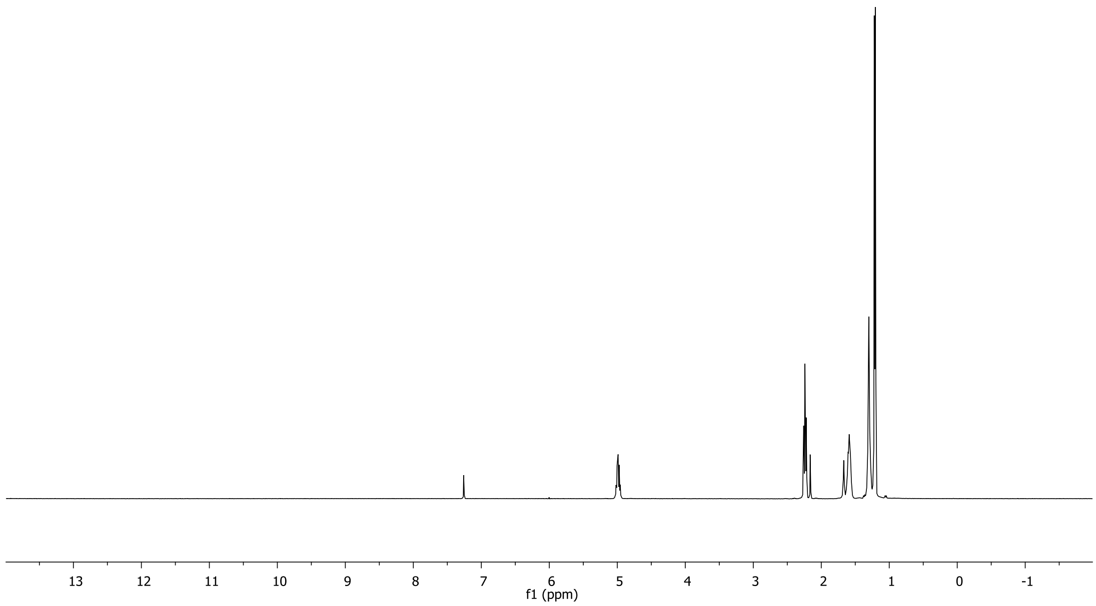

Figure A13 ^{1}H-NMR spectrum of DIAZ.

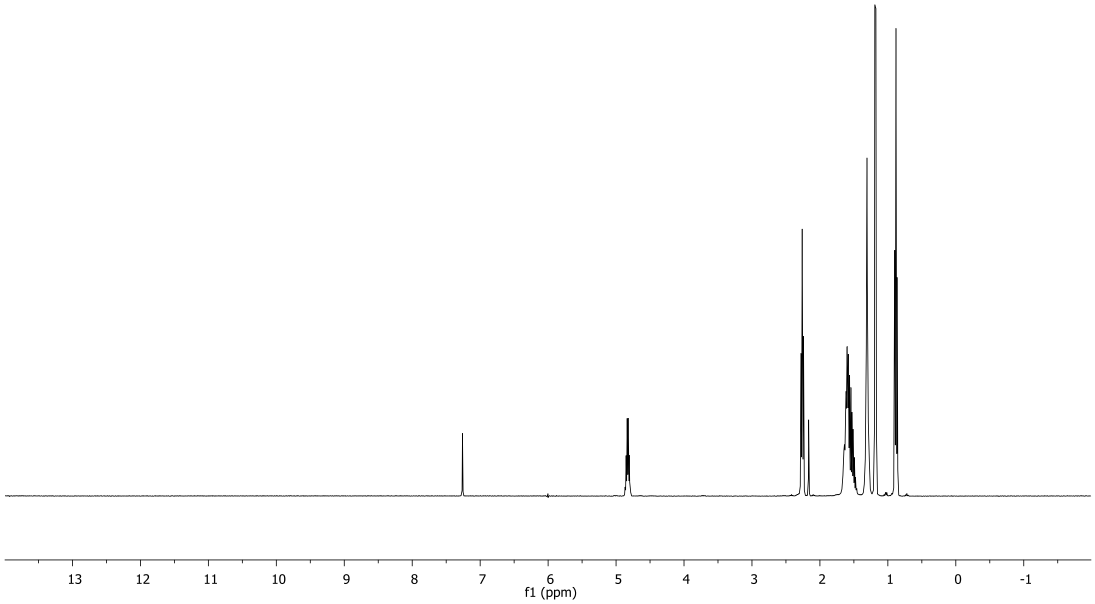

Figure A14 ^{1}H-NMR spectrum of DBAZ.

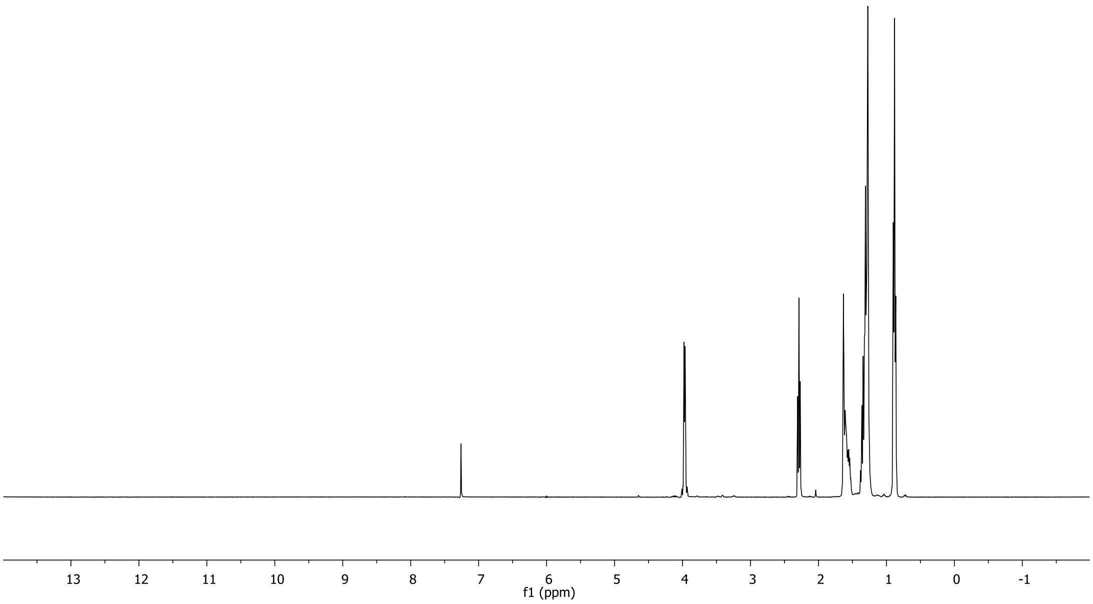

Figure A15 ^{1}H-NMR spectrum of DEAZ.

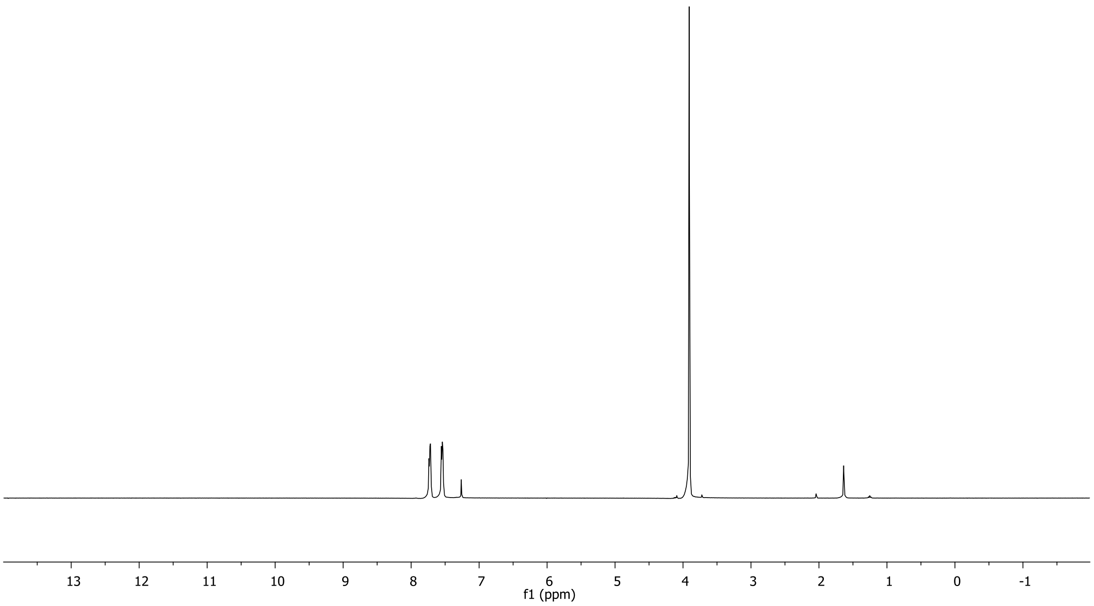

Figure A16 ^{1}H-NMR spectrum of DMP.

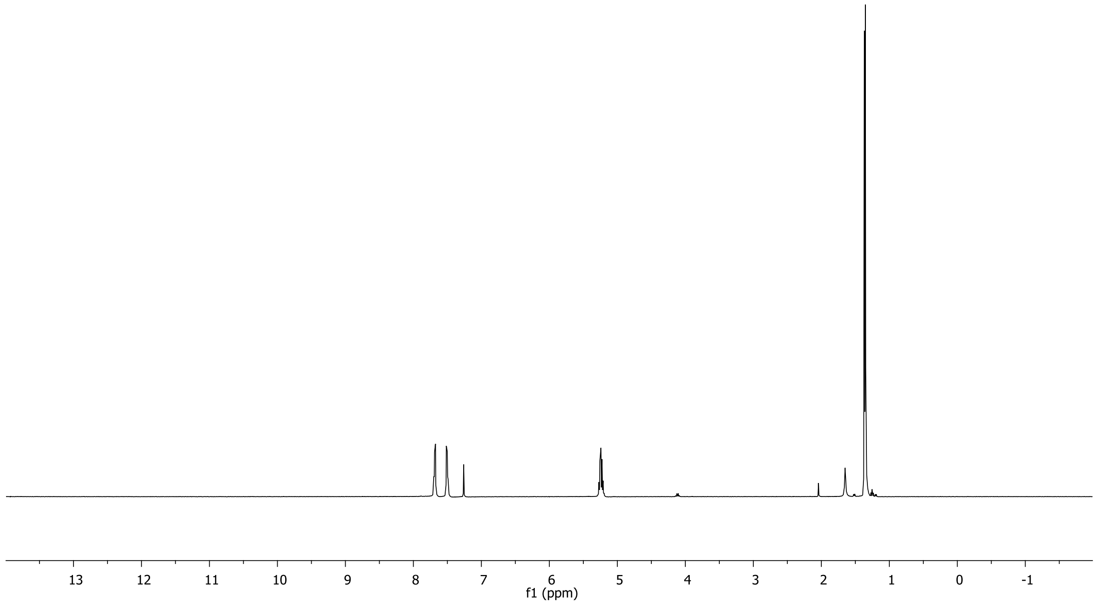

Figure A17 ^{1}H-NMR spectrum of DIP.

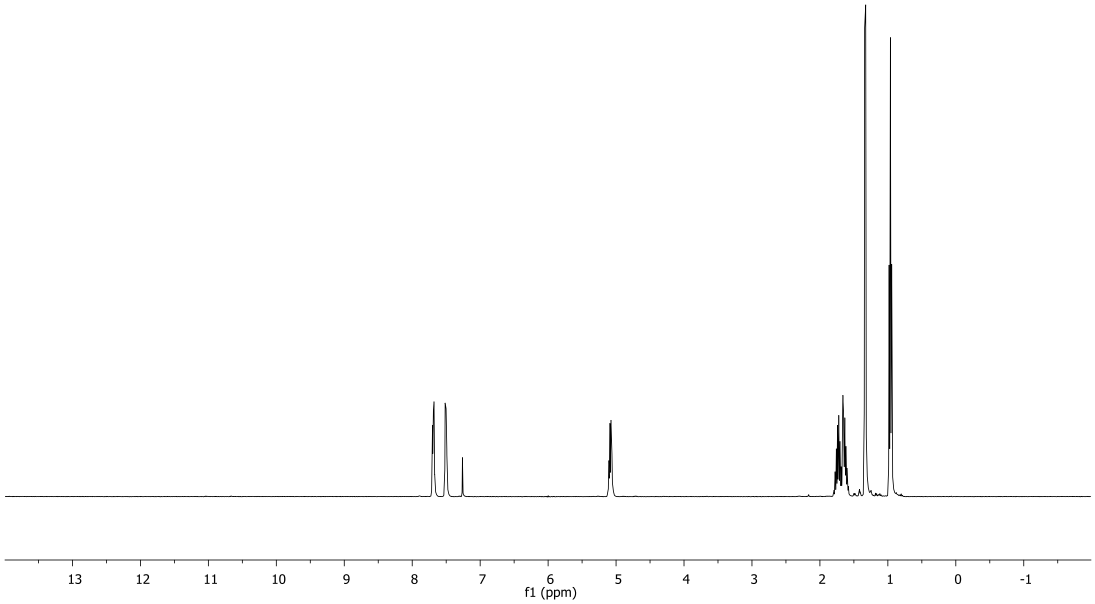

Figure A18 ^{1}H-NMR spectrum of DBP.

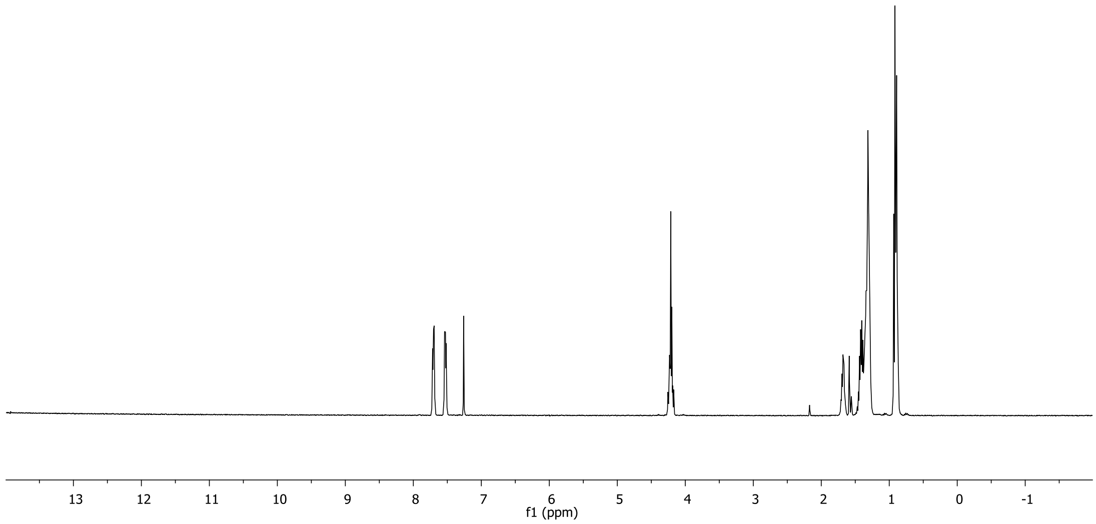

Figure A19 ^{1}H-NMR spectrum of DEP.

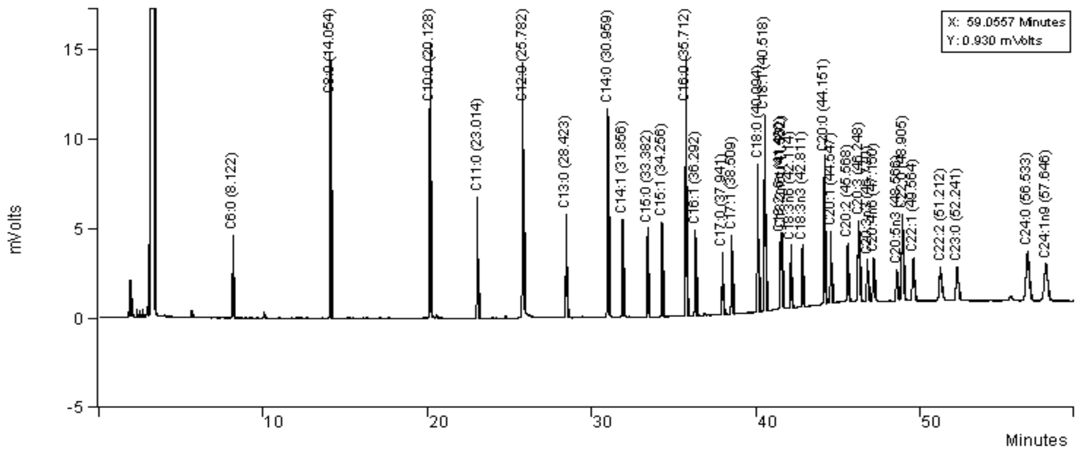

Identification (Peak Name)	Retention time (min)
C6:0 (Caproic)	8.122
C8:0 (Caprylic)	14.054
C10:0 (Capric)	20.128
C11:0 (Undecanoic)	23.014
C12:0 (Lauric)	25.782
C13:0 (Tridecanoic)	28.423
C14:0 (Myristic)	30.959
C14:1 (Myristoleic)	31.856
C15:0 (Pentadecanoic)	33.382
C15:1 (cis-10-Pentadecenoic)	34.256
C16:0 (Palmitic)	35.712
C16:1 (Palmitoleic)	36.292
C17:0 (Heptadecanoic) (Internal standard)	37.941
C17:1 (cis-10-Heptadecenoic)	38.509
C18:0 (Stearic)	40.094
C18:1n9c (Oleic)	40.518
C18:1n9t (Elaidic)	40.612
C18:2n6c (Linoleic)	41.480
C18:2n6t (Linolelaidic)	41.552
C18:3n6 (γ-Linolenic)	42.114
C18:3n3 (α-Linolenic)	42.811
C20:0 (Arachidic)	44.151
C20:1n9 (cis-11-Eicosenoic)	44.547
C20:2 (cis-11,14-Eicosadienoic)	45.568
C20:3n6 (cis-8,11,14-Eicosatrienoic)	46.248
C20:3n3 (cis-11,14,17-Eicosatrienoic)	46.770
C20:4n6 (Arachidonic)	47.150
C20:5n3 (cis-5,8,11,14,17-Eicosapentaenoic)	48.566
C22:0 (Behenic)	48.905
C22:1n9 (Erucic)	49.564
C22:2 (cis-13,16-Docosadienoic)	51.212
C23:0 (Tricosanoic)	52.241
C24:0 (Lignoceric)	56.533
C24:1n9 (Nervonic)	57.646

Figure A20 GC chromatogram of 37 FAMEs standard.

Data File: c:\star\joe\ptt glycerin\soybean bd
Channel: Front = FID RESULTS
Sample ID: soybean BD
Operator (Inj): bew
Injection Date: 19/04/2012 16:46:48
Injection Method: c:\labchem07\new method jo-1.2.mth
Run Time (min): 59.440
Workstation:
Instrument (Inj): gc

Operator (Calc): bew
Calc Date: 19/04/2012 18:22:49
Times Calculated: 11
Calculation Method: soybean bd 4;46;48 pm-front.mth
Instrument (Calc): gc
Run Mode: Analysis
Peak Measurement: Peak Area
Calculation Type: Percent
Calibration Level: N/A
Verification Tolerance: N/A

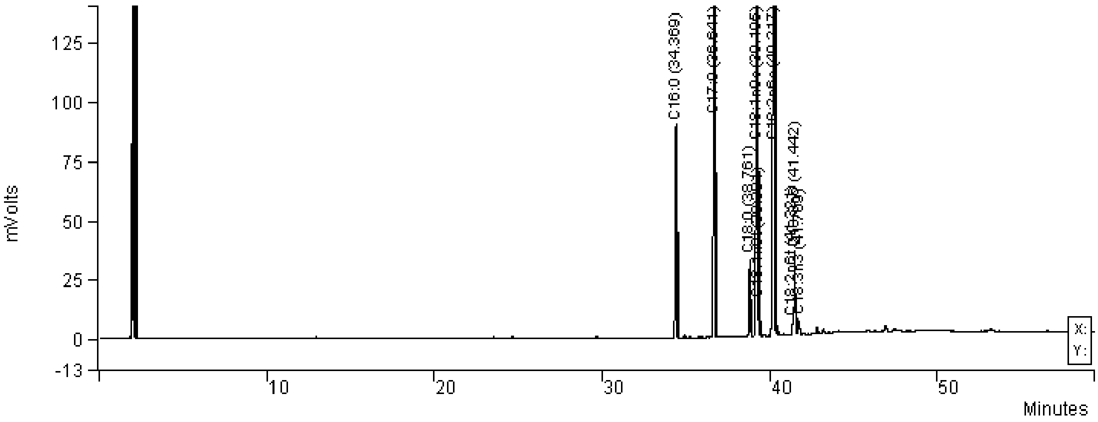

Peak No	Peak Name	Result()	Ret Time (min)	Time Offset (min)	Peak Area (counts)	Rel Ret Time	Sep. Code	Width 1/2 (sec)	Status Codes	Group
1	C16:0	9.0685	34.369	-0.312	429987	0.00	VB	4.5		0
2	C17:0	18.6961	36.641	-0.197	886487	0.00	VP	5.2		0
3	C18:0	3.5079	38.761	0.000	166329	0.00	BV	4.9		0
4	C18:1n9c	20.1584	39.195	0.000	955822	0.00	VV	5.3		0
5	C18:1n9t	1.0664	39.301	0.000	50564	0.00	VP	4.0		0
6	C18:2n6c	42.8505	40.217	-0.000	2451785	0.00	VP	6.2		0
7	C18:2n6t	0.5126	41.321	-0.000	24304	0.00	VV	5.6		0
8	C18:3n6	3.5126	41.442	-0.000	167647	0.00	VV	4.5		0
9	C18:3n3	0.6040	41.709	0.078	28638	0.00	VV	5.3		0
	Totals	**100.0001**		**-0.431**	5161563					

Figure A21 GC chromatogram of SME.

Data File: c:\star\joe\ptt glycerin\palm bd
Channel: Front = FID RESULTS
Sample ID: Palm BD
Operator (Inj): palm
Injection Date: 19/04/2012 14:04:00
Injection Method: c:\labchem07\new method jo-1.2.mth
Run Time (min): 59.440
Workstation:
Instrument (Inj): gc

Operator (Calc): palm
Calc Date: 19/04/2012 15:22:28
Times Calculated: 6
Calculation Method: palm bd 2;04;00 pm-front.mth
Instrument (Calc): gc
Run Mode: Analysis
Peak Measurement: Peak Area
Calculation Type: Percent
Calibration Level: N/A
Verification Tolerance: N/A

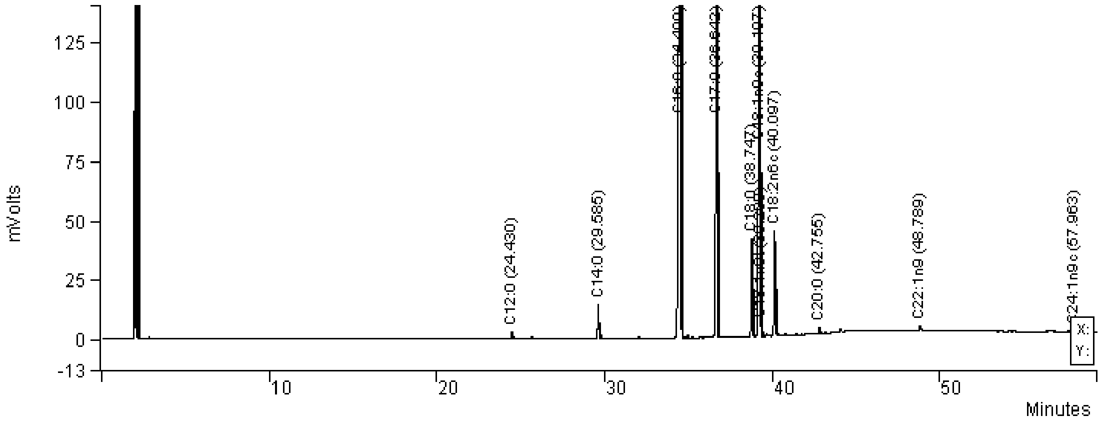

Peak No	Peak Name	Result()	Ret Time (min)	Time Offset (min)	Peak Area (counts)	Rel Ret Time	Sep. Code	Width 1/2 (sec)	Status Codes	Group
1	C12:0	0.1988	24.430	-0.205	11082	0.00	BB	4.0		0
2	C14:0	1.1397	29.585	-0.260	63534	0.00	VB	4.1		0
3	C16:0	51.9883	34.499	-0.182	2998134	0.00	VP	7.5		0
4	C17:0	17.6143	36.642	-0.196	981922	0.00	PP	5.4		0
5	C18:0	3.8784	38.747	0.000	216204	0.00	BV	4.9		0
6	C18:1n9c	20.2319	39.197	0.000	1257847	0.00	VV	5.5		0
7	C18:1n9t	0.2628	39.290	0.090	14652	0.00	VP	3.5		0
8	C18:2n6c	3.8833	40.097	-0.303	216479	0.00	BV	4.5		0
9	C20:0	0.2535	42.755	0.000	14133	0.00	BV	4.9		0
10	C22:1n9	0.3573	48.789	-0.000	19918	0.00	BB	7.6		0
11	C24:1n9c	0.1917	57.963	-0.000	10686	0.00	BB	17.7		0
	Totals	**100.0000**		**-1.056**	**5804591**					

Figure A22 GC chromatogram of PME.

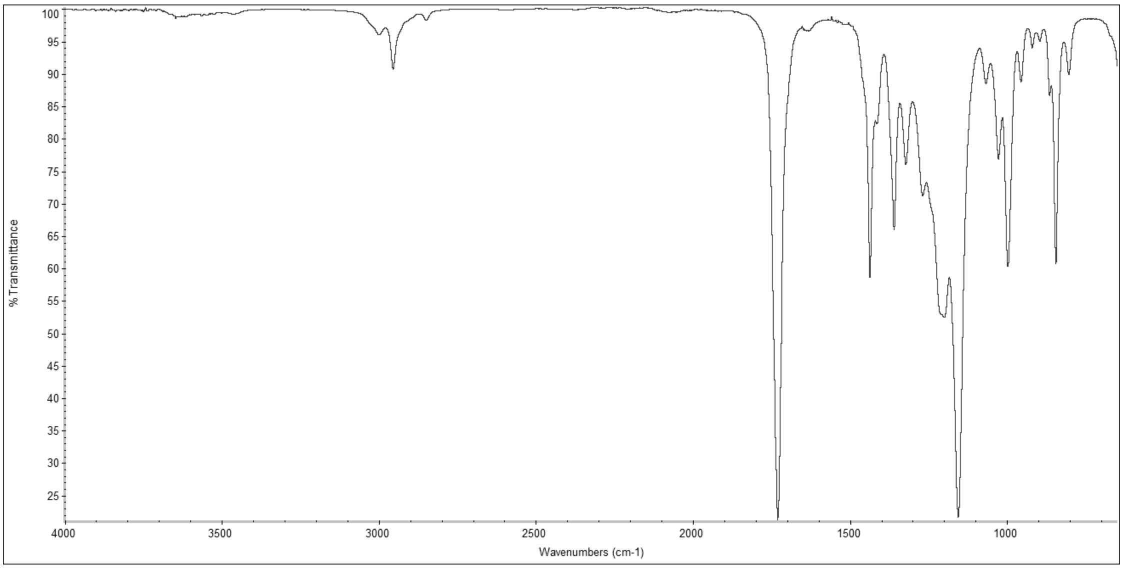

Figure A23 FT-IR spectrum of DMS.

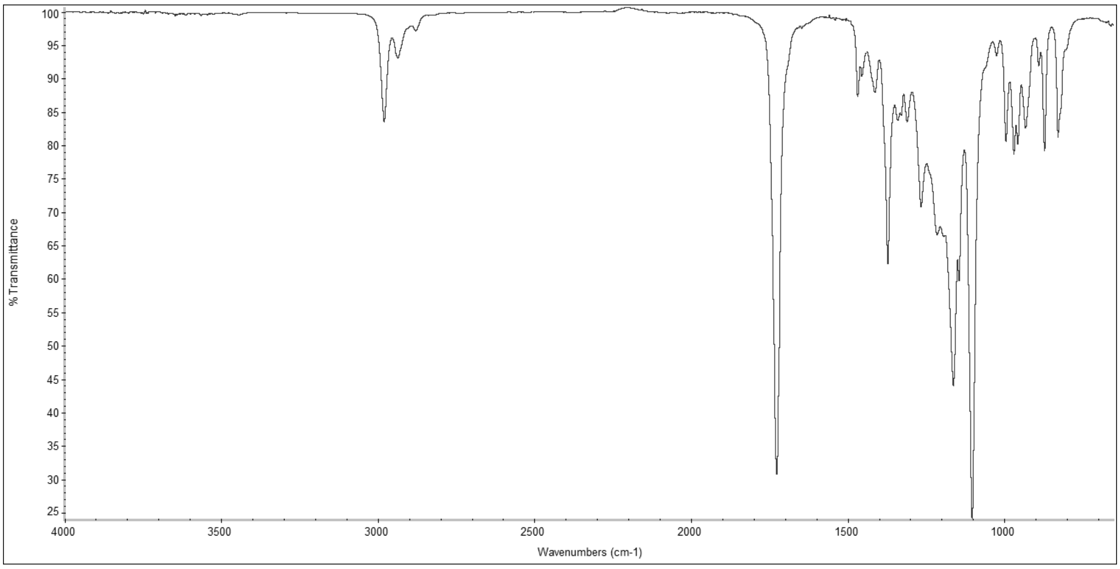

Figure A24 FT-IR spectrum of DIS.

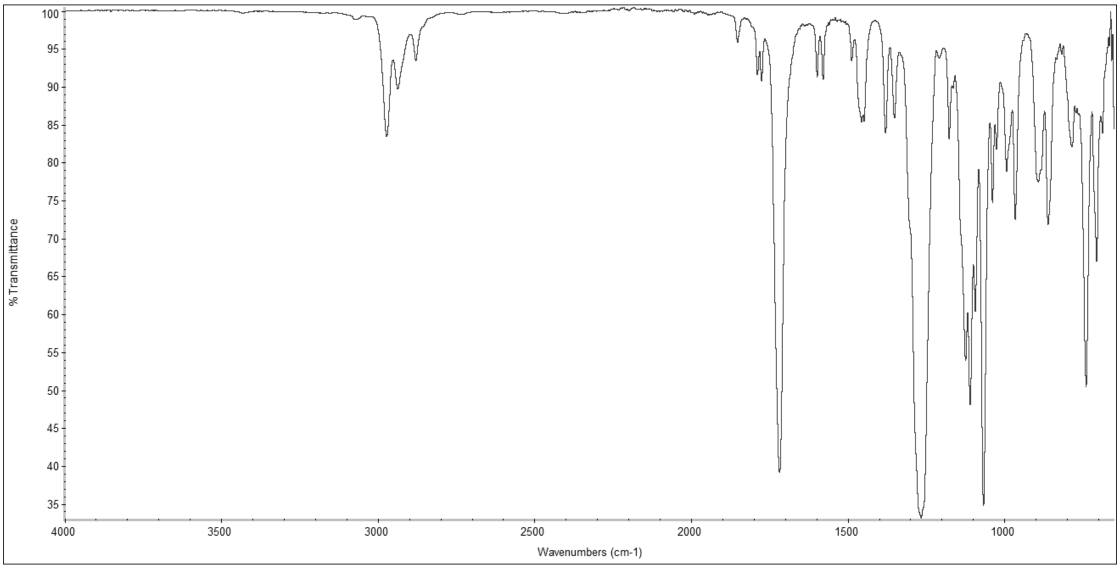

Figure A25 FT-IR spectrum of DBS.

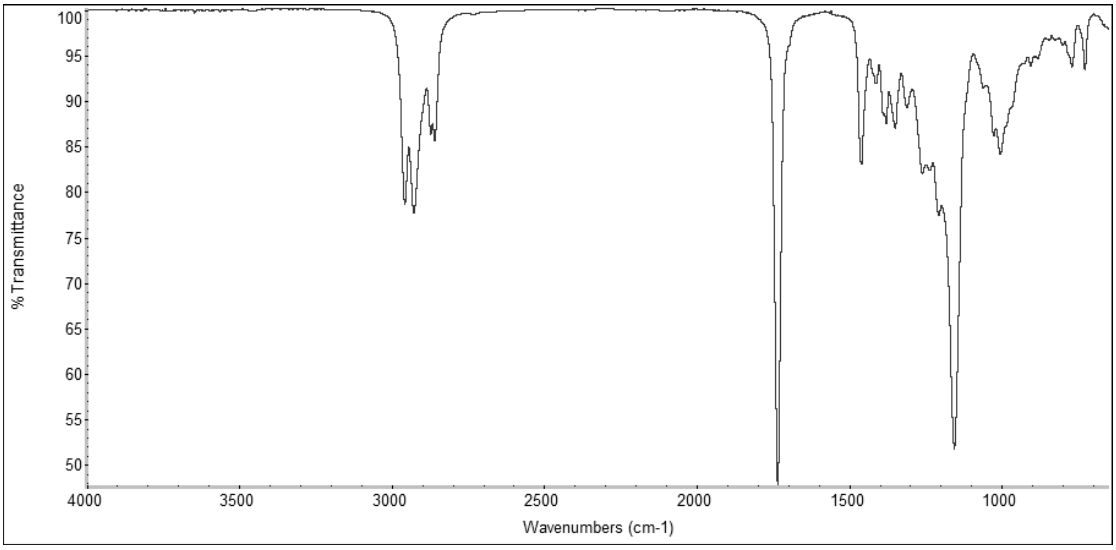

Figure A26 FT-IR spectrum of DES.

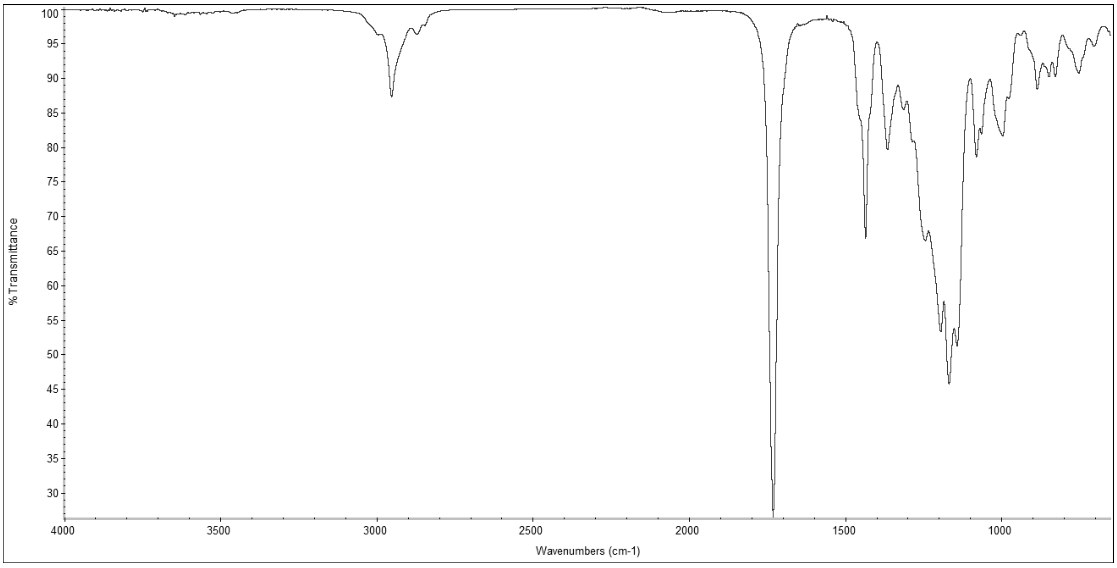

Figure A27 FT-IR spectrum of DMAD.

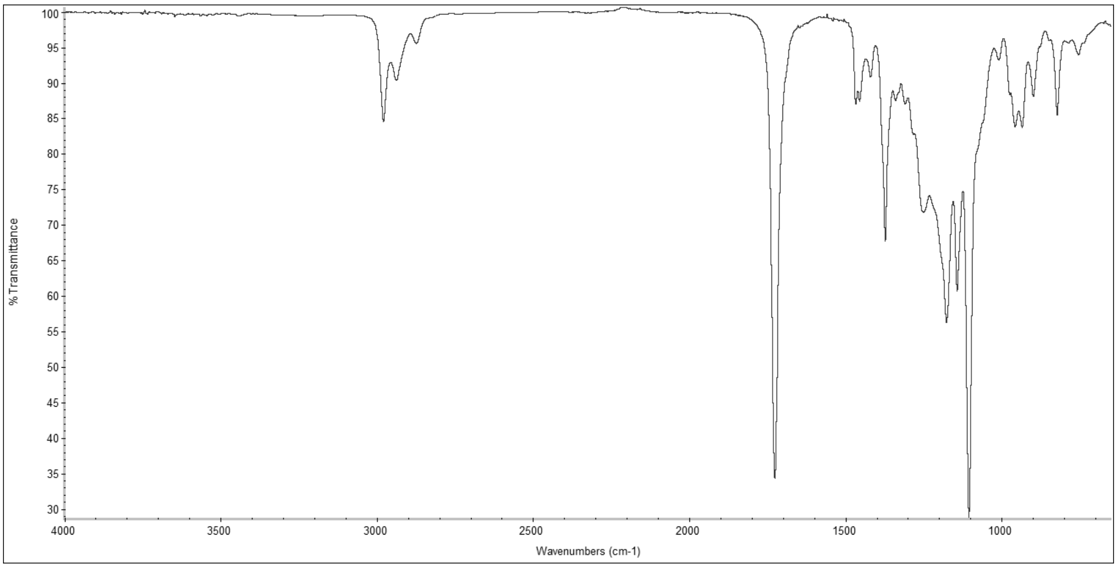

Figure A28 FT-IR spectrum of DIAD.

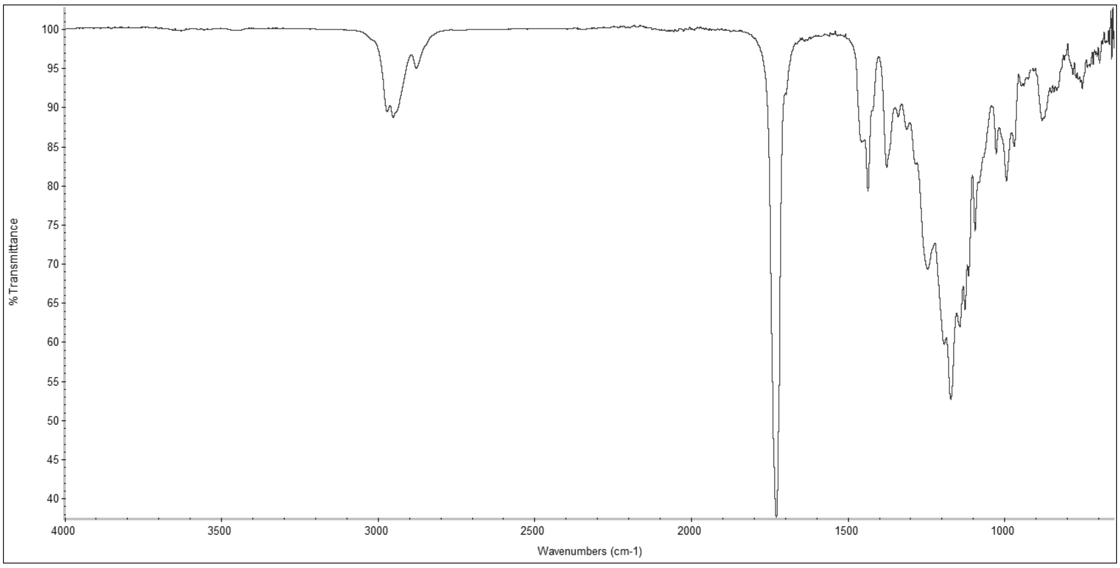

Figure A29 FT-IR spectrum of DBAD.

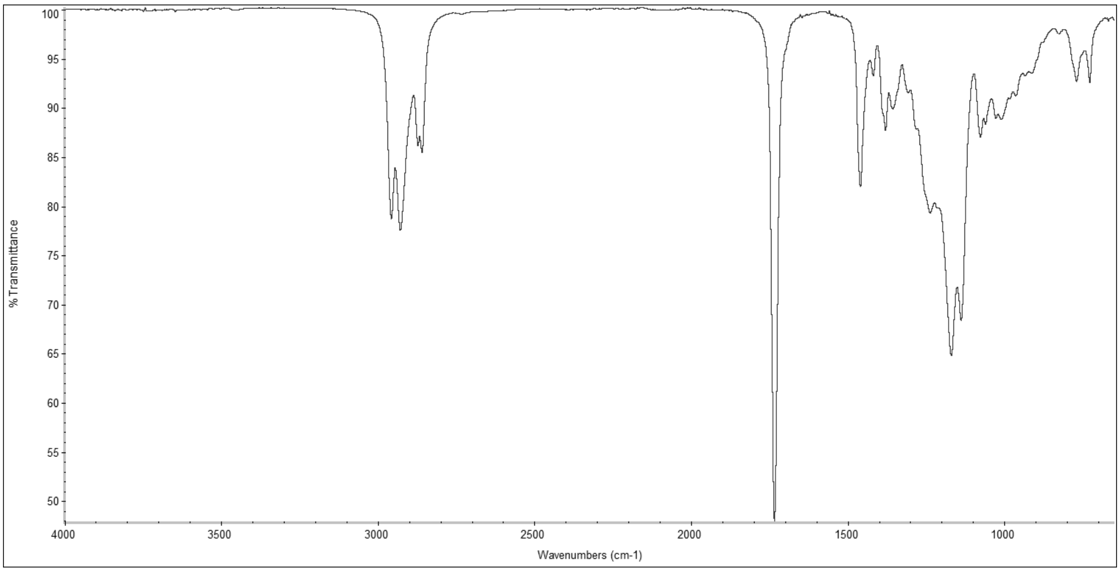

Figure A30 FT-IR spectrum of DEAD.

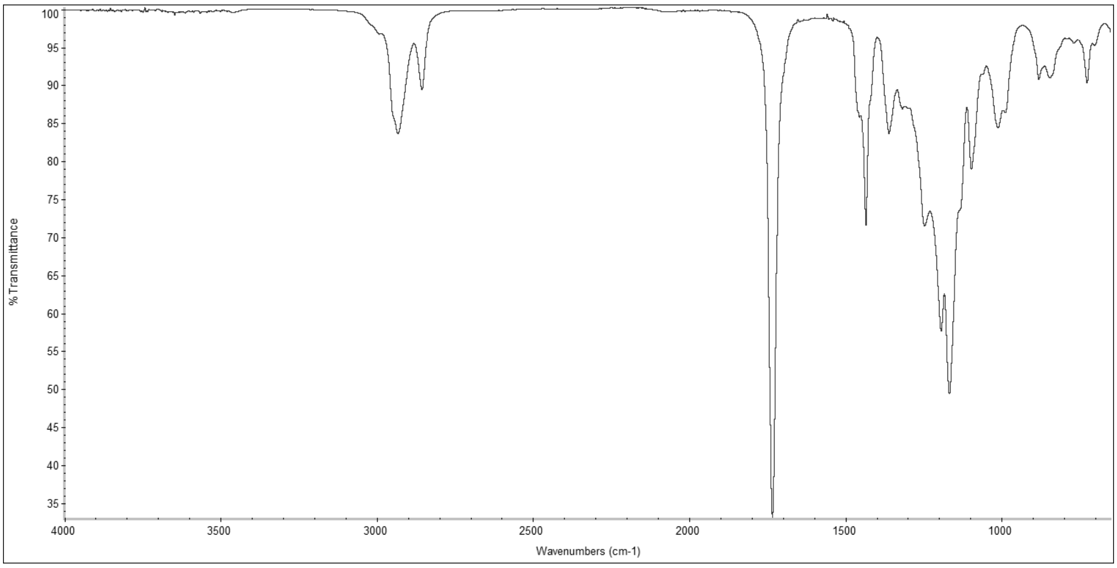

Figure A31 FT-IR spectrum of DMAZ.

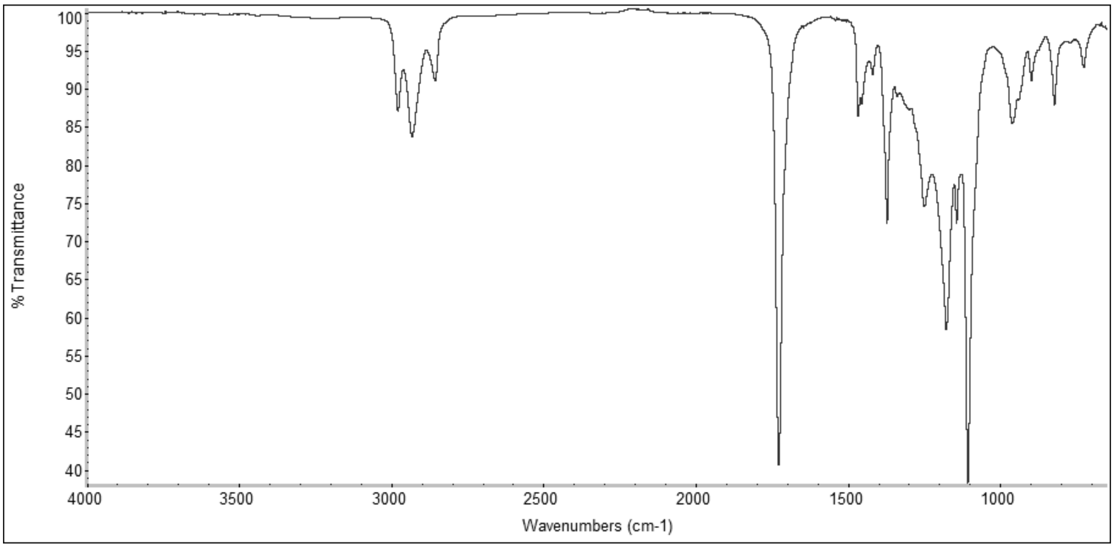

Figure A32 FT-IR spectrum of DIAZ.

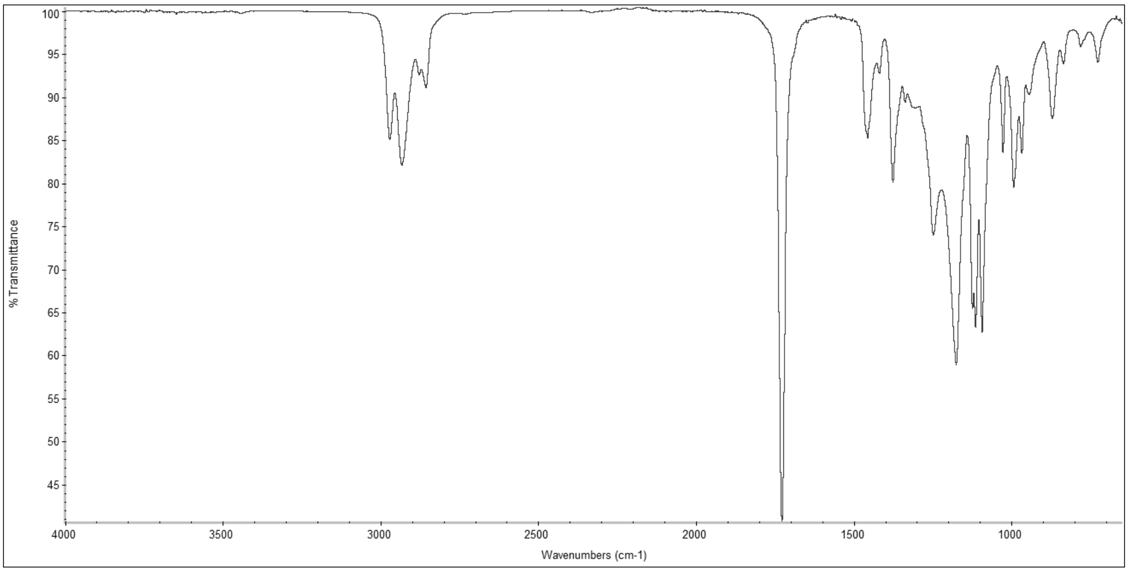

Figure A33 FT-IR spectrum of DBAZ.

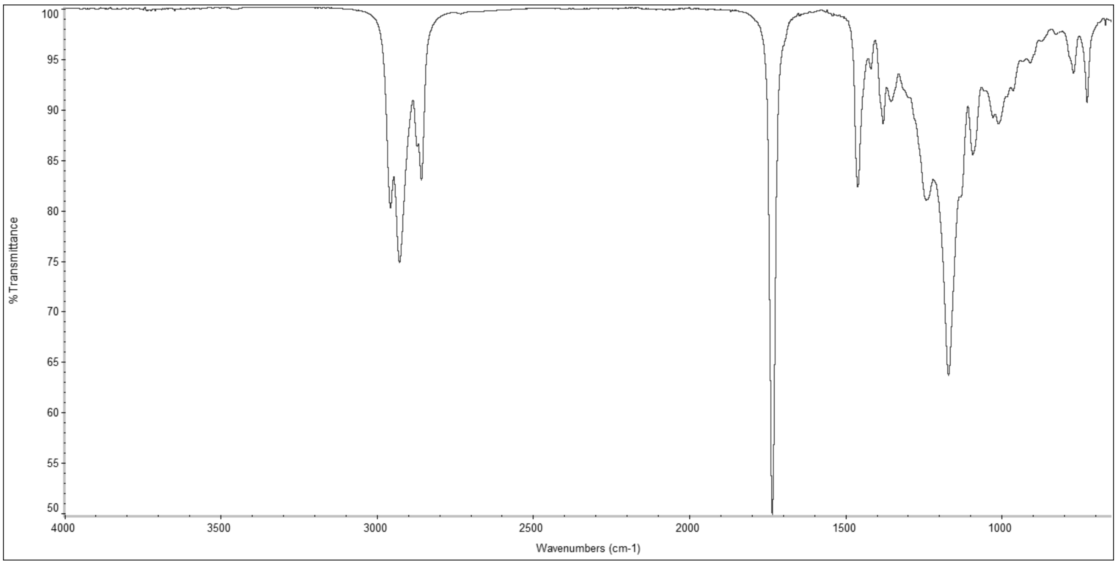

Figure A34 FT-IR spectrum of DEAZ.

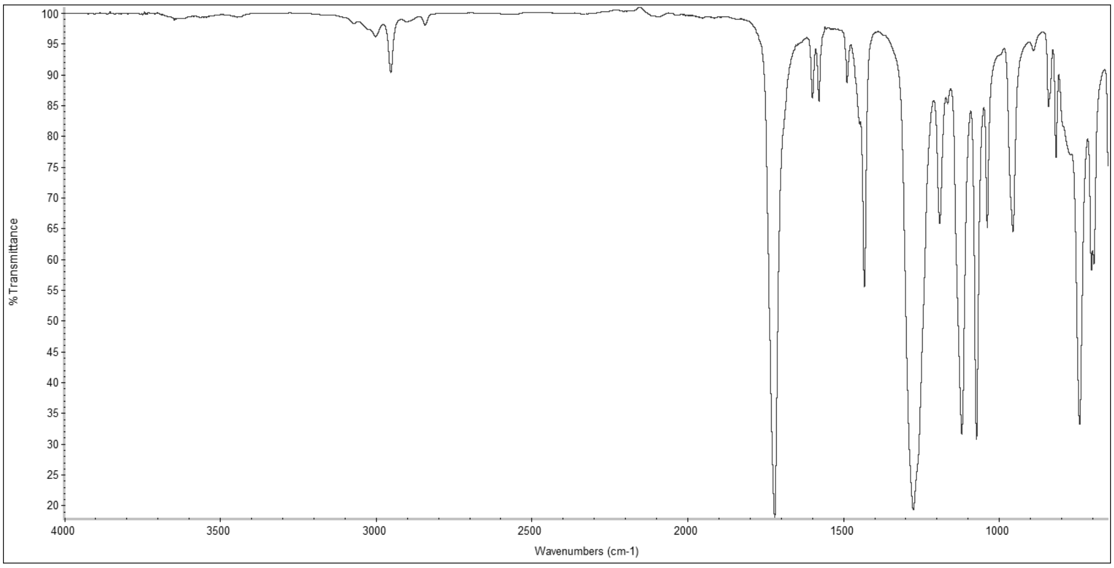

Figure A35 FT-IR spectrum of DMP.

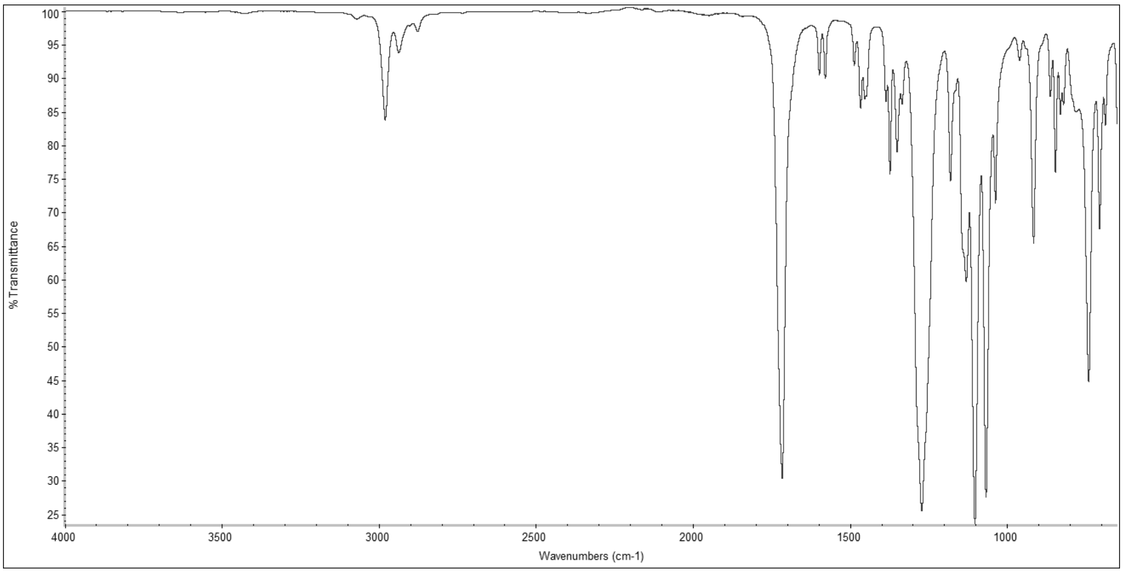

Figure A36 FT-IR spectrum of DIP.

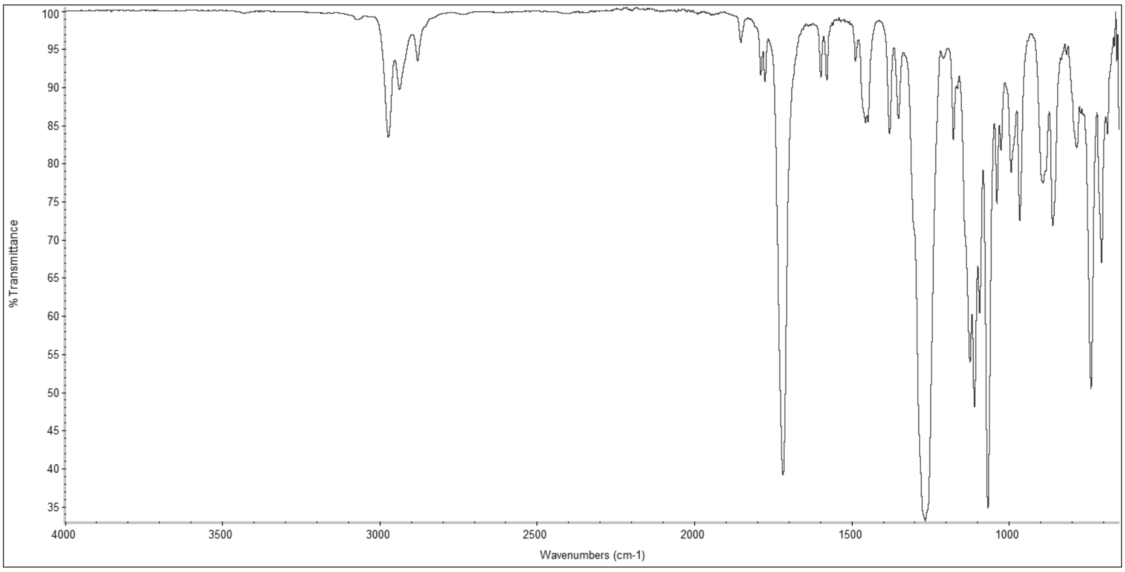

Figure A37 FT-IR spectrum of DBP.

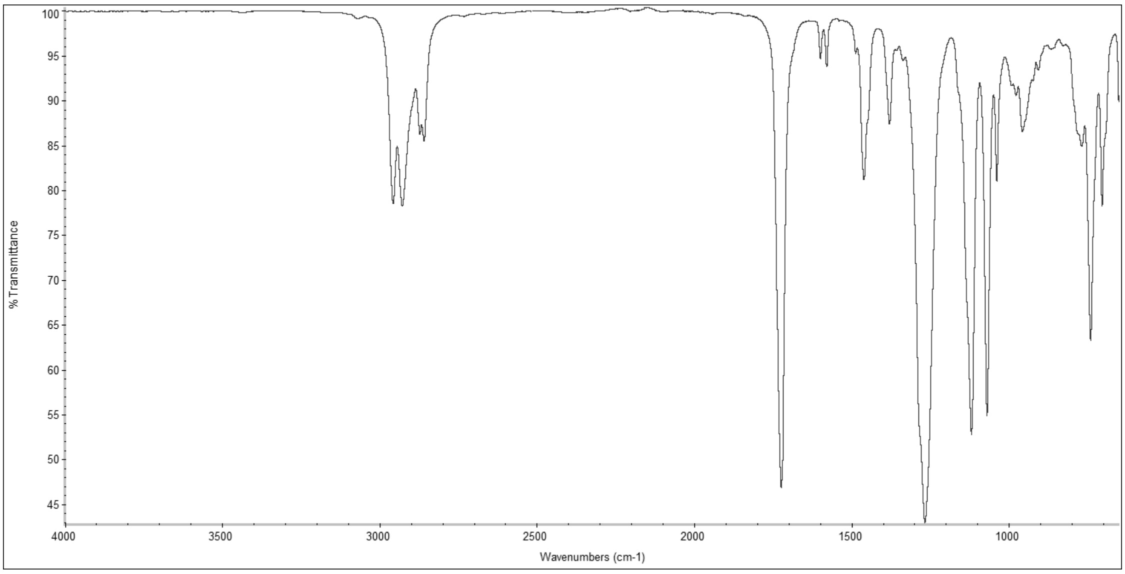

Figure A38 FT-IR spectrum of DEP.

APPENDIX B

VALUES OF CLOUD POINT AND POUR POINT OF SME AND PME

Table B1 Values of CP and PP of SME when using DMS as PPD.

Conc.(ppm)	CP (°C)			PP (°C)		
	CP_1	**CP_2**	**CP_{ave}**	**PP_1**	**PP_2**	**PP_{ave}**
0	2	2	2.00	0	0	0.00
10000	2	2	2.00	-0.2	-0.2	-0.20
100000	-0.2	-0.1	-0.15	-1.7	-1.7	-1.70
300000	-1.9	-1.7	-1.80	-2	-2	-2.00

Table B2 Values of CP and PP of PME when using DMS as PPD.

Conc.(ppm)	CP (°C)			PP (°C)		
	CP_1	**CP_2**	**CP_{ave}**	**PP_1**	**PP_2**	**PP_{ave}**
0	21	21	21.00	19	19	19.00
10000	20.9	20.7	20.80	18.5	18.5	18.50
100000	18.9	18.9	18.90	17.5	17.5	17.50
300000	16,5	16.5	16.50	14.3	14.3	14.30

Table B3 Values of CP and PP of SME using DIS as PPDs.

Conc.(ppm)	CP			PP		
	CP_1	**CP_2**	**CP_{ave}**	**PP_1**	**PP_2**	**PP_{ave}**
0	2	2	2.00	0	0	0.00
10000	1.6	1.5	1.55	-0.4	-0.4	-0.40
100000	-0.5	-0.5	-0.50	-2.2	-2.2	-2.20
300000	-2.5	-2.5	-2.50	-4.3	-4.3	-4.30

Table B4 Values of CP and PP of SME using DIS as PPDs.

Conc.(ppm)	CP			PP		
	CP_1	**CP_2**	**CP_{ave}**	**PP_1**	**PP_2**	**PP_{ave}**
0	21	21	21.00	19	19	19.00
10000	20.5	20.5	20.50	18.3	18.3	18.30
100000	18.4	18.4	18.40	16.8	16.8	16.80
300000	15.7	15.7	15.70	13.5	13.5	13.50

Table B5 Values of CP and PP of SME using DBS as PPDs.

Conc.(ppm)	**CP**			**PP**		
	CP_1	**CP_2**	**CP_{ave}**	**PP_1**	**PP_2**	**PP_{ave}**
0	2	2	2.00	0	0	0.00
10000	1.2	1.4	1.30	-0.7	-0.7	-0.70
100000	-0.8	-0.8	-0.80	-2	-2	-2.00
300000	-2.8	-2.8	-2.80	-4.7	-4.7	-4.70

Table B6 Values of CP and PP of Palm using DBS as PPDs.

Conc.(ppm)	**CP**			**PP**		
	CP_1	**CP_2**	**CP_{ave}**	**PP_1**	**PP_2**	**PP_{ave}**
0	21	21	21.00	19	19	19.00
10000	20.4	20.2	20.30	18	18	18.00
100000	18	18.2	18.10	16.5	16.5	16.50
300000	15.5	15.3	15.40	13.3	13.3	13.30

Table B7 Values of CP and PP of SME using DES as PPDs.

Conc.(ppm)	**CP**			**PP**		
	CP_1	**CP_2**	**CP_{ave}**	**PP_1**	**PP_2**	**PP_{ave}**
0	2	2	2.00	0	0	0.00
10000	1.7	1.7	1.70	-0.2	-0.2	-0.20
100000	-0.4	-0.4	-0.40	-1.9	-1.9	-1.90
300000	-2.2	-2.2	-2.20	-3.6	-3.6	-3.60

Table B8 Values of CP and PP of PME using DES as PPDs.

Conc.(ppm)	**CP**			**PP**		
	CP_1	**CP_2**	**CP_{ave}**	**PP_1**	**PP_2**	**PP_{ave}**
0	21	21	21.00	19	19	19.00
10000	20.6	20.7	20.65	18.5	18.5	18.50
100000	18.6	18.6	18.60	17.3	17.3	17.30
300000	16	16	16.00	13.7	13.7	13.70

Table B9 Values of CP and PP of SME using DMAD as PPDs.

Conc.(ppm)	**CP**			**PP**		
	CP_1	**CP_2**	**CP_{ave}**	**PP_1**	**PP_2**	**PP_{ave}**
0	2	2	2.00	0	0	0.00
10000	1.8	1.8	1.80	-0.5	-0.5	-0.50
100000	-0.1	-0.1	-0.10	-1.8	-1.8	-1.80
300000	-1.8	-1.8	-1.80	-3.4	-3.4	-3.40

Table B10 Values of CP and PP of PME using DMAD as PPDs.

Conc.(ppm)	**CP**			**PP**		
	CP_1	**CP_2**	**CP_{ave}**	**PP_1**	**PP_2**	**PP_{ave}**
0	21	21	21.00	19	19	19.00
10000	20.6	20.7	20.65	18.5	18.5	18.50
100000	19	18.8	18.90	17.5	17.5	17.50
300000	16.6	16.6	16.60	14.2	14.2	14.20

Table B11 Values of CP and PP of SME using DIAD as PPDs.

Conc.(ppm)	**CP**			**PP**		
	CP_1	**CP_2**	**CP_{ave}**	**PP_1**	**PP_2**	**PP_{ave}**
0	2	2	2.00	0	0	0.00
10000	1.5	1.5	1.50	-0.4	-0.4	-0.40
100000	-0.7	-0.6	-0.65	-2.3	-2.3	-2.30
300000	-2.6	-2.6	-2.60	-4.3	-4.3	-4.30

Table B12 Values of CP and PP of PME using DIAD as PPDs.

Conc.(ppm)	**CP**			**PP**		
	CP_1	**CP_2**	**CP_{ave}**	**PP_1**	**PP_2**	**PP_{ave}**
0	21	21	21.00	19	19	19.00
10000	20.1	20.3	20.20	18.2	18.2	18.20
100000	18.3	18.3	18.30	16.7	16.7	16.70
300000	15.5	15.5	15.50	13.4	13.4	13.40

Table B13 Values of CP and PP of SME using DBAD as PPDs.

Conc.(ppm)	CP			PP		
	CP_1	CP_2	CP_{ave}	PP_1	PP_2	PP_{ave}
0	2	2	2.00	0	0	0.00
10000	1.3	1.3	1.30	-0.7	-0.7	-0.70
100000	-0.8	-0.8	-0.80	-2.1	-2.1	-2.10
300000	-2.8	-2.8	-2.80	-5.7	-5.7	-5.00

Table B14 Values of CP and PP of PME using DBAD as PPDs.

Conc.(ppm)	CP			PP		
	CP_1	CP_2	CP_{ave}	PP_1	PP_2	PP_{ave}
0	21	21	21.00	19	19	19.00
10000	19.8	20	19.90	18.1	18.1	18.10
100000	18	18	18.00	16.3	16.3	16.30
300000	15.3	15.3	15.30	13.2	13.2	13.20

Table B15 Values of CP and PP of SME using DES as PPDs.

Conc.(ppm)	CP			PP		
	CP_1	CP_2	CP_{ave}	PP_1	PP_2	PP_{ave}
0	2	2	2.00	0	0	0.00
10000	1.6	1.6	1.60	-0.6	-0.6	-0.60
100000	-0.5	-0.5	-0.50	-1.8	-1.8	-1.80
300000	-2.4	-2.5	-2.45	-3.9	-3.9	-3.90

Table B16 Values of CP and PP of PME using DES as PPDs.

Conc.(ppm)	CP			PP		
	CP_1	CP_2	CP_{ave}	PP_1	PP_2	PP_{ave}
0	21	21	21.00	19	19	19.00
10000	20.3	20.5	20.40	18.4	18.4	18.40
100000	18.5	18.5	18.50	16.9	16.9	16.90
300000	16.5	16.5	16.50	13.7	13.7	13.70

Table B17 Values of CP and PP of SME using DMAZ as PPDs.

Conc.(ppm)	CP			PP		
	CP_1	CP_2	CP_{ave}	PP_1	PP_2	PP_{ave}
0	2	2	2.00	0	0	0.00
10000	1.9	1.7	1.80	-0.2	-0.2	-0.20
100000	-0.3	-0.3	-0.30	-1.8	-1.8	-1.80
300000	-2	-2	-2.00	-4.5	-4.5	-4.50

Table B18 Values of CP and PP of PME using DMAZ as PPDs.

Conc.(ppm)	CP			PP		
	CP_1	CP_2	CP_{ave}	PP_1	PP_2	PP_{ave}
0	21	21	21.00	19	19	19.00
10000	20.5	20.5	20.50	18.4	18.4	18.40
100000	18.7	18.7	18.70	17.3	17.3	17.30
300000	16.3	16.3	16.30	14	14	14.00

Table B19 Values of CP and PP of SME using DIAZ as PPDs.

Conc.(ppm)	CP			PP		
	CP_1	CP_2	CP_{ave}	PP_1	PP_2	PP_{ave}
0	2	2	2.00	0	0	0.00
10000	1.5	1.5	1.50	-0.5	-0.5	-0.50
100000	-0.7	-0.9	-0.85	-2.5	-2.5	-2.50
300000	-3	-2.8	-2.90	-5.2	-5.2	-5.20

Table B20 Values of CP and PP of PME using DIAZ as PPDs.

Conc.(ppm)	CP			PP		
	CP_1	CP_2	CP_{ave}	PP_1	PP_2	PP_{ave}
0	21	21	21.00	19	19	19.00
10000	20.3	20.4	20.35	18	18	18.00
100000	18	18	18.00	16.7	16.7	16.70
300000	15.3	15.4	15.35	13.2	13.2	13.20

Table B21 Values of CP and PP of SME using DBAZ as PPDs.

Conc.(ppm)	**CP**			**PP**		
	CP_1	**CP_2**	**CP_{ave}**	**PP_1**	**PP_2**	**PP_{ave}**
0	2	2	2.00	0	0	0.00
10000	1.2	1.2	1.20	-0.8	-0.8	-0.80
100000	-1	-1	-1.00	-2.8	-2.8	-2.80
300000	-3.1	-3.2	-3.15	-5.4	-5.4	-5.40

Table B22 Values of CP and PP of PME using DBAZ as PPDs.

Conc.(ppm)	**CP**			**PP**		
	CP_1	**CP_2**	**CP_{ave}**	**PP_1**	**PP_2**	**PP_{ave}**
0	21	21	21.00	19	19	19.00
10000	19.6	19.5	19.55	17.7	17.7	17.70
100000	17.8	17.8	17.80	16.2	16.2	16.20
300000	15	15	15.00	13	13	13.00

Table B23 Values of CP and PP of SME using DEAZ as PPDs.

Conc.(ppm)	**CP**			**PP**		
	CP_1	**CP_2**	**CP_{ave}**	**PP_1**	**PP_2**	**PP_{ave}**
0	2	2	2.00	0	0	0.00
10000	1.7	1.8	1.75	-0.3	-0.3	-0.30
100000	-0.4	-0.5	-0.45	-2.1	-2.1	-2.10
300000	-2.7	-2.7	-2.70	-4.9	-4.9	-4.90

Table B24 Values of CP and PP of PME using DEAZ as PPDs.

Conc.(ppm)	**CP**			**PP**		
	CP_1	**CP_2**	**CP_{ave}**	**PP_1**	**PP_2**	**PP_{ave}**
0	21	21	21.00	19	19	19.00
10000	20.6	20.4	20.50	18.4	18.4	18.40
100000	18.4	18.3	18.35	17	17	17.00
300000	15.9	16	15.90	13.7	13.7	13.70

Table B25 Values of CP and PP of SME using DMP as PPDs.

Conc.(ppm)	**CP**			**PP**		
	CP_1	**CP_2**	**CP_{ave}**	**PP_1**	**PP_2**	**PP_{ave}**
0	2	2	2.00	0	0	0.00
10000	1.5	1.5	1.50	-0.6	-0.6	-0.60
100000	-0.1	-0.1	-0.10	-1.4	-1.4	-1.40
300000	-0.8	-0.6	-0.70	-2.7	-2.7	-2.70

Table B26 Values of CP and PP of PME using DMP as PPDs.

Conc.(ppm)	**CP**			**PP**		
	CP_1	**CP_2**	**CP_{ave}**	**PP_1**	**PP_2**	**PP_{ave}**
0	21	21	21.00	19	19	19.00
10000	20.8	20.9	20.85	18.5	18.5	18.50
100000	19	19	19.00	17.3	17.3	17.30
300000	16.7	16.5	16.60	14.9	14.9	14.90

Table B27 Values of CP and PP of SME using DIP as PPDs.

Conc.(ppm)	**CP**			**PP**		
	CP_1	**CP_2**	**CP_{ave}**	**PP_1**	**PP_2**	**PP_{ave}**
0	2	2	2.00	0	0	0.00
10000	1.4	1.4	1.40	-1	-1	-1.00
100000	-0.3	-0.3	-0.30	-1.7	-1.7	-1.70
300000	1.2	1.2	-1.20	-4	-4	-4.00

Table B28 Values of CP and PP of PME using DIP as PPDs.

Conc.(ppm)	**CP**			**PP**		
	CP_1	**CP_2**	**CP_{ave}**	**PP_1**	**PP_2**	**PP_{ave}**
0	21	21	21.00	19	19	19.00
10000	20.5	20.6	20.55	18.2	18.2	18.20
100000	18.8	18.9	18.85	17.1	17.1	17.10
300000	15.3	15.5	15.40	14.5	14.5	14.50

Table B29 Values of CP and PP of SME using DBP as PPDs.

Conc.(ppm)	**CP**			**PP**		
	CP_1	**CP_2**	**CP_{ave}**	**PP_1**	**PP_2**	**PP_{ave}**
0	2	2	2.00	0	0	0.00
10000	1.3	1.1	1.20	-1	-1	-1.00
100000	-0.3	-0.4	-0.35	-1.9	-1.9	-1.90
300000	-1.4	-1.4	-1.40	-4.2	-4.2	-4.20

Table B30 Values of CP and PP of PME using DBP as PPDs.

Conc.(ppm)	**CP**			**PP**		
	CP_1	**CP_2**	**CP_{ave}**	**PP_1**	**PP_2**	**PP_{ave}**
0	21	21	21.00	19	19	19.00
10000	20.2	20.2	20.20	18.1	18.1	18.10
100000	18.9	18.8	18.85	16.9	16.9	16.90
300000	15.2	15.2	15.20	14.4	14.4	14.40

Table B31 Values of CP and PP of SME using DEP as PPDs.

Conc.(ppm)	**CP**			**PP**		
	CP_1	**CP_2**	**CP_{ave}**	**PP_1**	**PP_2**	**PP_{ave}**
0	2	2	2.00	0	0	0.00
10000	1.5	1.5	1.50	-0.7	-0.7	-0.70
100000	-0.1	-0.2	-0.15	-1.5	-1.5	-1.50
300000	-1.2	-1	-1.10	-3.4	-3.4	-3.40

Table B32 Values of CP and PP of PME using DEP as PPDs.

Conc.(ppm)	**CP**			**PP**		
	CP_1	**CP_2**	**CP_{ave}**	**PP_1**	**PP_2**	**PP_{ave}**
0	21	21	21.00	19	19	19.00
10000	20.5	20.5	20.50	18.3	18.3	18.30
100000	18.8	18.7	18.75	17.3	17.3	17.30
300000	15.5	15.3	15.40	14.7	14.7	14.70

APPENDIX C

CALCULATIONS

1. Calculated % ester content of SME and PME from ^{1}H-NMR spectrum

The percentage ester content of SME and PME was calculated as follow:

$$\boxed{\%\ \text{Ester content} = [(2I_{OMe}) / (3I_{CH2})] \times 100}$$

I_{OMe} = Integration value of the protons of the methyl esters, appear at δ 3.7 ppm

I_{CH2} = Integration value of the methylene protons, appear at δ 2.3 ppm

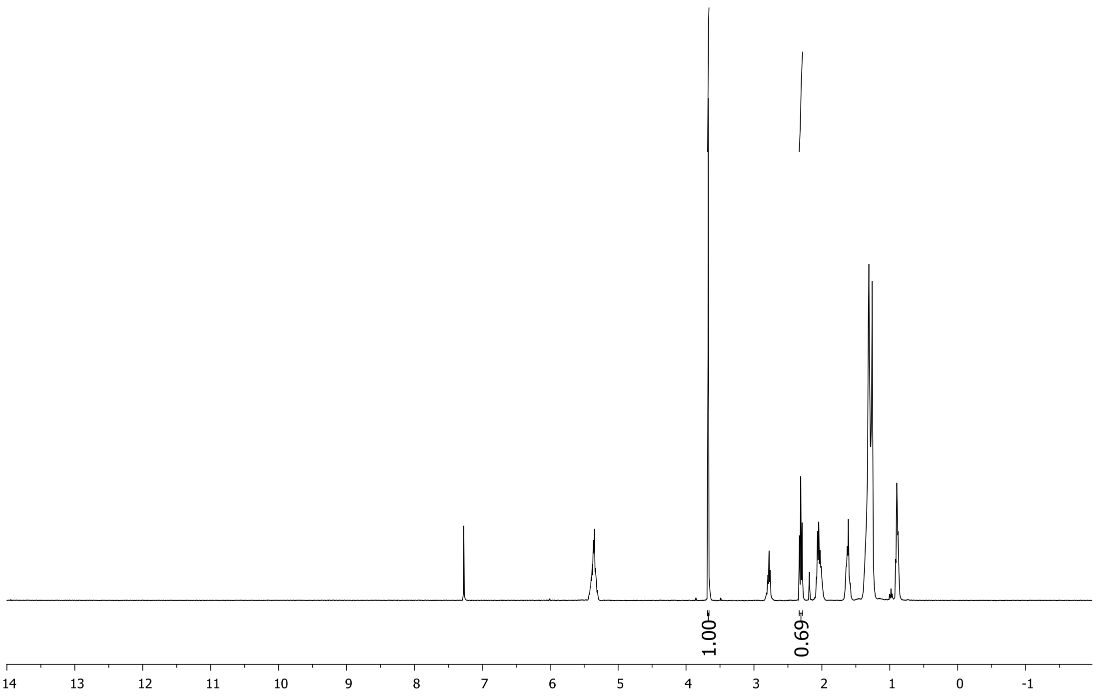

% Ester content of SME = [(2 ×1) / (3 × 0.69)] × 100

= 96.62 %

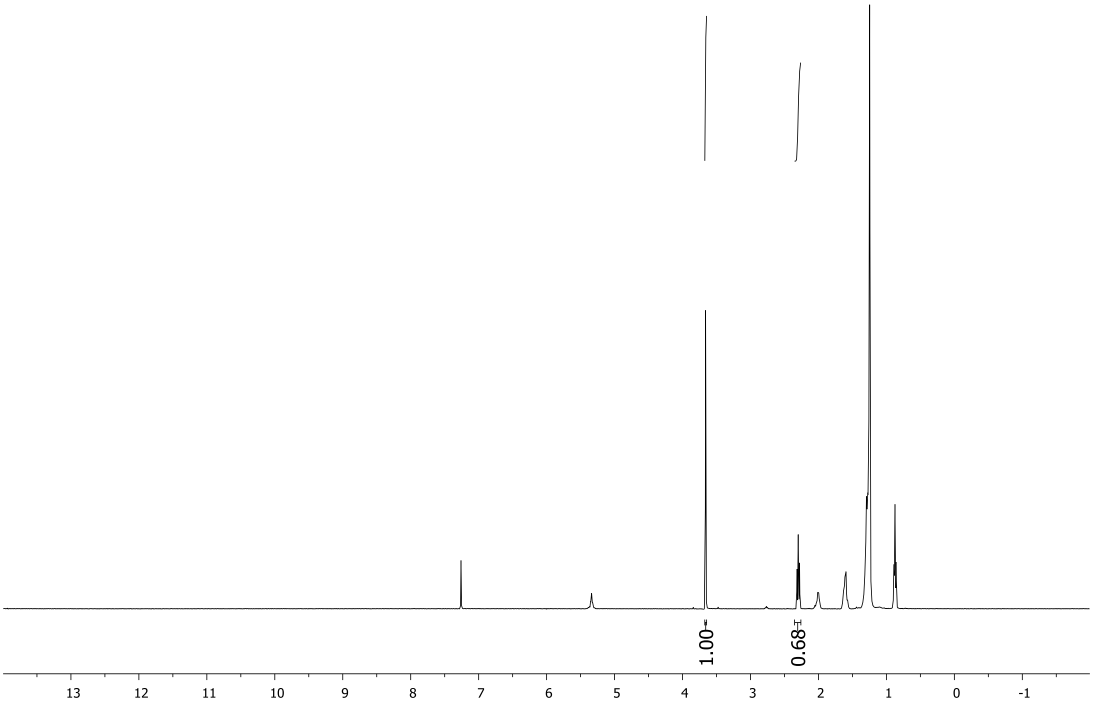

$$\% \text{ Ester content of PME} = [(2 \times 1) / (3 \times 0.68)] \times 100$$

$$= 98.04\ \%$$

2. Calculated % conversion of PPDs from ^{1}H-NMR spectrum

The percentage conversion of dimethyl esters were calculated as follow:

$$\boxed{\% \text{ Conversion} = [(4I_{OMe}) / (6I_{CH2})] \times 100}$$

I_{OMe} = Integration value of the protons of the methyl esters, appear at δ 3.7 ppm

I_{CH2} = Integration value of the methylene protons, appear at δ 2.3 ppm

*Integration value of the aromatic protons, appear at δ 7.5 and δ 7.6 ppm

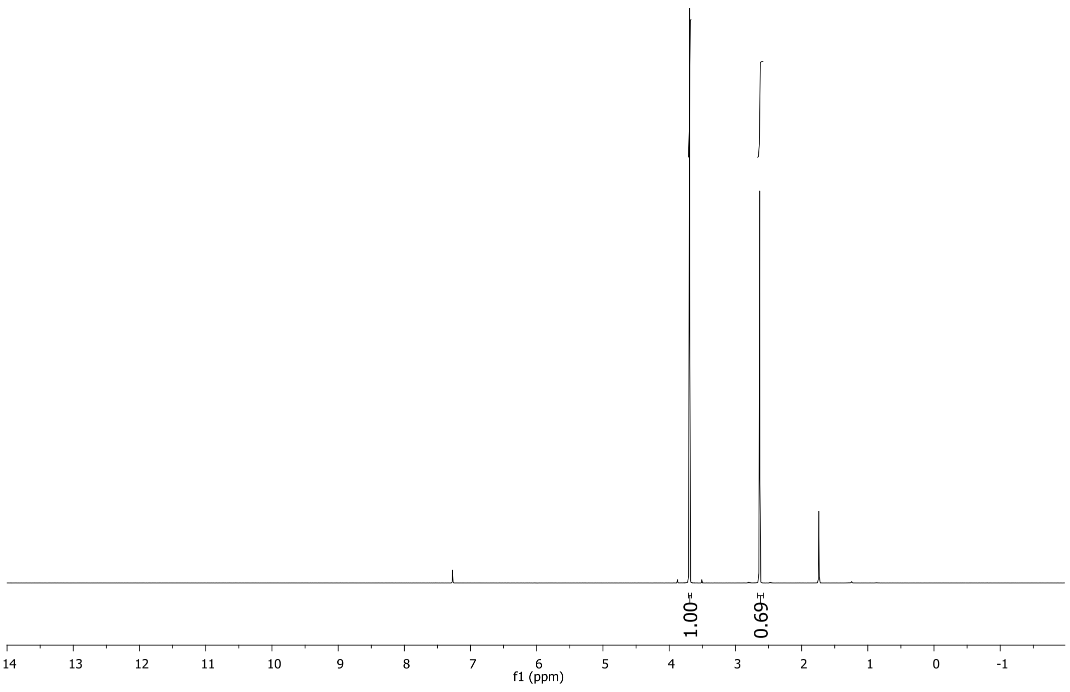

% Conversion of DMS = $[(4 \times 1) / (6 \times 0.69)] \times 100$

= 96.62 %

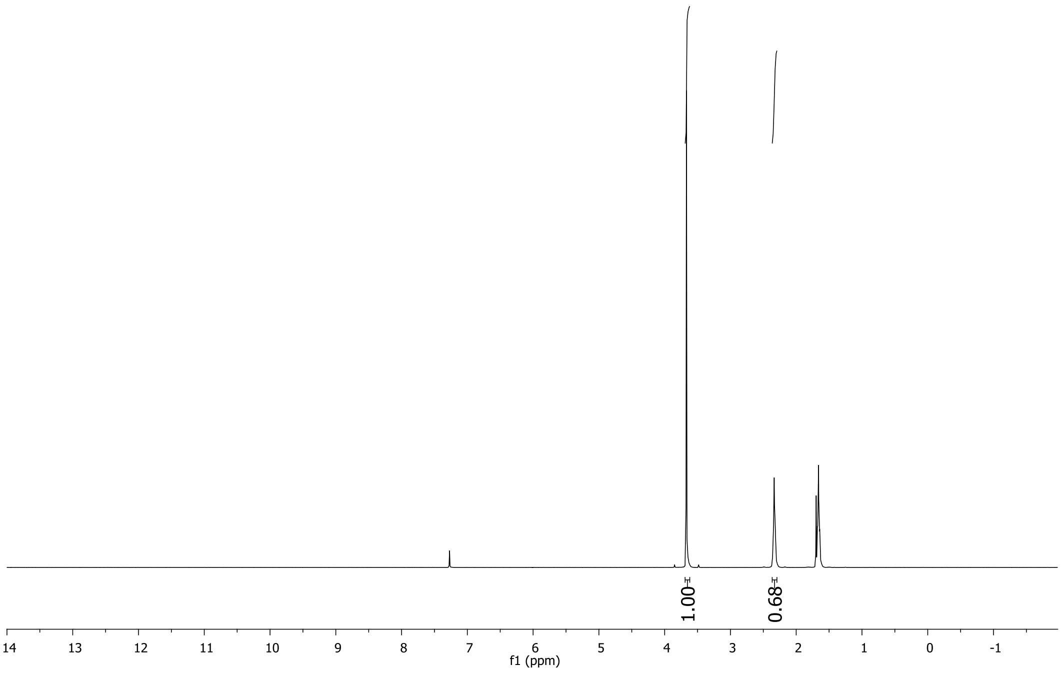

% Conversion of DMAD = $[(4 \times 1) / (6 \times 0.68)] \times 100$

= 98.04 %

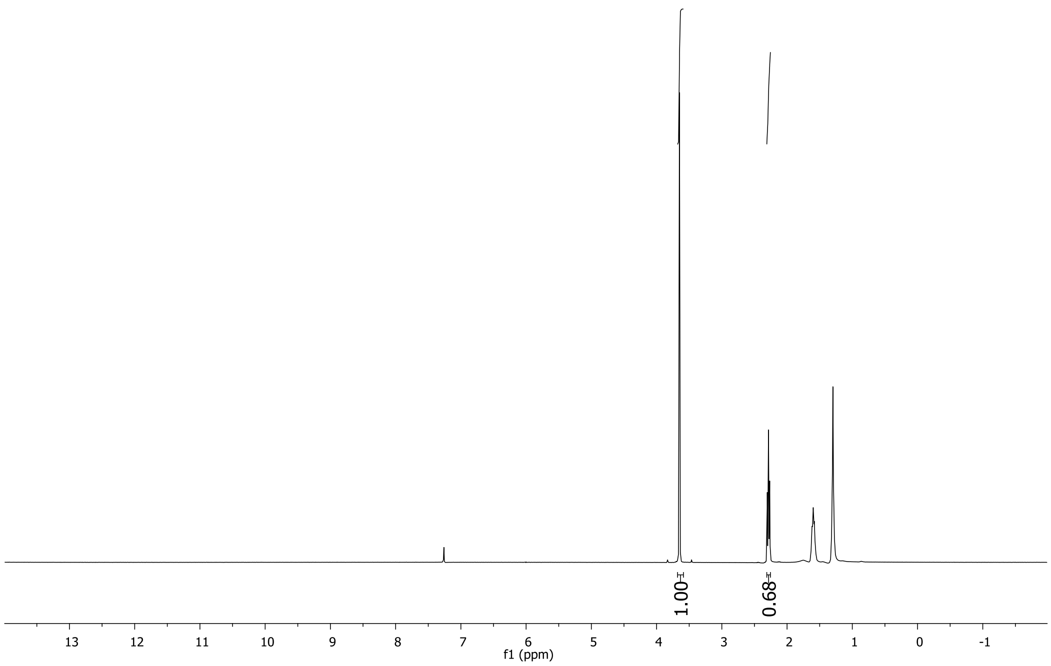

% Conversion of DMAZ = $[(4 \times 1) / (6 \times 0.68)] \times 100$

= 98.04 %

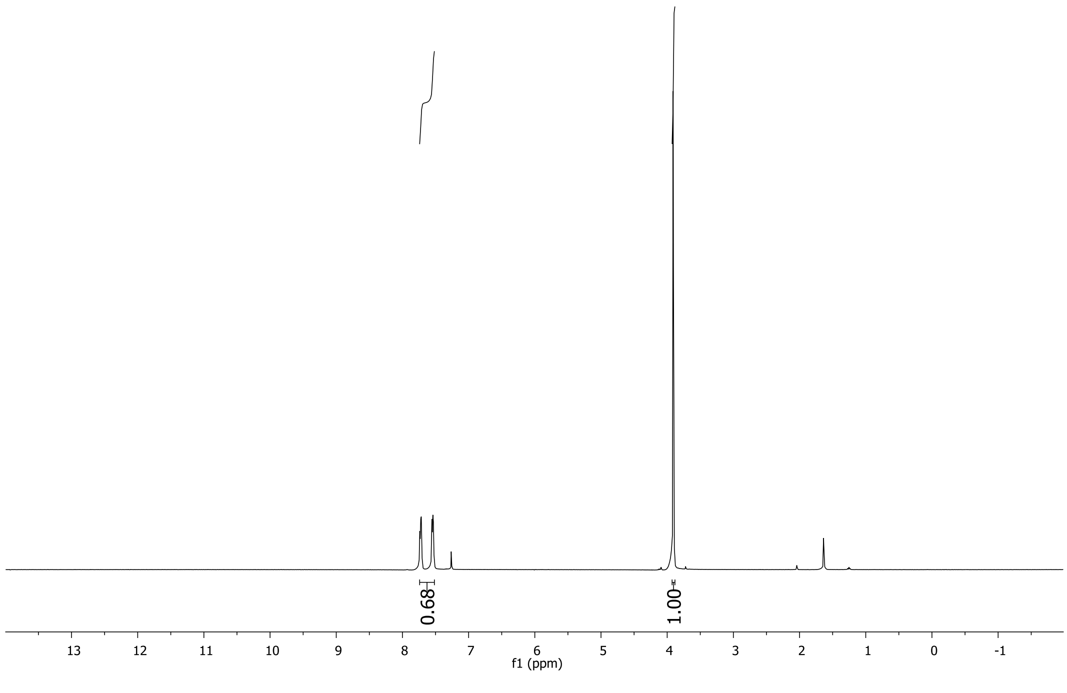

% Conversion of DMP = $[(4 \times 1) / (6 \times 0.68)] \times 100$

= 98.04 %

The percentage conversion of diisopropyl esters were calculated as follow:

$$\boxed{\%\ \text{Conversion} \quad = \quad [(4I_{O\underline{CH}(CH3)2} / 2I_{CH2}] \times 100}$$

$I_{O\underline{CH}(CH3)2}$ = Integration value of the protons of the iso-propyl esters, appear at δ 5.0 ppm

I_{CH2} = Integration value of the methylene protons, appear at δ 2.3 ppm

*Integration value of the aromatic protons, appear at δ 7.5 and δ 7.6 ppm

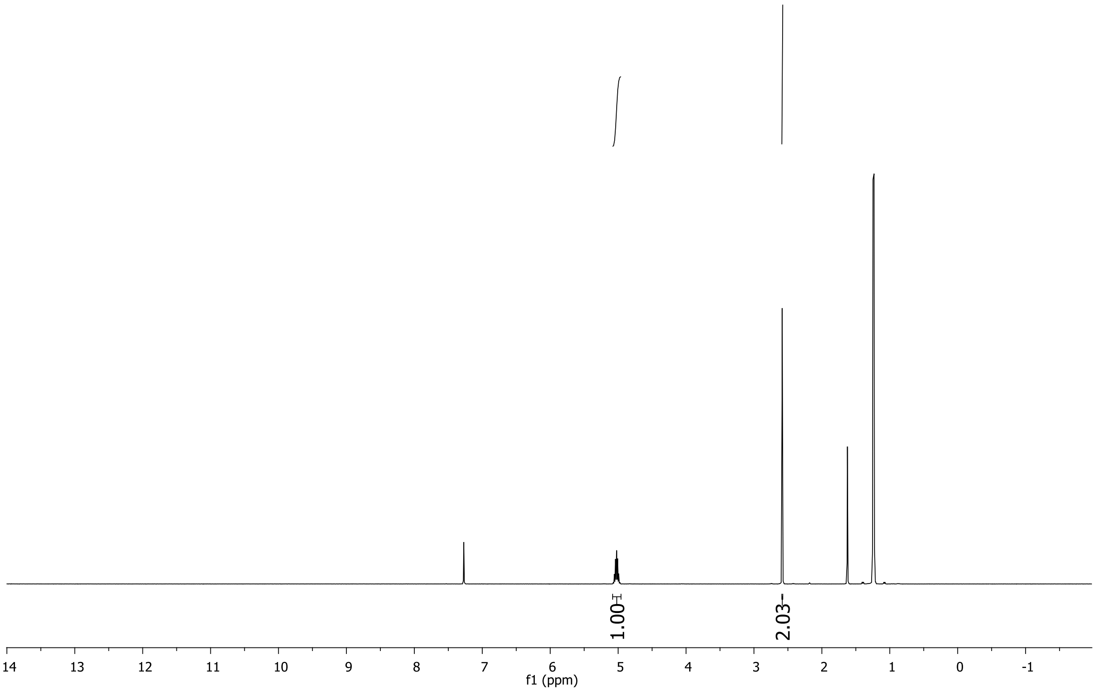

$$\%\ \text{Conversion of DIS} = [(4 \times 1) / (2 \times 2.03)] \times 100$$
$$= 98.52\ \%$$

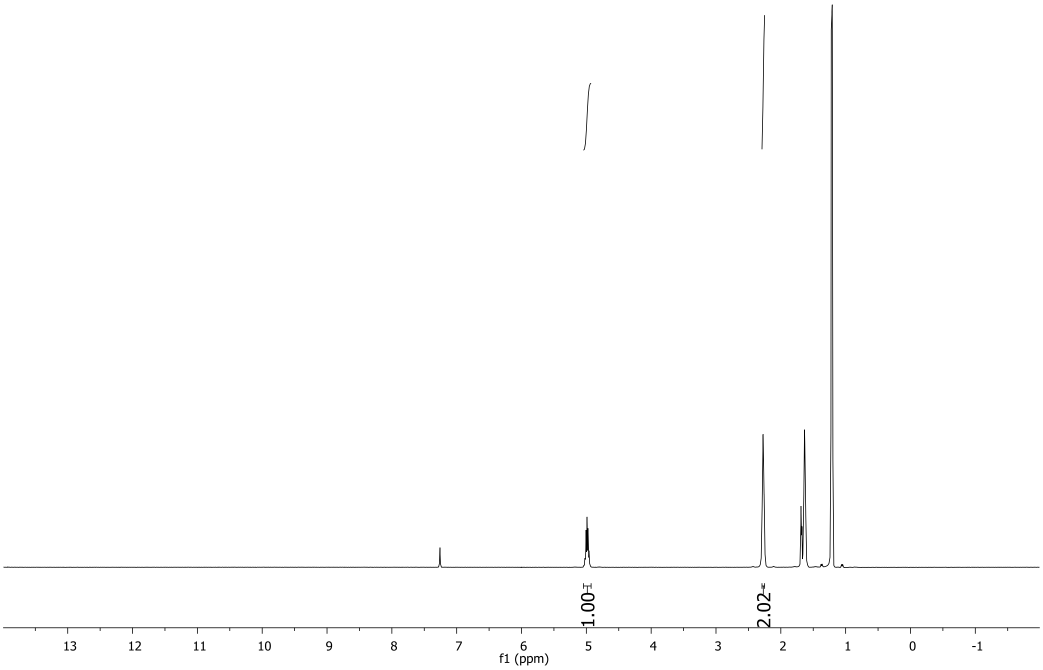

% Conversion of DIAD = [(4 × 1) / (2 ×2.02)] × 100

= 99.01 %

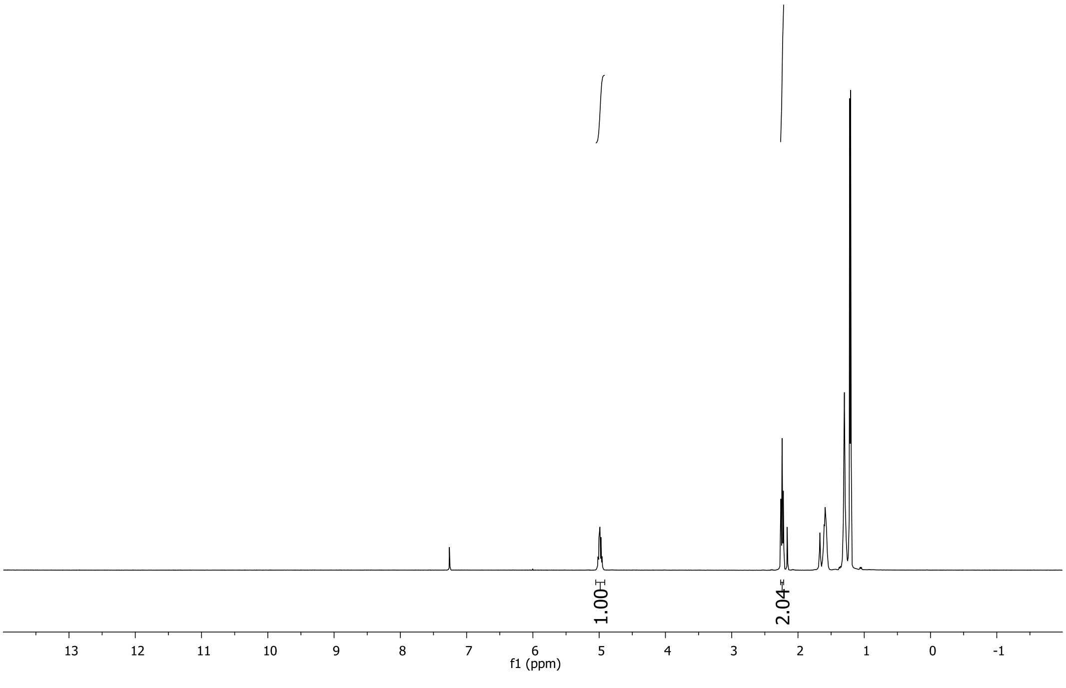

% Conversion of DIAZ = [(4 × 1) / (2 ×2.04)] × 100

= 98.04 %

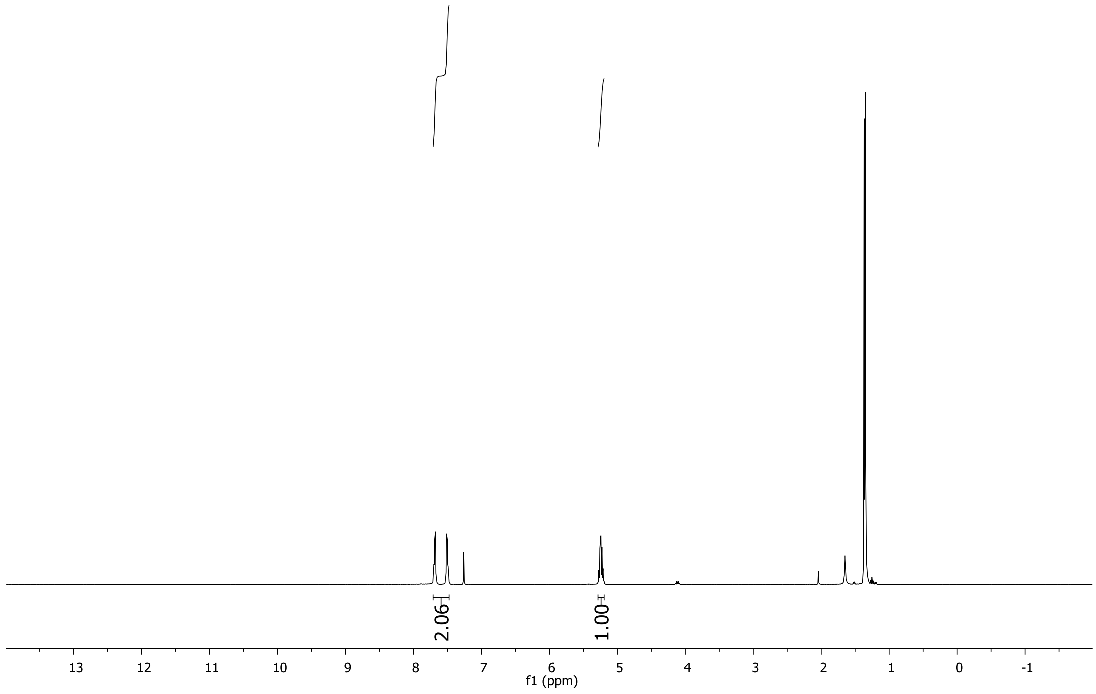

% Conversion of DIP = [(4 × 1) / (2 ×2.06)] × 100

= 97.09 %

The percentage conversion of di-2-butyl esters were calculated as follow:

$$\boxed{\%\ \text{Conversion} \quad = \quad [(4I_{O\underline{CH}CH2(CH3)} / 2I_{CH2}] \times 100}$$

$I_{O\underline{CH}\,CH2(CH3)3}$ = Integration value of the protons of the 2-butyl esters, appear at δ 4.8 ppm

I_{CH2} = Integration value of the methylene protons, appear at δ 2.3 ppm

*Integration value of the aromatic protons, appear at δ 7.5 and δ 7.6 ppm

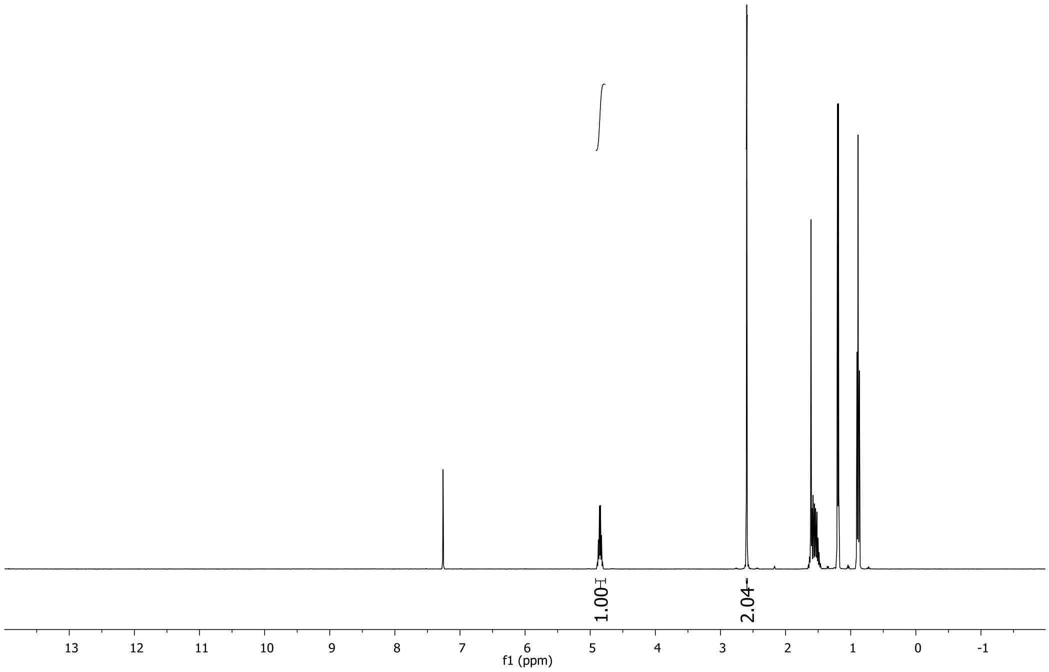

% Conversion of DBS = [(4 × 1) / (2 ×2.04)] × 100

= 98.04 %

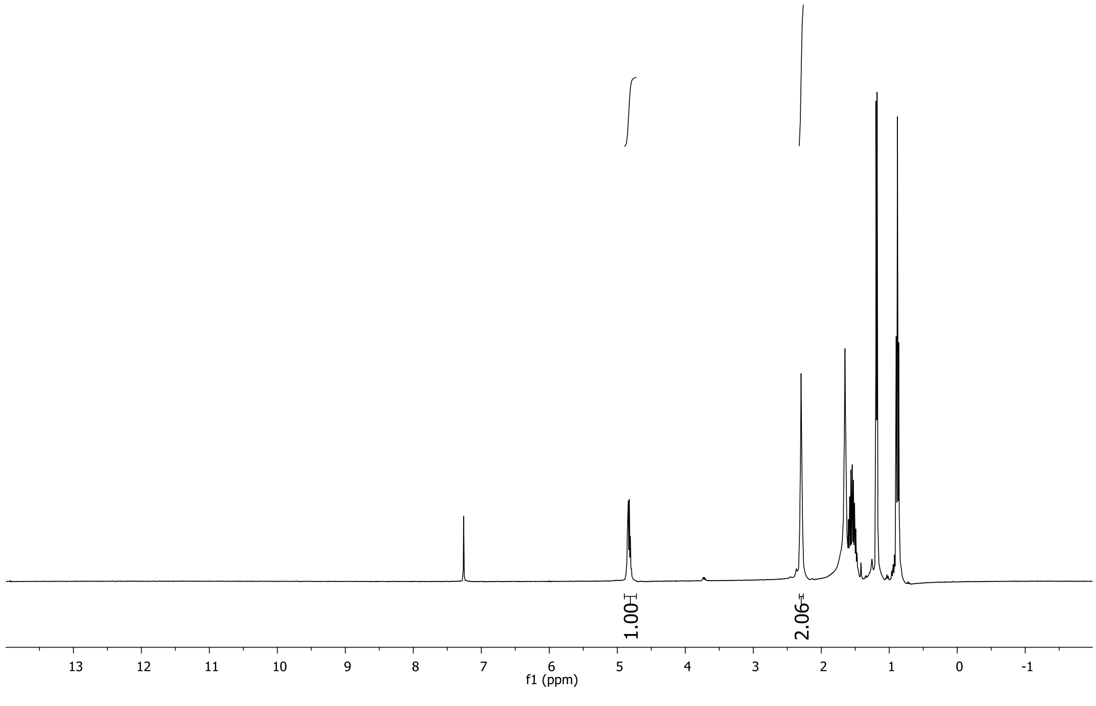

% Conversion of DBAD = [(4 × 1) / (2 ×2.06)] × 100

= 97.09 %

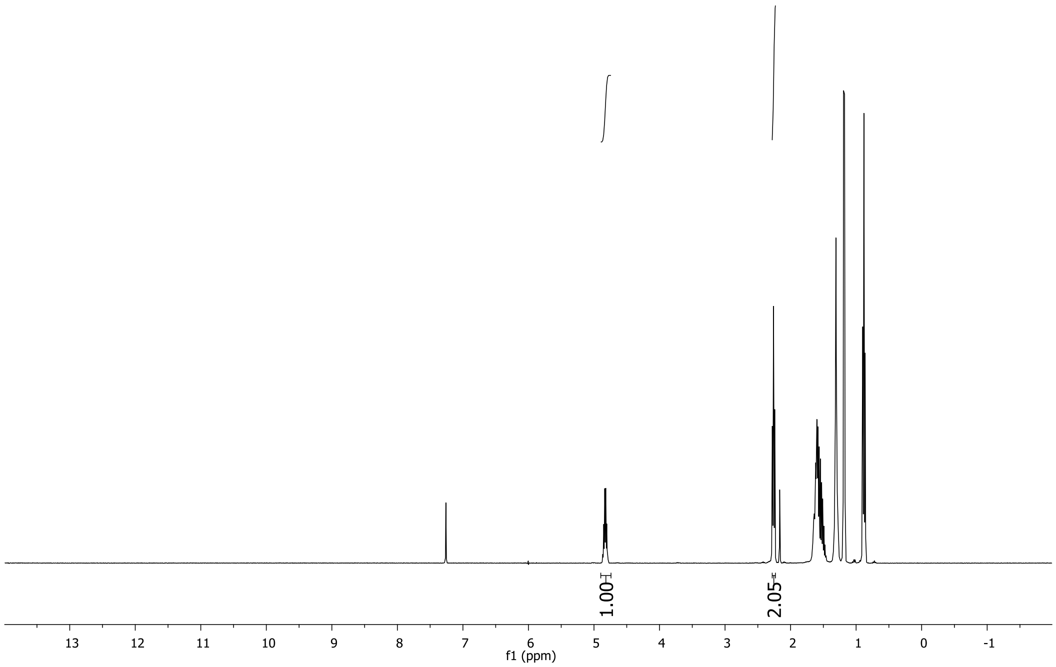

% Conversion of DBAZ = [(4 × 1) / (2 ×2.05)] × 100

= 97.56 %

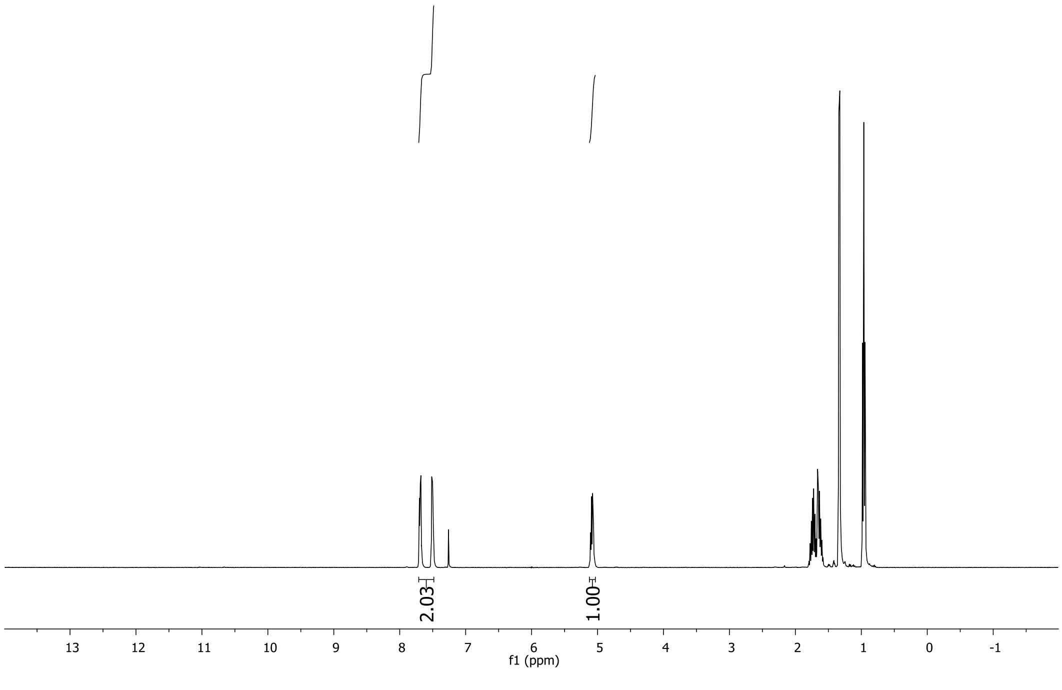

% Conversion of DBP = [(4 × 1) / (2 ×2.03)] × 100

= 98.52 %

The percentage conversion of di-2-ethyl hexyl esters were calculated as follow:

$$\boxed{\%\ \text{Conversion} \quad = \quad [(4I_{OCH2CH(CH2CH3)(CH2)3(CH3)}) / 4I_{CH2}] \times 100}$$

$I_{O\underline{CH2}CH(CH2CH3)(CH2)3(CH3)}$ = Integration value of the protons of the 2-ethyl hexyl esters, appear at δ 4 ppm

I_{CH2} = Integration value of the methylene protons, appear at δ 2.3 ppm

*Integration value of the aromatic protons, appear at δ 7.5 and δ 7.6 ppm

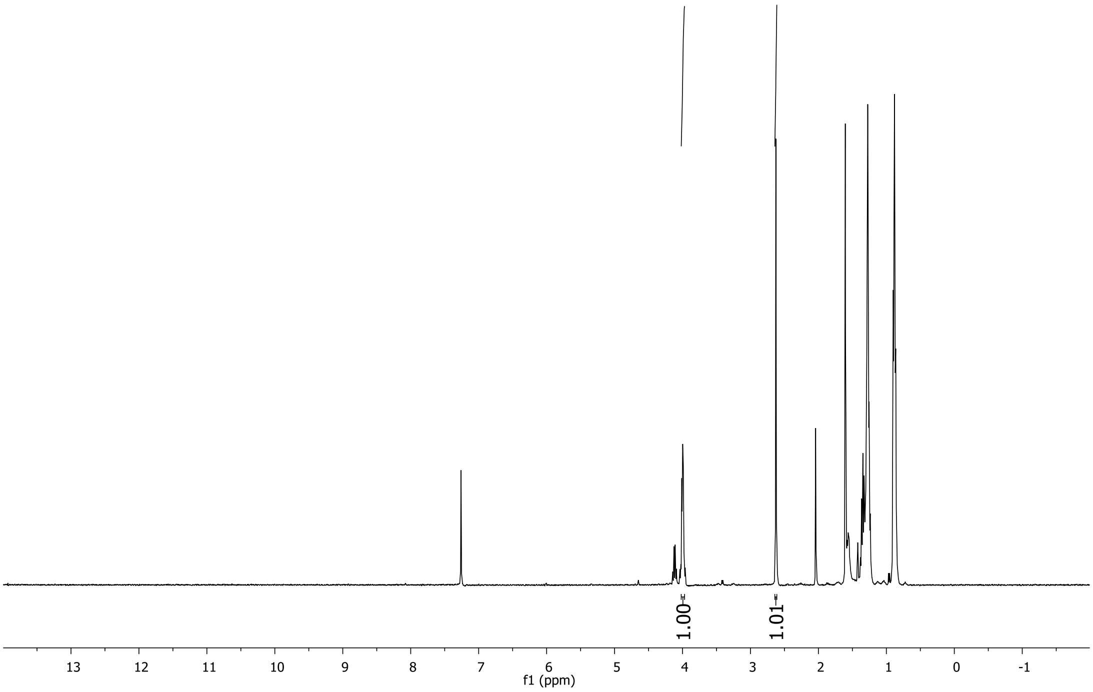

% Conversion of DES = [(4 × 1) / (4 ×1.01)] × 100

= 99.01 %

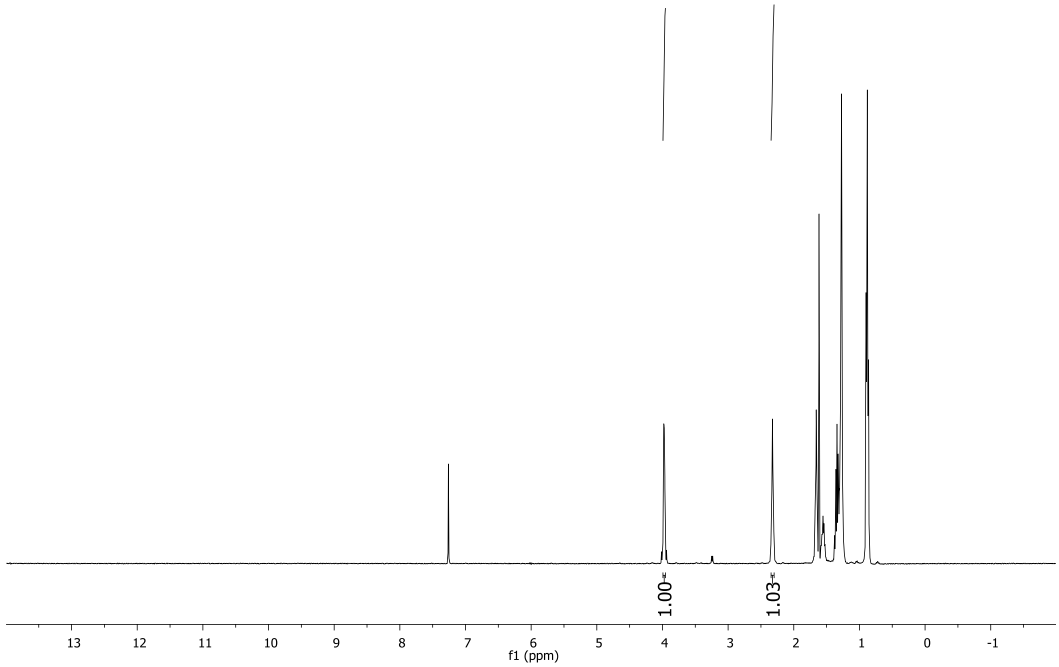

% Conversion of DEAD = [(4 × 1) / (4 ×1.03)] × 100

= 97.09 %

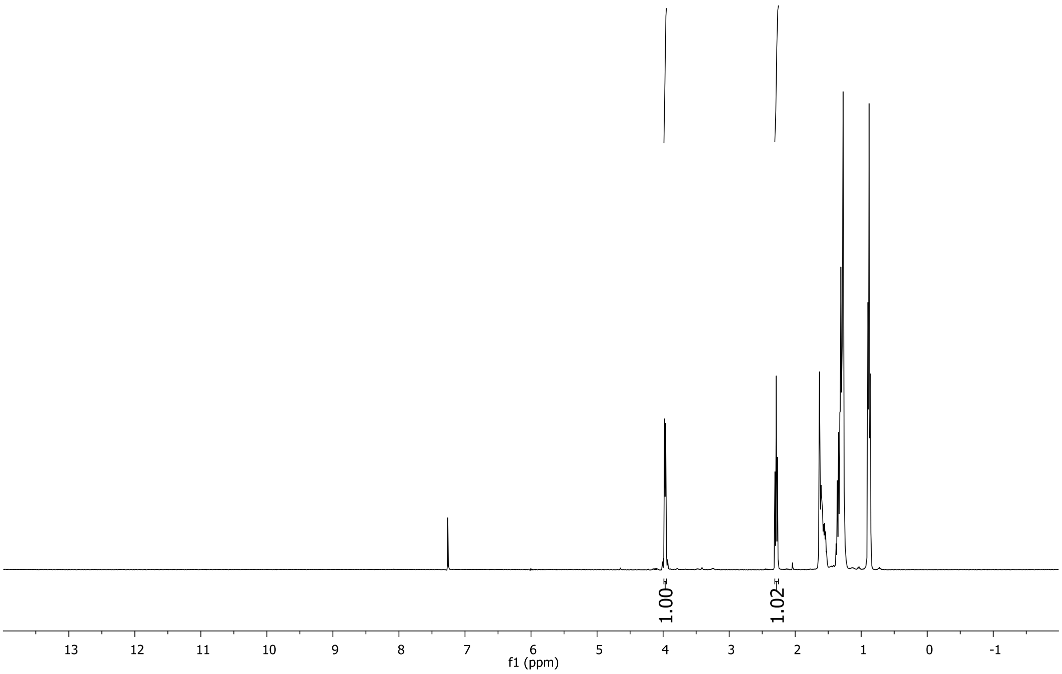

% Conversion of DEAZ = [(4 × 1) / (4 ×1.02)] × 100

= 98.04 %

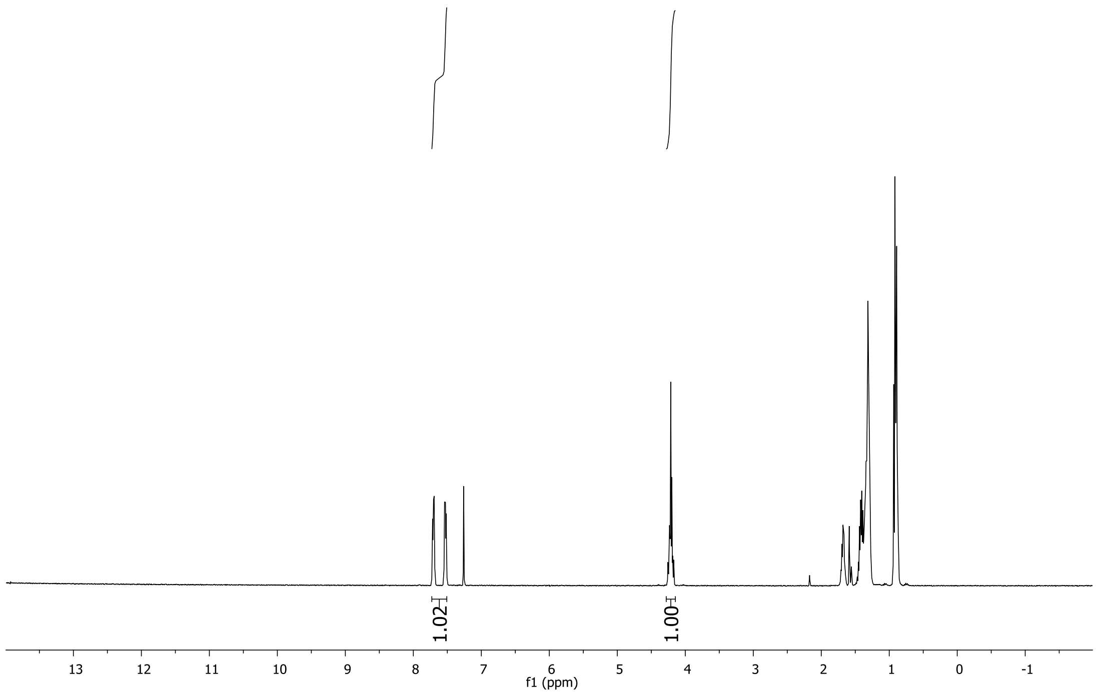

% Conversion of DEP = $[(4 \times 1) / (4 \times 1.02)] \times 100$

= 98.04 %

3. Determine the % free fatty acid (ASTM D5555)

Reagent

1. Ethanol
2. Phenolphthalein
3. 0.25 N NaOH

To the 250 ml of Erlenmeyer flask, oil sample (1 g), ethanol (75 ml) and 2ml of 1% phenolphthalein were added. The mixture was subject to titrate with 0.25 N sodium hydroxide solutions until the pink color was occurred. The ml of alkali solution used was recorded.

The percentage of free fatty acid (FFA) was calculated as follows:

% FFA = (ml of alkali x N x 28.2) / weight of sample

N = normality of alkaline solution

ml of alkali = ml of sodium hydroxide solution

Table C1 Values of free fatty acid contain in soybean oil.

Sample	**Weight of sample (g)**	**Volume of titrant (ml)**	**Concentration of NaOH (N)**	**% FFA**
Soybean oil	1.0285	0.11	0.2415	0.73
	1.0323	0.11	0.2415	0.73
% FFA average				0.73

4. Determination of the Saponification number (ASTM D5558)

Reagent

1. Phenolphthalein
2. Alcoholic KOH solution
3. 0.5 N HCl

To the 250 ml of Erlenmeyer flask, oil sample (1 g), alcoholic potassium hydroxide (25 ml) and 1 ml of 1% phenolphthalein were added. The mixture was subject to titrate with 0.5 N of hydrochloric acid until the pink color has disappeared. Prepare a blank determination and carried out same with the sample. The ml of acid solution used was recorded.

The saponification number (SN) was calculated as follows:

SN = $56.1 \times N \times (A - B)$ / weight of sample
A = titration of blank
B = titration of sample
N = normality of hydrochloric acid solution
Alcoholic KOH = 40 g of potassium hydroxide dissolved in 1 L of ethanol

Table C2 Saponification number of soybean oil.

Sample	**Weight of sample (g)**	**Volume of titrant (ml)**	**Volume of blank (ml)**	**SN**
Soybean oil	1.0225	23.95	30.55	180.40[a]
	1.0323	23.90	30.55	180.05[a]
SN average				180.23[a]

Remark : a = 0.4982 N

5. Determination of the Iodine value (ASTM D5554)

Reagent

1. KI solution
2. Wijs solution
3. 0.1 N $Na_2S_2O_3$
4. Starch

To the 500 ml of glass-stopper flask, oil sample (0.1 g), Wijs solution (25 ml) was added. Store the flasks in a dark place for 30 min. From storage, removed the flasks and add 20 ml of KI solution followed by 100 ml of distilled water. The mixture was subject to titrate with 0.1 N of sodium thiosulfate until the yellow color has almost disappeared, add 2 ml of starch indicator solution, and continued the titration until the blue color has just disappeared. Prepare a blank determination and carried out same with the sample. The ml of sodium thiosulfate used was recorded.

The iodine value (IV) was calculated as follows:

Iodine value = $(B - S) \times N \times 12.69$ / weight of sample
B = titration of blank
S = titration of sample
N = normality of $Na_2S_2O_3$ solution

Table C3 Iodine value of Soybean oil.

Sample	**Weight of sample (g)**	**Volume of titrant (ml)**	**Volume of blank (ml)**	**IV**
Soybean oil	0.1057	40.45	50.75	121.80[a]
	0.1035	40.40	50.75	124.99[a]
IV average				123.40[a]

Remark : a = 0.0985 N

6. Determination of the acid value (ASTM D974)

Reagent

1. p-naphtholbenzein indicator solution
2. 0.1 M alcoholic KOH solution
3. Titration solvent (250 ml toluene + 250 ml isopropyl alcohol)

To the 250 ml of Erlenmeyer flask, oil sample (2 g), titration solvent (25 ml) and 0.125 ml of 1% p-naphtholbenzein indicator solution were added. The mixture was subject to titrate with 0.1 M alcoholic KOH until the green color was occured. Prepare a blank determination and carried out same with the sample. The ml of acid solution used was recorded.

The acid value was calculated as follows:

Acid value = $[(A - B) \times N \times 56.1]$ / weight of sample
A = titration of sample
B = titration of blank
N = normality of alcoholic KOH solution
Alcoholic KOH = 0.6 g of potassium hydroxide dissolved in 100 ml of isopropyl alcohol

Table C4 Acid value of SME, PME and PPDs.

Sample	Weight of sample (g)	Volume of titrant (ml)	Volume of blank (ml)	AV
SME	2.0054	0.15	0.05	0.26^a
	2.0048	0.15	0.05	0.26^a
PME	2.0041	0.2	0.05	0.39^a
	2.0035	0.2	0.05	0.39^a
DMS	2.0002	0.05	0.05	0.00^a
	2.0021	0.05	0.05	0.00^a
DMAD	2.0062	0.05	0.05	0.00^a
	2.0046	0.05	0.05	0.00^a
DMAZ	2.0009	0.05	0.05	0.00^a
	2.0012	0.05	0.05	0.00^a
DMP	2.0031	0.05	0.05	0.00^a
	2.0003	0.05	0.05	0.00^a
DIS	2.0007	0.05	0.05	0.00^a
	2.0032	0.05	0.05	0.00^a
DIAD	2.0056	0.05	0.05	0.00^a
	2.0018	0.05	0.05	0.00^a
DIAZ	2.0029	0.05	0.05	0.00^a
	2.0005	0.05	0.05	0.00^a

Sample	**Weight of sample (g)**	**Volume of titrant (ml)**	**Volume of blank (ml)**	**AV**
DIP	2.0012	0.05	0.05	0.00[a]
	2.0034	0.05	0.05	0.00[a]
DBS	2.0047	0.05	0.05	0.00[a]
	2.0038	0.05	0.05	0.00[a]
DBAD	2.0009	0.05	0.05	0.00[a]
	2.0016	0.05	0.05	0.00[a]
DBAZ	2.0034	0.05	0.05	0.00[a]
	2.0048	0.05	0.05	0.00[a]
DBP	2.0024	0.05	0.05	0.00[a]
	2.0051	0.05	0.05	0.00[a]
DES	2.0008	0.05	0.05	0.00[a]
	2.0042	0.05	0.05	0.00[a]
DEAD	2.0015	0.05	0.05	0.00[a]
	2.0020	0.05	0.05	0.00[a]
DEAZ	2.0041	0.05	0.05	0.00[a]
	2.0052	0.05	0.05	0.00[a]
DEP	2.0034	0.05	0.05	0.00[a]
	2.0004	0.05	0.05	0.00[a]

Remark : a = 0.0934 N

7. Determination of viscosity (ASTM D445)

Viscosity is the unit specifying the resistance to flow; therefore viscosity is normally a specific value.

7 ml of each sample were added into the Viscometer tube, and insert the viscometer into the bath. After insertion, allow the viscometer to reach bath temperature, Use suction to adjust the head level of the test sample to a position in the capillary arm of the instrument about 7 mm above the first timing mark. With the sample flowing freely, measure, in seconds to within 0.1 s, the time required for the meniscus to pass from the first to the second timing mark. The time of sample used was recorded.

The viscosity was calculated as follows:

viscosity = Ct

C^a = Constant of viscometer tube (mm^2/s^2)

a=constant values of no.100 of viscometer tube

(0.01434)

time = measured flow times for *t1* and *t2*, respectively(s)

$$\text{Viscosity (cSt)} = C^a \times \frac{\text{time1(s)+time2(s)}}{2}$$

Table C5 Viscosity of SME, PME and PPDS.

Sample	Time1 (s)	Time2 (s)	Viscosity (cSt)
SME	288	288	4.13
PME	292	291	4.18
DMS	105	105	1.51
DMAD	132	132	1.89
DMAZ	200	200	2.87
DMP	389	388	5.57
DIS	147	147	2.11
DIAD	202	201	2.89
DIAZ	318	318	4.56
DIP	629	629	9.02

Sample	Time1 (s)	Time2 (s)	Viscosity (cSt)
DBS	185	185	2.65
DBAD	242	242	3.47
DBAZ	347	347	4.98
DBP	921	921	13.21
DES	265	264	3.79
DEAD	350	351	5.03
DEAZ	360	360	5.16
DEP	1750	1750	25.10

Table C6 Viscosity of SME when blend with 300000 ppm of PPDs**.**

Additives	Time1 (s)	Time2 (s)	Viscosity (cSt)
DMS	209	209	3.00
DMAD	228	228	3.27
DMAZ	258	258	3.70
DMP	301	300	4.31
DIS	233	232	3.33
DIAD	263	262	3.76
DIAZ	284	284	4.07
DIP	318	317	4.55
DBS	254	254	3.64
DBAD	228	228	3.81
DBAZ	308	308	4.42
DBP	305	305	4.37
DES	291	291	4.17
DEAD	312	311	4.47
DEAZ	319	318	4.57
DEP	410	409	5.87

Table C7 Viscosity of PME when blend with 300000 ppm of PPDs.

Additives	Time 1 (s)	Time 2 (s)	Viscosity (cSt)
DMS	209	210	3.00
DMAD	223	222	3.19
DMAZ	259	259	3.71
DMP	294	294	4.22
DIS	233	233	3.34
DIAD	252	251	3.61
DIAZ	298	299	4.28
DIP	310	309	4.44
DBS	253	253	3.63
DBAD	262	262	3.76
DBAZ	303	303	4.35
DBP	334	333	4.78
DES	288	288	4.13
DEAD	262	262	4.47
DEAZ	313	313	4.49
DEP	404	404	5.79

VITA

Miss Sujitra warasanam was born on October 16, 1988 in Roi-et, Thailand. She graduated at Strisuksa School in 2005. She received the Bachelor Degree of Science in Chemistry, Mahidol University in 2009. She continued her Master study in Program of Petrochemistry and Polymer Science, Faculty of Science, Chulalongkorn University in 2009 and completed the program in 2012.

Conference

15-16 July 2012 “Synthesis of pour point depressant from dicarboxylic acid for biodiesel”
ICCEEI’2012: International Conference on Chemical Processes and Environmental issue
Planetary Scientific Research Center (PSRC), Singapore